A survey of the alpha-nucleon interaction

S. Ali

International Centre for Theoretical Physics, Trieste, Italy
and Physics Department, University of Dhaka, Dhaka-2, Bangladesh

A. A. Z. Ahmad

Physics Department, Bright Star University of Technology, P.O. Box 58158, Ajdabia, Libya

N. Ferdous

Physics Department, University of Dhaka, Dhaka-2, Bangladesh

This paper gives a survey of the alpha-nucleon interaction and then describes experimental work on angular distributions of differential scattering cross sections and polarizations in proton-alpha and neutron-alpha scattering. The phenomenological approach, which includes the study of both local and nonlocal potentials reproducing the experimental alpha-nucleon scattering data, is discussed. Basic studies of the alpha-nucleon interaction attempting to build an interaction between an alpha particle and a nucleon from first principles are then described. The authors then present a critical discussion of the results with some concluding remarks suggesting the direction for further investigation.

CONTENTS

I. INTRODUCTION

Considerable interest has been shown by both the theorists and the experimentalists in the study of alpha-nucleon scattering, as this process gives insight into nuclear structural problems and also throws some light on the basic two-body interaction. Added interest is also due to the fact that it essentially involves the study of $A=5$ systems. Incidentally, there is no experimental evidence, so far, for the existence of bound states of five-baryon systems except that of $^5_\Lambda$He. The other facet of this study is the domain of alpha-nucleus scattering, models of which are built from the alpha-nucleon interaction, the simplest of all nucleon-nucleus interactions. However, so far no attempt has been made to give a broad survey of the whole subject of alpha-nucleon interaction except a very early review by Hodgson (1958).

In the present review we have made an attempt to present such a survey of the subject. The format of the review will be as follows.

We shall first review the experimental work on the alpha-nucleon scattering, which will include the angular distributions of differential scattering cross sections and polarization and phase shift analyses of the combined data. We shall then describe the phenomenological studies of alpha-nucleon interaction (both local and nonlocal). Discussion of basic or fundamental studies of the alpha-nucleon interaction will then follow. Finally, a critical discussion of the results with some concluding remarks indicating possible trends for further investigation into the subject will be given.

II. REVIEW OF EXPERIMENTAL WORK ON ALPHA-NUCLEON SCATTERING

A. Double scattering and other early experiments

In the presentation of the alpha-nucleon scattering results, proton-alpha scattering usually features first, because it was initiated earlier than neutron-alpha scattering. Experiments on the scattering of alpha particles by hydrogen nuclei yield the same information as those on the scattering of protons by helium nuclei. Incidentally, in the earliest experiments, the alpha particles emanating from alpha emitters were used as projectiles. Later, with the advent of accelerators, protons were more frequently used as projectiles. It is, however, quite amusing to find that just sixty years after the first experiment on the scattering of alpha particles by hydrogen, the alphas circulated in 1982 for sixty hours in one of the CERN Intersecting Storage Rings (ISR) before colliding with protons in another ring for a total c.m. energy of 88 GeV (Faessler, 1983).

To date, a large number of experiments on p-α and n-α scattering have been performed. Tables I and II list the p-α and n-α scattering experiments and the energy ranges covered. Although some of the earlier scattering works

TABLE I. p-α scattering experiments.

Source of particles	Energy range covered[a]	Type of analysis	References
	0—10 (MeV)		
Natural emitter of α particles $R_a(B+C)$		Angular distribution	Chadwick and Bieler (1921)
Radioactive source $R_a(B+C)$		Angular distribution	Mohr and Pringle (1937)
Cockroft-Walton-type accelerator	0.200—0.500	Polarization	Ad'yasevich *et al.* (1966)
Electrostatic generator	0.994	Angular distribution	Heydenberg and Roberts (1939)
Van de Graaff	3	Polarization	Scott and Segel (1955)
Van de Graaff	0.5—3	Differential cross section	Kraus and Linck (1974)
Electrostatic generator	1—3	Angular distribution	Heydenberg and Ramsey (1941)
Tandem accelerator	0.9—3.2	Polarization and phase shifts	Brown and Trächslin (1967)
Tandem accelerator	1—3.5	Angular distribution	Freier *et al.* (1949)
Tandem accelerator	3.5	Polarization	Heusinkveld and Freier (1952)
Van de Graaff	3.58	Polarization	Scott (1958)
Van de Graaff	4.5	Polarization	Manduchi *et al.* (1964)
Electrostatic generator	4.04—4.78	Polarization	Drigo *et al.* (1964)
Cyclotron	5.1	Angular distribution	Braden (1951)
Van de Graaff	2—5.5	Angular distribution and polarization	Miller and Phillips (1958); Phillips and Miller (1959)
Cyclotron	5.78	Differential cross section and phase shifts	Kreger *et al.* (1954)
Cyclotron	6.0	Polarization	Juveland and Jentschke (1956)
Cyclotron	6.25[b]	Polarization	Rosen and Brolley (1957)
Cyclotron	7.5	Differential cross section and phase shifts	Putnam *et al.* (1956)
Tandem accelerator	2—9	Analyzing power and phase shifts	Brandan *et al.* (1976)
Cyclotron	9.48	Angular distribution	Putnam (1952)
Cyclotron	9.5	Angular distribution	Freemantle *et al.* (1954)
Linear accelerator	9.79	Differential cross section	Williams and Rasmussen (1955)
Linear accelerator	9.9	Angular distribution	Cork and Hartsough (1954)
Linear accelerator	10.0	Polarization	Sanada (1960)
Linear accelerator	10.0	Polarization and phase shifts	Plummer *et al.* (1968)
Tandem Van de Graaff	2—11	Phase shifts, excitation function, angular distribution	Barnard *et al.* (1964)
Tandem accelerator	6—11	Polarization and phase shifts	Jahns and Bernstein (1967)
Tandem accelerator	4—12	Polarization	Brown *et al.* (1963)
	10—20 (MeV)		
Tandem accelerator	12.00	Polarization standards	Keaton *et al.* (1972)
Tandem accelerator	12.03	Analyzing power	Ohlsen *et al.* (1971)
Tandem accelerator	11—14	Scattering cross section	Dodder *et al.* (1977)
Tandem accelerator	11.93 and 17.00	Analyzing power	Hardekopf and Ohlsen (1977)
Cyclotron	17.5	Differential cross section and phase shifts	Brockman (1956)
Cyclotron	11.4 and 18.0	Differential cross section	Brockman (1957)
Cyclotron	11—18	Polarization	Brockman (1958)
Cyclotron	12—17.5	Differential cross section, phase shifts, and polarization	Garreta *et al.* (1969)
Tandem accelerator	3—18	Polarization and phase shifts	Schwandt *et al.* (1971)
	20—50 (MeV)		
Cyclotron	22	Polarization	Conzett *et al.* (1960)
Cyclotron	22—25	Differential cross section and polarization	Darriulat *et al.* (1968)
Tandem accelerator	17—27	Polarization and phase shift	Weitkamp and Haeberli (1966)

TABLE I. (*Continued*).

Source of particles	Energy range covered[a]	Type of analysis	References
Tandem accelerator	20—28	Differential cross section	Allison and Smythe (1968)
Linear accelerator	25—30	Polarization and differential cross section	Plummer *et al.* (1971)
Linear accelerator	31	Energy spectra and differential cross section	Bunch *et al.* (1964)
Linear accelerator	31.6	Absolute differential cross section	Cork (1953)
Linear accelerator	38.4	Polarization	Hwang *et al.* (1962)
Linear accelerator	40.0	Differential cross section and angular distribution	Brussel and Williams (1957)
Cyclotron	26.8, 34.2, 44.1	Polarization and cross section measurement	Boschitz *et al.* (1965)
Cyclotron	20—45	Angular distribution and polarization	Bacher *et al.* (1972)
Cyclotron	22—46	Excitation function	Bunker *et al.* (1969)
Cyclotron	21.85—47.65	Cross-section measurements and phase-shift analysis	Houdayer *et al.* (1978)
Cyclotron	18—48	Total reaction cross section	Sourkes *et al.* (1974); Sourkes *et al.* (1976)
Linear accelerator	22—48	Polarization	Craddock *et al.* (1963)
Linear accelerator	48	Spin-rotation parameter	Griffith *et al.* (1965,1966)
Linear accelerator	49	Differential cross section and phase shift	Davies *et al.* (1967)
	50—100 (MeV)		
Synchrocyclotron	53	Differential cross section	Cairns *et al.* (1964)
Synchrocyclotron	56	Differential cross section	Hayakawa *et al.* (1964)
Cyclotron	63	Polarization	Boschitz *et al.* (1965)
Cyclotron	45.0, 52.3, 59.6 64.9	Angular distribution of analyzing power and cross section	Imai *et al.* (1979)
Cyclotron	66	Polarization	Cormack *et al.* (1959)
Cyclotron	70, 80	Analyzing power	Stetz and Stetz (1968)
Cyclotron	70, 80	Polarization and phase shifts	Perez-Mendez *et al.* (1969)
Cyclotron	85	Differential cross section	Votta *et al.* (1974)
Cyclotron	95	Angular distribution	Selove and Teem (1958)
Cyclotron	100	Angular distribution	Goldstein *et al.* (1970)
High-energy accelerators (synchrocyclotrons, bevatrons, etc.)	>100 MeV (in units of GeV)	Mostly elastic differential scattering cross section	see below

At proton energies which are a few tenths of a GeV or a few GeV's, a number of p-α scattering experiments have been performed on various high-energy accelerators. The data consist mostly of the measurements of the elastic differential cross sections, although in some cases polarization was also measured. These experiments, which correspond to different ranges of t (the four-momentum transfer squared) were performed at 0.147 (Cormack *et al.*, 1959; Palmieri and Goloskie, 1964), 0.156 (Comparat *et al.*, 1975), 0.206 (Gotow, 1959), 0.225 (Greeniaus *et al.*, 1979), 0.310 (Aslanides *et al.*, 1977), 0.315 (Chamberlain *et al.*, 1956), 0.327 (Greeniaus *et al.*, 1979), 0.500 (Moss *et al.*, 1983), 0.520 (Greeniaus *et al.*, 1979), 0.560 (Klem *et al.*, 1977; Courant *et al.*, 1979), 0.580 (Boschitz *et al.*, 1972; Verbeck *et al.*, 1975), 0.600 (Fain *et al.*, 1976), 0.65 (Aslanides *et al.*, 1977), 0.720 (Verbeck *et al.*, 1975), 0.725 (McManigal *et al.*, 1965), 0.800 (Klem *et al.*, 1977; Courant *et al.*, 1979), 0.992 (Velicho *et al.*, 1982), 1.00 (Palevsky *et al.*, 1967), 1.03 (Klem *et al.*, 1977; Courant *et al.*, 1979), 1.05 (Baker *et al.*, 1974; Geaga *et al.*, 1977; Aslanides *et al.*, 1977), 1.15 (Aslanides *et al.*, 1977), 1.24 (Courant *et al.*, 1979), 1.27 (Klem *et al.*, 1977), 1.73 (Klem *et al.*, 1977; Courant *et al.*, 1979), 2.68 (Nasser *et al.*, 1978), 18.6 (Bruton *et al.*, 1978), 23.1 (Berthot *et al.*, 1975), 50—300 (Burq *et al.*, 1981), and 45—400 GeV (Bujak *et al.*, 1981). The inverse reaction ^{4}He-p elastic scattering at 1.75, 2.5, and 4.13 GeV/nucleon has been reported (Beznokikh *et al.*, 1978). In fact, in the experiment of Geaga *et al.* a 7.0-GeV/c α-particle beam at the bevatron was used. This is equivalent to proton incident on ^{4}He at 1.05 GeV bombarding energy. More recently, in the CERN intersecting storage rings (ISR), beams of α-particles were stored for the first time. After circulating for 60 h, an α beam (momentum 63 GeV/c) in one ring collided with a proton beam in the other ring (momentum 31.7 GeV/c). The α-p scattering experiments could be performed for $\sqrt{s}=88$ GeV (Bell *et al.*, 1982; Faessler, 1983) and $\sqrt{s}=89$ GeV (Ambrosio *et al.*, 1982), where $\sqrt{s}$ is the total c.m. energy. These c.m. energies at the present moment are the world-record ones for the collision of nuclei.

[a]The broad energy ranges used for purposes of grouping of data are only approximate. Energies used in some of the experiments are seen to exceed the ranges somewhat.
[b]In this experiment 25-MeV α's were used. This is equivalent to 6.25-MeV protons on ^{4}He.

TABLE II. n-α scattering experiments.

Source of neutrons	Energy range covered[a]	Type of analysis	References
	0–10 (MeV)		
Ra + Be	Thermal neutrons	Total cross section	Carroll (1941)
Heavy water reactor	Thermal neutrons	Total cross section	Harris (1950)
Radioactive ^{24}Na-D photoneutron source	0.262	Polarization	Jewell *et al.* (1966)
^{9}Be$(d,n)^{10}$B reaction	1.0	Angular distribution	Gaerttner *et al.* (1939)
^{9}Be$(d,n)^{10}$B reaction	1.0	Cross section	Staub and Stephens (1939)
^{7}Li$(p,n)^7$Be	0.5–1.33	Differential cross section and angular distribution	Cramer and Cranberg (1972)
^{7}Li$(p,n)^7$Be	0.6–1.6	Angular distribution	Hall and Koontz (1947)
T$(p,n)^3$He	2.0	Polarization	May *et al.* (1962)
^{7}Li$(p,n)^7$Be	1.01, 2.44	Polarization and phase shift	Sawers *et al.* (1968)
D$(d,n)^3$He	0.95–2.5	Cross section	Staub and Tatel (1940a,1940b)
D$(d,n)^3$He (E_d=0.2–0.5 MeV) T$(d,n)^4$He (E_d=0.1–0.3 MeV)		Polarization	Pasma (1958)
T$(p,n)^3$He	0.400–2.73	Angular distribution	Adair (1952)
D$(d,n)^3$He	3	Polarization	White and Farley (1957)
D$(d,n)^3$He	2–3	Angular distribution and phase shifts	Demanins *et al.* (1962)
D$(d,n)^3$He	2.5–3.1	Angular distribution	Barschall and Kanner (1940)
D$(d,n)^3$He	3–4	Angular distribution	Huber and Baldinger (1952)
^{9}Be$(\alpha,n)^{12}$C	3.38	Polarization and phase shifts	Stammbach *et al.* (1970)
D$(d,n)^3$He	2.6–4.1	Differential cross section	Streibel and Huber (1957)
^{7}Li$(p,n)^7$Be and D$(d,n)^3$He	0.4–4.9	Total neutron cross section	Bashkin *et al.* (1951)
T$(p,n)^3$He	6.0	Polarization	May *et al.* (1962)
Photoneutrons through bombarding Pb by electrons	1.5–6	Analyzing power	Bond and Firk (1976)
^{7}Li$(p,n)^7$Be	0.1–6.2	Total neutron cross section	Vaughn *et al.* (1959)
^{7}Li$(p,n)^7$Be ^{12}C$(d,n)^{13}$N T$(p,n)^3$He	0.2–7.0	Angular distribution and phase shifts	Morgan and Walter (1968)
^{9}Be$(\alpha,n)^{12}$C	7.8	Polarization and phase shifts	Stammbach *et al.* (1970)
T$(p,n)^3$He	1.6–10.9	Polarization	Walter *et al.* (1962)
	10–20 (MeV)		
T$(d,n)^4$He (E_d=1.8 MeV)		Polarization	Levintov *et al.* (1957)
T$(d,n)^4$He (E_d=1–7 MeV)		Polarization	Perkins and Simmons (1961)
T$(d,n)^4$He	9.8–11.4	Polarization	Trostin *et al.* (1961)
D$(d,n)^3$He	4.2–12.1	Polarization	Dubbeldam and Walter (1961)
^{7}Li$(p,n)^7$Be (E_p=3–6 MeV) D$(d,n)^3$He (E_d=2.45 MeV)		Polarization	Baicker and Jones (1960)
D$(d,n)^3$He (E_d=8.2 MeV)		Polarization	Daehnick(1959)
T$(d,n)^4$He	2.6–14.0	Angular distribution	Seagrave (1953)
D$(d,n)^3$He	10.5–14.0	Polarization	Trostin and Smotryaev (1963)
^{3}H$(d,n)^4$He	14.1	Angular distribution	Smith (1954)
^{3}H$(p,n)^3$He ^{2}H$(d,n)^3$He ^{3}H$(d,n)^4$He	1–15	Total neutron cross section	Battat *et al.* (1959)
T$(d,n)^4$He	15	Angular distribution	Malaroda *et al.* (1963)
T$(p,n)^3$He	6.8–15.4	Polarization	Alekseev *et al.* (1963)
^{15}N$(d,n)^{16}$O ^{3}H$(d,n)^4$He	12.0, 16.2	Polarization	Büsser *et al.* (1966)
T$(d,n)^4$He	15.95–16.90	Polarization	Boreli *et al.* (1965a,1965b)
D$(d,n)^3$He	14.0, 17.1	Polarization	Lisowski *et al.* (1975)
D$(d,n)^3$He	1–18	Polarization and phase shifts	Levintov *et al.* (1957)
D$(d,n)^3$He	12.7–19.3	Polarization and phase shifts	Christiansen *et al.* (1965)
T$(p,n)^3$He, D$(d,n)^3$He, T$(d,n)^4$He	12.1–19.8	Total cross section	Vaughn *et al.* (1959)
D$(d,n)^4$He	10.9–20.4	Polarization	Alekseev *et al.* (1963)
^{3}H$(d,n)^4$He	11.9–21.4	Polarization	Busse *et al.* (1967)

TABLE II. (*Continued*).

Source of neutrons	Energy range covered[a]	Type of analysis	References
$D(d,n)^3He$	2–23	Angular distribution, phase shift, and total cross section	Austin *et al.* (1962)
$T(p,n)^3He$, $D(d,n)^3He$, $T(d,n)^4He$	2–24	Angular distribution	May *et al.* (1963)
$T(d,n)^4He$	16–26	Angular distribution (total cross section)	Shamu and Jenkin (1964)
$^3H(d,n)^4He$, $^{14}N(d,n)^{15}O$, $D(d,n)^3He$	16–23.4	Angular distribution	Bonner *et al.* (1959)
	20–50 (MeV)		
$T(d,n)^4He$	23.0	Polarization	Perkins and Glashausser (1964)
$T(d,n)^4He$	17–23.7	Differential and total	Niiler *et al.* (1971)
$T(d,n)^4He$	20–29	Total cross section	Shamu *et al.* (1963)
Electron bombardment of conversion target	1–30	Total cross section	Goulding *et al.* (1973)
$D(d,n)^3He$ and $T(d,n)^4He$	6–30	Angular distribution and phase shifts	Hoop and Barschall (1966)
p + Be reaction	10–30	Total cross section	Swartz (1952)
$^3H(d,n)^4He$	20–30	Analyzing power	Lisowski *et al.* (1976)
$T(d,n)^4He$ and $D(t,n)^4He$	11–30.3	Polarization	Broste *et al.* (1972)
$T(d,n)^4He$	19.0–30.5	Polarization	Mutchler *et al.* (1971)
$T(d,n)^4He$	25, 28, 34	Polarization	Arifkhanov *et al.* (1965)
$T(d,n)^4He$	21.1–35.9	Polarization	Alekseev *et al.* (1964)
$p + {}^8Be$ reaction	47.5	Total cross section	Hillman *et al.* (1954)
	50 MeV and above		
$^2H(d,n)^3He$	50.4	Analyzing power	York *et al.* (1983)
$p + {}^8Be$ reaction	88	Total cross section	Hillman *et al.* (1954)
$^9Be(d,n)^{10}B$	90	Cross section, angular distribution	Tannenwald (1953)
$D(p,n)^2H$	80–150	Cross section, angular distribution	Measday and Palmieri (1966)

[a]In cases where neutron energies are not quoted, the energies of the projectile for the neutron producing reaction have been mentioned. The broad neutron energy intervals used here for the grouping of data are only approximate and cannot strictly confine the neutron energies of all experiments within these intervals.

have either been discarded or improved upon later, we include them in the present review for the sake of completeness. In describing the experimental work, we could have chosen a chronological order, which would have been fine in principle. But since this would lead to unavoidable repetitions and to presentation of unrelated facts, we chose instead to describe the experimental results and analyses in order of energy regions, from low to high. In a way, this will be in part a chronological ordering, also, because the various proton energies became available that way. Today the p-α experimental work is vastly rich, ranging from a few keV's to a few GeV's. The recent work on intermediate and high-energy p-α scattering is part of the general program of proton-nucleus research. The added interest in this work is due to its prospects in testing various theoretical models—the Glauber multiple scattering theory, the optical model, etc. Although Table I includes the recent experiments with GeV energies, we shall not deal with them extensively but shall refer the reader to an excellent review by Igo (1978) of some recent intermediate and high-energy proton-nucleus research. These experiments are yet to be conclusive and consistent with each other, and a correct parametrization of the nucleon-nucleon amplitudes in the analysis of the high-energy data is yet to emerge. In our review, we shall focus our attention principally on the work done with proton energies less than 100 MeV, although we shall comment on the results of the very recent high-energy scattering experiments.

Since the study of polarization in alpha-nucleon scattering is an important aid in the understanding of nuclear structure, considering the concepts and definitions used in the α-N polarization work in some detail will be worthwhile. Polarization of nucleons (i.e., more nucleons spinning "up" than "down" or vice versa, relative to the plane of the scattering event) in a scattering can be caused by the spin dependence of forces (inhomogeneous magnetic field, tensor forces, spin-orbit forces, etc.). Naturally, nucleon-polarization in α-N scattering has proved to be of great interest. First, this experiment was one of the first experimental evidences which proved the existence of spin-orbit forces in nuclear physics. Second, α-N scattering gives rise to the polarization of nucleons over a wide range of energies through the mechanism of spin-orbit forces so as to make it the most useful polarization analyzer for double-scattering experiments. Thus α-N polarization experiments are one of the convenient sources for producing polarized nucleons needed for different reactions, although for polarized protons the best sources are polarized ion sources.

It was first pointed out by Schwinger (1946,1948) that the spin-orbit coupling could be observed by doing a double scattering experiment of neutrons off helium. He suggested that the anomaly in n-α scattering was due to the presence of a $P_{1/2}$-$P_{3/2}$ doublet in ^{5}He with a splitting of 0.4 MeV, but at that time it was difficult to perform double scattering with 1-MeV neutrons. In fact, it was shown later that the splitting of the $P_{1/2}$-$P_{3/2}$ doublet in ^{5}He is much larger than Schwinger had thought. Then Wolfenstein (1949) came forward with a suggestion for p-α scattering assuming that a similar effect would be observed in the mirror nucleus ^{5}Li which should also exhibit a large splitting between the $P_{1/2}$ and $P_{3/2}$ levels. This experiment was then done by Heusinkveld and Freier (1952).

The object of interest in a double scattering experiment as shown in Fig. 1 is primarily a direct measurement of polarization. It has been shown by Enge (1966) that for a given scattering angle θ the intensity of the particles emerging from the second scattering center can be written as

$$I_2(\theta,\varphi)=I_2\left[\theta,\frac{\pi}{2}\right](1+P_1P_2\cos\varphi) ,$$

where φ is the angle between the two scattering planes and $P_1=P_1(\theta)$ and $P_2=P_2(\theta)$ are the polarizations which would result from the first and second scattering events, respectively, if the incoming beams on both the centers were unpolarized. For identical scattering targets and scattering angles, one obtains

$$I_2(\theta,\varphi)=I_2\left[\theta,\frac{\pi}{2}\right](1+P^2\cos\varphi) .$$

Thus for a given energy and a given θ a determination of the polarization parameter needs the measurements of intensities at two values of φ—for example, $\varphi=0$ and $\pi/2$. However, in most of the double-scattering experiments the polarizations are not measured individually but only as inseparable parts of a product of two polarizations. The quantities of interest, namely, polarization $P(\theta)$ and the asymmetry $\varepsilon(\theta)$ in the second scattering, may be defined (Wolfenstein, 1956) for spin-$\frac{1}{2}$ particles as

$$P(\theta)=\frac{N_+(\theta)-N_-(\theta)}{N_+(\theta)+N_-(\theta)}$$

and

$$\varepsilon(\theta)=\frac{(LL)-(LR)}{(LL)+(LR)}=P_1P_2 .$$

Here $N_+(\theta)$ is the number of particles in the beam with spin component parallel to a preferred direction and $N_-(\theta)$, the number of particles with antiparallel spin component. (LL) and (LR) denote the number of particles for both spin up and spin down which are twice scattered to the left and once to the left and once to the right, respectively. While scattering polarized nucleon beams experimenters often use the notation $\varepsilon(\theta)=(L-R)/(L+R)$, where L and R now denote the coincidence counts in the left and right detectors. A term which is often used in the literature is the analyzing power $A(\theta)$, which for ^{4}He is given by

$$A(\theta)=\varepsilon(\theta)/P_1 ,$$

where $P_1=P_B$ is the incident beam polarization which is determined from data taken simultaneously in the polarimeter. Since the analyzing power $A(\theta)$ is the same as the polarization $P_2(\theta)$ for the elastic scattering case, the terms "analyzing power" and "polarization" are often used interchangeably in the literature.

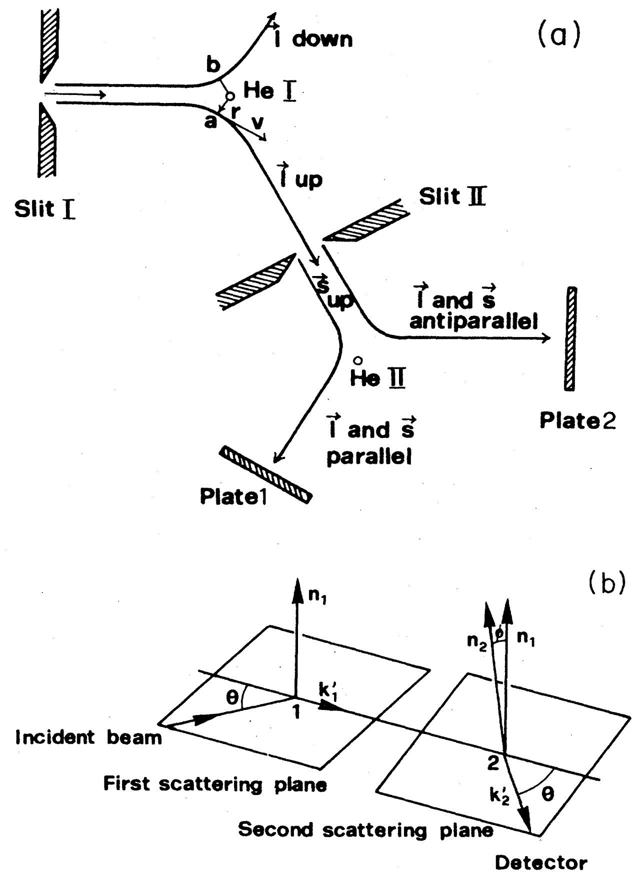

FIG. 1. (a) Schematic drawing of double scattering of protons by ^{4}He, the first scattering producing polarization and the second demonstrating or "analyzing" it (Mayer and Jensen, 1955, p. 55). (b) Double scattering experiment to measure polarization. The vectors $\mathbf{n}_1$ and $\mathbf{n}_2$ are unit vectors normal to the scattering planes. The second scattering plane forms an angle φ with the first scattering plane. The apparatus is set up so that the scattering angle θ is the same in both events (Enge, 1966, p. 75).

The experimental work on α-N scattering consists primarily of the measurements of angular distributions of differential scattering cross section $(d\sigma/d\Omega)(\theta)$ and polarization $P(\theta)$. These and also the spin rotation parameter β are connected with each other. The connecting relations are

$$\frac{d\sigma}{d\Omega}(\theta)=|g|^2+|h|^2 ,$$

$$P(\theta)=\frac{2\,\mathrm{Re}(g^*h)}{|g|^2+|h|^2} ,$$

and

$$\beta=\arctan\left[\frac{2\,\mathrm{Im}(gh^*)}{|g|^2-|h|^2}\right] .$$

A quantity which is also measured especially in high-energy p-α scattering experiments is the Wolfenstein R parameter, which is defined to be the component of the final polarization vector perpendicular to the outgoing direction, when the incident beam is completely polarized, and is given by

$$R(\theta)=[1-P^2(\theta)]^{1/2}\cos(\beta-\theta).$$

In the above relations, $g(\theta)$ and $h(\theta)$ are the spin-independent (non-spin-flip) and spin-dependent (spin-flip) scattering amplitudes,

$$g(\theta)=f_c(\theta)+\frac{1}{k}\sum_l[(l+1)e^{i\delta_l^+}\sin\delta_l^+ +le^{i\delta_l^-}\sin\delta_l^-]\times e^{2i\sigma_l}P_l(\cos\theta)$$

and

$$h(\theta)=\frac{i}{k}\sum_l(e^{i\delta_l^+}\sin\delta_l^+ -e^{i\delta_l^-}\sin\delta_l^-)e^{2i\sigma_l}\times\sin\theta\frac{d}{d\cos\theta}P_l(\cos\theta) ,$$

where f_c is the pure Coulomb scattering amplitude and σ_l the Coulomb phase shift. δ_l^+ and δ_l^- are the nuclear phase shift for $J=l+\frac{1}{2}$ and $J=l-\frac{1}{2}$ corresponding to whether l and s are parallel or antiparallel, respectively.

In order to see the sensitivity of $(d\sigma/d\Omega)(\theta)$ and $P(\theta)$ to phase shifts, the above expressions can be recast differently. One can write (Scott, 1958)

$$P=\frac{P\frac{d\sigma}{d\Omega}}{\frac{d\sigma}{d\Omega}} ,$$

with

$$P\frac{d\sigma}{d\Omega}=2\lambda\!\!\!^{-2}\sin\theta\sin(\delta_1^+-\delta_1^-)\left[\left[\frac{\alpha}{2s^2}\right]\sin(\delta_1^++\delta_1^-+\sigma_1+\alpha\ln s^2)-\sin\delta_0\sin(\delta_1^++\delta_1^-+\sigma_1-\delta_0)-3\cos\theta\sin\delta_1^+\sin\delta_1^-\right]$$

and

$$\frac{d\sigma}{d\Omega}=\lambda\!\!\!^{-2}\left\{\left|\frac{-\alpha}{2s^2}\exp(-i\alpha\ln s^2)+\sin\delta_0\exp(i\delta_0)+\cos\theta\{2\sin\delta_1^+\exp[i(\delta_1^++\sigma_1)]+\sin\delta_1^-\exp[i(\delta_1^-+\sigma_1)]\}\right|^2+\sin^2\theta\sin^2(\delta_1^+-\delta_1^-)\right\} ,$$

where θ is the scattering angle, δ_0 is the s-wave phase shift, δ_1^+ is the p-wave phase shift for $j=\frac{3}{2}$, δ_1^- is the p-wave phase shift for $j=\frac{1}{2}$, $s=\sin\theta/2$, $\alpha=ze^2\mu/k\hbar^2$, $\sigma_1=2\tan^{-1}\alpha$, and $\lambda\!\!\!^-=\hbar/m\vartheta$, ϑ is the incident velocity, μ is the reduced mass of the proton, and P measures percentage polarization. The expressions given above include s and p waves only.

From these expressions, one immediately sees that phase shifts provide a link between cross section and polarization. One can calculate phase shifts from the differential cross sections and then predict polarizations through the above connecting formulas. In fact, earlier, the literature indicates that this had been done, but it was noted that the calculation of phase shifts from only angular distributions not only makes the phase-shift solutions less unique but their use in the prediction of polarization also yields uncertainties. Since polarization depends on phase shifts differently from angular distribution in that all the terms are proportional to a trigonometric function of the difference of the two p phase shifts, polarization is found to be more sensitive than angular distribution to errors in phase shifts. This point had been illustrated in detail by Scott (1958). Thus, in order to obtain more unique phase-shift solutions at given energies, a combined analysis of the available cross-section and polarization data is usually made, making it as statistically significant as possible.

B. p-^{4}He, n-^{4}He cross sections and polarizations

There has been an early recognition of charge symmetry between the p-^{4}He (^{5}Li) and n-^{4}He (^{5}He) systems. Since a comparison of p-^{4}He and n-^{4}He scattering has been useful in providing a test of the validity of the charge symmetry hypothesis for nuclear forces, it is fitting to consider p-^{4}He and n-^{4}He cross sections and polarizations together. In reviewing the experimental results

TABLE III. p-α phase shifts (in degrees). The quantities in parentheses are inelastic parameters $\tau[=\exp(-2\,\mathrm{Im}\delta)]$.

Proton energy	$s_{1/2}$	$p_{1/2}$	$p_{3/2}$	$d_{3/2}$	$d_{5/2}$	$f_{5/2}$	$f_{7/2}$	$g_{7/2}$	$g_{9/2}$	$h_{9/2}$	$h_{11/2}$	$\chi^2_{\sigma+p}$	References
0–10 (MeV)													
0.94	−11.20	0.25	4.80										Brown *et al.* (1967)
1.35	−16.20	2.90	16.10										
1.765	−20.50	6.00	33.70										
2.18	−24.20	9.50	59.80										
2.59	−27.20	12.8	82.50										
3.00	−31.00	16.0	95.0										
3.00	148.67	16.26	94.21	0.03	0.07							0.46	Schwandt *et al.* (1971)[a]
	148.48	16.18	94.26	0.06	0.07							0.48	
3.20	149.36	18.27	101.46	0.07	0.08								
	147.04	18.14	98.88	0.07	0.08								
4.58	138.06	31.51	111.61	0.16	0.21							0.35	
	138.39	31.89	111.46	0.16	0.21							0.61	
5.95	131.14	43.09	112.63	0.31	0.41	0.04	0.05					0.64	
	131.39	43.14	112.91	0.31	0.41	0.04	0.05					0.66	
7.89	123.99	53.05	111.45	0.59	0.82	0.09	0.12					0.56	
	123.27	52.83	111.12	0.59	0.82	0.09	0.12					0.74	
9.89	117.32	59.65	108.56	1.49	2.19	0.35	0.46					0.68	
	123.27	59.15	105.09	1.49	2.19	0.35	0.46					0.97	
10–20 (MeV)													
11.99	110.96	59.65	105.74	1.49	2.19	0.35	0.46					0.82	
	110.37	59.15	105.09	1.49	2.19	0.35	0.46					0.98	
14.23	103.74	58.76	101.33	2.15	3.23	0.59	0.79					0.77	
	104.89	59.30	101.99	2.15	3.23	0.59	0.79					0.96	
17.45	99.20	58.44	98.68	3.27	5.08	1.09	1.48					0.82	
	98.36	58.20	98.06	3.27	5.08	1.09	1.48					0.97	
20–50 MeV													
19.94	94.01	56.00	94.24	4.67	6.20	1.73	1.96	−0.10	−0.20			0.41	Plattner *et al.* (1972)
22.46	91.13	53.28	90.92	8.17	7.67	2.26	2.97	0.33	0.03			1.09	
22.96	90.12	52.95	90.15	11.10	7.85	2.17	2.89	0.15	0.31			0.91	
23.16	89.48	53.01	89.87	15.36	8.41	1.94	2.80	0.07	0.11			0.73	
23.48	89.95	53.10	89.56	7.44	8.47	2.85	3.53	0.79	0.53			0.94	
	(1.000)	(1.000)	(0.994)	(0.636)	(1.000)	(0.995)	(1.000)	(1.000)	(1.000)				
24.51	87.86	51.54	88.63	6.18	9.90	3.41	3.97	0.93	0.74			0.64	
	(1.000)	(1.000)	(0.994)	(0.814)	(0.993)	(1.000)	(1.000)	(1.000)	(1.000)				
28.13	85.21	48.35	84.08	6.73	12.71	4.50	5.05	1.25	1.01			0.50	
	(0.995)	(0.960)	(0.971)	(0.744)	(0.950)	(0.995)	(0.997)	(0.962)	(1.000)				
30.43	83.06	46.99	80.95	7.48	14.08	5.86	6.67	1.04	1.40			0.73	
	(0.940)	(0.954)	(0.957)	(0.705)	(0.882)	(0.995)	(0.990)	(0.975)	(1.000)				

TABLE III. (*Continued*).

Proton energy	$s_{1/2}$	$p_{1/2}$	$p_{3/2}$	$d_{3/2}$	$d_{5/2}$	$f_{5/2}$	$f_{7/2}$	$g_{7/2}$	$g_{9/2}$	$h_{9/2}$	$h_{11/2}$	$\chi^2_{\sigma+p}$	References
32.17	81.64	45.53	78.60	8.35	14.85	6.79	7.93	1.13	2.09			0.76	
	(0.935)	(0.953)	(0.963)	(0.687)	(0.869)	(0.992)	(0.971)	(0.963)	(1.000)				
34.30	80.24	44.13	76.54	9.40	15.91	7.90	9.64	0.97	1.82			0.79	
	(0.909)	(0.961)	(0.961)	(0.675)	(0.826)	(0.983)	(0.966)	(0.973)	(0.998)				
36.93	77.54	41.70	73.58	10.57	17.61	8.78	11.47	0.83	2.03			1.04	
	(0.872)	(0.982)	(0.953)	(0.664)	(0.800)	(0.970)	(0.948)	(0.967)	(1.000)				
39.80	75.76	39.69	70.84	12.00	19.50	9.17	13.11	0.71	2.25			0.87	
	(0.842)	(1.000)	(0.940)	(0.655)	(0.771)	(0.953)	(0.917)	(0.962)	(0.992)				
												$\chi^2_{\rm tot}$	
42.45	70.88	35.24	66.76	11.61	18.43	8.31	13.27	0.42	1.98			1.20	Houdayer *et al.* (1978)[b]
	(0.785)	(0.996)	(0.914)	(0.648)	(0.741)	(0.941)	(0.912)	(0.957)	(0.992)				
44.05	71.64	34.03	65.28	12.00	19.49	7.81	13.82	0.32	1.77			1.61	
	(0.770)	(0.998)	(0.908)	(0.643)	(0.731)	(0.934)	(0.903)	(0.955)	(0.898)				
47.65	68.88	33.23	63.42	12.78	21.00	7.78	14.29	0.21	1.45	0.15	0.012	1.18	
	(0.761)	(0.997)	(0.895)	(0.650)	(0.704)	(0.914)	(0.876)	(0.953)	(0.980)	(0.997)	(0.998)		
48.8	70.83	33.31	63.07	13.82	22.45	6.98	15.10	0.05	1.32	0.00	0.003	1.13	
	(0.761)	(0.998)	(0.892)	(0.636)	(0.700)	(0.905)	(0.875)	(0.948)	(0.978)	(0.995)	(1.000)		
50 MeV and above													
55.0	64.61	32.86	61.39	11.92	24.44	6.23	14.85	−0.59	1.23	−0.132	0.079	0.93	
	(0.763)	(0.997)	(0.882)	(0.657)	(0.693)	(0.879)	(0.871)	(0.934)	(0.959)	(0.994)	(0.995)		
63.0	−135	24.0	46.5	10.9	25.7	4.6	12.6	0.00	2.3	0.171	2.3		Perez-Mendez *et al.* (1969)
	(0.98)	(0.86)	(0.96)	(0.75)	(0.72)	(0.82)	(0.95)	(0.89)	(0.90)	(0.95)	(0.83)		
70.0	−136	22.4	41.2	5.7	19.5	4.0	12.6	−5.7	4.0	−8.0	6.9		
	(1.0)	(0.67)	(0.89)	(0.71)	(0.70)	(0.93)	(0.76)	(0.92)	(0.71)	(0.98)	(0.69)		
80.0	−135.5	24.0	42.5	6.3	25.2	−4.0	11.0	0.05	9.15	3.42	3.4		
	(0.88)	(0.92)	(0.81)	(0.69)	(0.67)	(0.76)	(0.71)	(0.92)	(0.78)	(1.0)	(0.87)		
94.0	−137	29.8	32.1	16.8	17.2	0.00	8.0	−4.0	5.1	0.57	1.15		
	(1.0)	(0.92)	(0.78)	(0.57)	(0.65)	(0.52)	(0.74)	(0.67)	(0.83)	(0.94)	(0.95)		

[a]The first set of phase shifts of Schwandt *et al.* are the results of searches for the best s- and p-wave phase shifts, the d- and f-wave phases being fixed by effective range expansion. The second set gives the results of calculations using the final effective range phase shifts.

[b]The $\chi^2_{\rm tot}$ values quoted in the analysis of Houdayer *et al.* have been defined as $\chi^2_{\rm tot}=\chi^2/(A+B+C)$, where

$$\chi^2=\frac{A}{N_\sigma}\sum_{i=1}^{N_\sigma}\left[\frac{\sigma^{\rm th}(\theta_i)-\sigma^{\rm expt}(\theta_i)}{\Delta\sigma(\theta_i)}\right]^2+\frac{B}{N_A}\sum_{j=1}^{N_A}\left[\frac{A^{\rm th}(\theta_j)-A^{\rm expt}(\theta_j)}{\Delta A(\theta_j)}\right]^2+C\left[\frac{\sigma_R^{\rm th}-\sigma_R^{\rm expt}}{\Delta\sigma_R}\right]^2,$$

$\sigma^{\rm th}(\theta_i)$, and $\sigma^{\rm expt}(\theta_i)$ are the calculated and experimental differential cross sections at the N_σ c.m. scattering angles θ_i, $A^{\rm th}(\theta_i)$, and $A^{\rm expt}(\theta_i)$ are the calculated and experimental analyzing powers at the N_A c.m. scattering angles θ_j, $\sigma_R^{\rm th}$ and $\sigma_R^{\rm expt}$ are the calculated and experimental total reaction cross sections, and $\Delta\sigma(\theta_i)$, $\Delta A(\theta_j)$, and $\Delta\sigma_R$ are the corresponding experimental errors. The quantities A, B, and C are weighting factors which were set equal to 9, 5, and 1 to enhance the sensitivity with respect to the analyzing power data and the reaction cross-section datum. Other combinations of weighting factors were also tried, leading to essentially the same final result.

TABLE IV. n-α phase shifts (in degrees).

Neutron energy	$s_{1/2}$	$p_{1/2}$	$p_{3/2}$	$d_{3/2}$	$d_{5/2}$	$f_{5/2}$	$f_{7/2}$	$g_{7/2}$	$g_{9/2}$	χ^2	References
0–10 (MeV)											
0.50	163	2	11								Hoop and Barschall (1966)
0.80	159	4	33								
1.00	156	6	61								
1.20	154	7	81								
1.50	151	10	108								
2.00	146	15	118								
3.00	138	25	122								
4.00	132	35	121								
6.00	121	47	115								
8.00	113.0	55.0	110.0		1.0						Hoop and Barschall (1966)
10.00	106.0	60	107.0		2.0						
10–20 (MeV)											
12.00	101.0	61.0	103.0	1.0	2.0						
14.00	98.0	60.0	100.0	2.0	3.0						
16.00	96.0	58.0	97.0	2.0	5.0	1.0	1.0				
18.00	93.0	56.0	95.0	3.0	6.0	1.0	1.0				
20.00	91.0	54.0	93.0	4.8	8.0	2.0	2.0				
20–50 (MeV)											
22.00	89.0	53.0	92.0	19.0	10.0	3.0	3.0				
23.8	−102.6	42.9	79.1	11.0	10.6	5.0	5.8	2.8	3.6	0.91	Broste *et al.* (1972)[a]
				(0.766)							
25.7	−100.7	38.5	77.8	9.2	9.6	3.7	5.1	2.2	2.0	2.51	
				(0.748)	(0.881)						
27.3	−105.8	39.3	73.8	3.7	14.5	1.1	0.3	3.8	4.0	2.84	
				(0.895)	(0.933)	(0.760)					
30.3	−102.9	26.4	77.1	−7.7	16.0	−0.3	0.4	−0.5	1.2	1.56	
				(0.95)	(0.66)	(0.81)					
50.4	64.7	27.8	61.2	21.6	27.1	9.41	16.2	2.27	5.42	0.32	York *et al.* (1983)[b]
	(0.633)	(0.930)	(0.825)	(0.574)	(0.494)	(0.917)	(0.947)	(0.931)	(0.978)		

[a]Only the central phase-shift values have been quoted. In the analysis of Broste *et al.* the definition

$$\chi^2=\left[\sum_{i=1}^{r}\left[\frac{N_iO_i(p)-O_i(\text{exp})}{\Delta O_i(\text{exp})}\right]^2+\sum_{j=1}^{s}\left[\frac{N_j-1}{\Delta N_j}\right]^2\right]\Big/(\text{number of data}-\text{number of parameters})$$

was used. Here $O_i(\text{exp})$ is the experimental value of the observable, $\Delta O_i(\text{exp})$ is its experimental uncertainty, $O_i(p)$ is the value of the observable calculated from the parameters p (phase shifts and absorptions), N_j is the normalization factor of the jth data set (cross section or polarization), and ΔN_j is the experimental uncertainty in N_j.

[b]In the investigation of York *et al.* a small admixture of $h_{9/2}$ and $h_{11/2}$ phase shifts of amounts of 1.34° (1.000) and 0.91° (0.986) were also admitted. The χ^2 values of York *et al.* were the usual χ^2 per datum point as defined by Eq. (2.1) in the text.

for these, one faces a major problem in that not only the experimenters' energy regions are different, but the inputs of their experimental analyses also vary. In some cases, the inputs are cross sections only or polarizations only, while in others they are a combination of both. In a few cases, besides scattering cross sections and polarizations, reaction data have also been used. Furthermore, while some experimenters confine themselves to the phase-shift analysis of their data only, others include the measurements of previous investigations and make a combined analysis. Different data have been normalized in different ways and the χ^2 criterion of fits has been defined differently, depending on the inputs used. Thus it often becomes quite difficult to make a direct comparison of the data, although the judgments for phase-shift selections have been specified in almost all cases. However, in the present review we chose to present, whenever possible, results of combined phase-shift analysis of cross-section and polarization data.

In the presentation of the scattering experiments and also the results of analyses, we chose a number of energy regions. The regions are 0–10 MeV including the $P_{3/2}$ and $P_{1/2}$ resonances; from there to about 20 MeV, the region of data from tandem accelerators and fixed energy cyclotrons; 20–50 MeV, the region of data from variable energy cyclotrons and proton linear accelerators; and 50 MeV and above, with data from synchrocyclotrons. This division is naturally not rigid, as there will always be some overlaps. Since all of the experiments are listed in Tables I and II, and since the results of some experiments have been superseded by others, we have not commented on all of them. We have tried to identify the experimental results and analyses that made significant progress towards the final solutions. In Tables III and IV are listed the most recent, and as far as possible, final phase-shift solutions.

1. 0—10 MeV

In this energy range, a number of phase-shift analyses have been made. We have quoted in Table III the results of analyses of Brown *et al.* (1967) and of Schwandt *et al.* (1971) which have proved to be fairly reliable. The measurements of Brown and Trächslin (1967) of the left-right asymmetry in proton-alpha scattering in the energy range 0.9—3.2 MeV were analyzed by Brown *et al.* to determine the polarization of the proton beam in order to find the phase shifts that best fit the polarization and cross-section data for proton energies below 3.2 MeV. In fact, Brown *et al.* used the polarization measurements of Brown and Trächslin and the cross sections of Freier *et al.* (1949) extrapolated to the energies of the polarization measurements. The experimental uncertainty of the cross section was 3%, which included no additional error for interpolation. Brown *et al.* observed that the best-fit values of the s phases can be shifted to the values given by the hard-sphere calculation without destroying the quality of fit provided adjustments in the p phases were made. Although not quoted against the phase shifts, χ^2 values were calculated by Brown *et al.* for all the solutions. For a fixed s phase, searches were made at each energy for the $P_{1/2}$ and $P_{3/2}$ phase shifts so as to minimize the error fraction

$$\chi^2_{\sigma+p}=\frac{1}{n+m}\left[\sum_{i=1}^{n}\left[\frac{P_{\rm cal}(\theta_i)-P_{\rm expt}(\theta_i)}{\Delta P_i}\right]^2+\sum_{j=1}^{m}\left[\frac{\sigma_{\rm cal}(\theta_j)-\sigma_{\rm expt}(\theta_j)}{\Delta\sigma_j}\right]^2\right], \qquad (2.1)$$

where $P(\theta)$ and $\sigma(\theta)$ are the polarization and differential cross section at angle θ, ΔP, $\Delta\sigma$ are their respective experimental uncertainties, and the subscripts cal and expt designate values calculated from the trial phase shifts and values directly obtained from the experimental data, respectively. The designates m and n are the number of experimental cross-section and polarization data points, respectively. The final values of the phase shifts were obtained by taking the s phase to be the hard-sphere value and the p phases to be the best-fit values for the fixed s phase. d phases were found to be negligible at these energies. These phase shifts are plotted in Fig. 2. The hard-sphere s phases were calculated for an interaction radius of 2.48 fm. This hard-sphere radius was close to the value of 2.5 fm determined by Barnard *et al.* (1964) on the basis of phase shifts for energies up to 10 MeV. The phase shifts of Brown *et al.* agreed essentially with the earlier ones of Critchfield and Dodder (1949), although evidently a much more accurate determination of the p-wave splitting could be obtained.

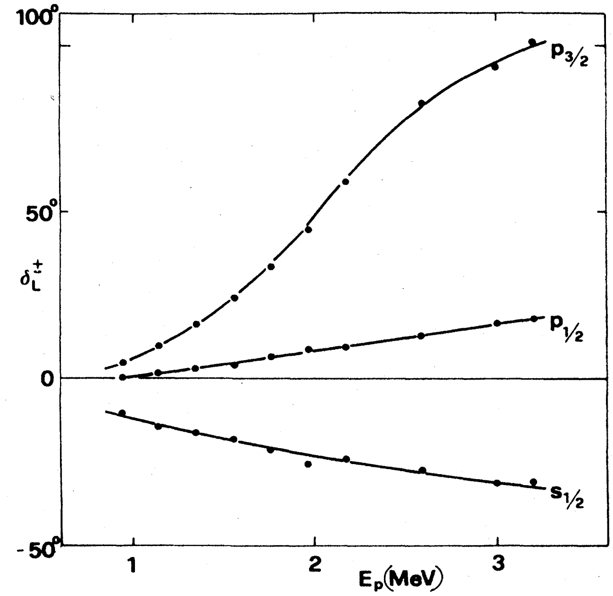

FIG. 2. s- and p-wave p-α phase shifts as function of energy (Brown *et al.*, 1967). The points are from searches made by Brown *et al.* for assumed zero d-wave phases and beam polarization 0.480. The smooth curve drawn through the s-wave phases is calculated for a hard-sphere potential with an interaction radius of 2.48 fm. The smooth curves for the p-phases are drawn through values that give the best fit to the experimental data for δ_0 fixed at the hard-sphere value.

The next set of p-α phase shifts considered is that of Schwandt *et al.* (1971), who measured angular distributions of the polarization for proton energies near 4.6, 6.0, 7.9, 9.9, and 11.9 MeV and performed a phase-shift analysis of available cross-section and polarization angular distributions between 3.0 and 17.5 MeV. They used the cross-section data of Garreta *et al.* (1969) and suitably extrapolated the cross-section data of Miller and Phillips (1958), Phillips and Miller (1959), Brockman (1957), and Barnard *et al.* (1964). Since it is difficult to determine the d- and f-wave phase shifts with great accuracy from the data at any one given energy, Schwandt *et al.* thought it best to obtain the energy dependence of the f- and d-wave phase shifts by using the following effective range expansion:

$$C_l^2(\eta)k^{2l+1}[\cot\delta_l^j+2\eta H(\eta)/C_0^2(\eta)]=\sum_{n=0} a_{nlj}E^n ,$$

where E is the proton laboratory energy (MeV), k is the wave number, μ the reduced mass of the α-p system,

$$\eta=\mu z_p z_\alpha e^2/\hbar^2 k ,$$

$$c_0^2(\eta)=2\pi\eta(e^{2\pi\eta}-1)^{-1} ,$$

$$c_l^2(\eta)=c_{l-1}^2(\eta)(1+\eta^2/l^2) ,$$

$$H(\eta)=\eta^2\sum_{s=1}^{\infty}\frac{1}{s(s^2+\eta^2)}-In\eta-\gamma$$

with $\gamma=0.577\,216$ (Euler's constant).

With f- and d-wave phase shifts fixed at values calculated from the effective range expansion, cross-section and polarization data at each energy were analyzed to determine optimum values of the s- and p-wave phase shifts. These solutions are plotted in Fig. 3, the numerical values being shown in Table III along with the quality of fit criterion $\chi^2_{\sigma+p}$ [defined by Eq. (2.1)]. Excellent fits to the data with $\chi^2_p \leq 1$ (not shown) were obtained. The phase-shift predictions of Schwandt *et al.* for energies below 3 MeV were in good agreement with the best-fit phases of Brown *et al.* discussed earlier.

The reason we have tabled the 3-MeV p-α phase shifts twice, once from Brown *et al.* and once from Schwandt *et al.*, is to point out that the negative s-wave phase shifts can be interpreted either as due to a repulsive potential or (by adding π) as reflecting the presence of a bound state in the potential.

It was pointed out by Schwandt *et al.* that the linear expansion for the d- and f-wave phases breaks down above 20 MeV. Thus the effective range expansion of Schwandt *et al.* is not useful beyond about 22 MeV, because, as pointed out by Darriulat *et al.* (1968), the $d_{3/2}$ state in ^{5}Li around 23 MeV becomes effective. Their phase-shift solutions are therefore unique only as long as the constraints imposed on the d- and f-waves are valid. The polarization calculated by them is plotted in Fig. 4 as a function of the laboratory energy and angle. Curves of constant polarization are labeled by percentage values. A feature of practical utility that emerges from the calculations of Schwandt *et al.* is that their 12-MeV phase shift solutions predict values of polarization at $\theta_{\rm lab}=111.5°$ which are very nearly unity and are insensitive to the phase shifts, i.e., $0.997 \leq P(\theta) \leq 0.999$. Thus, at this energy and angle, p-^{4}He scattering would seem to provide an accurate and nearly absolute calibration of proton polarization.

As far as the n-α phases in the (0—10)-MeV region are concerned, these have been provided through the investigations, among others, of Hoop and Barschall (1966), Morgan and Walter (1968), and Stammbach *et al.* (1970). For quite some time, a reliable n-^{4}He phase-shift analysis has been that of Hoop and Barschall, who measured the n-α differential scattering cross sections for neutron energies between 6 and 30 MeV and fitted their data as well as the earlier measurements of elastic scattering and total cross section and polarization, with phase shifts, as shown in Fig. 5. For reasons mentioned later, we have included these phase shifts in Table IV only up to 22 MeV. The phase shifts of Hoop and Barschall for the entire region 6—30 MeV were based largely on the p-α phase shifts. Below 10 MeV they found that the phase-shift set DGS proposed by Dodder and Gammel (1952) gave a satisfactory representation of the existing data, with the $P_{3/2}$

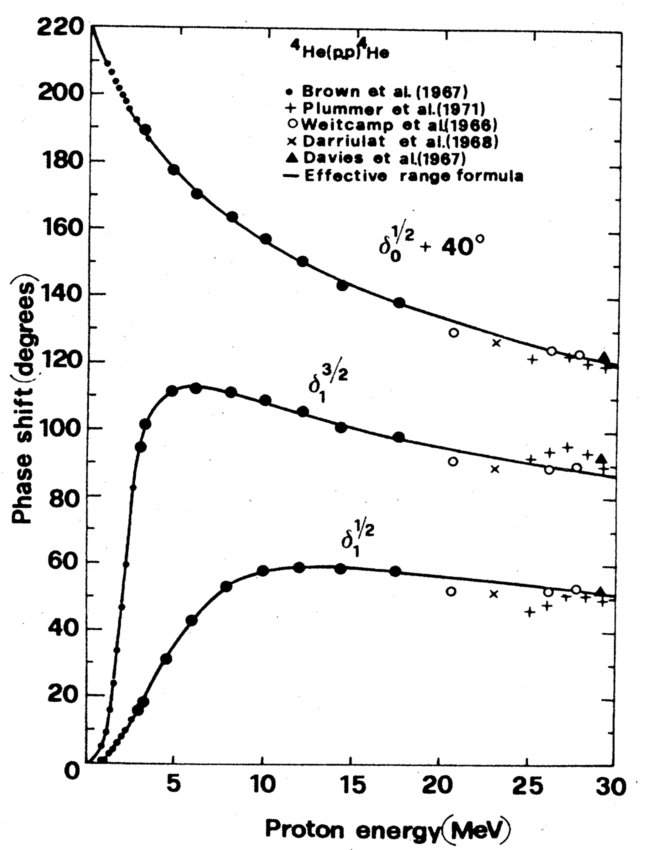

FIG. 3. s- and p-wave p-α phase shifts of Schwandt *et al.* (1971) as functions of proton laboratory energy. The large solid circles represent their single energy solutions between 3 and 18 MeV, and the curves show their effective range expansion fits.

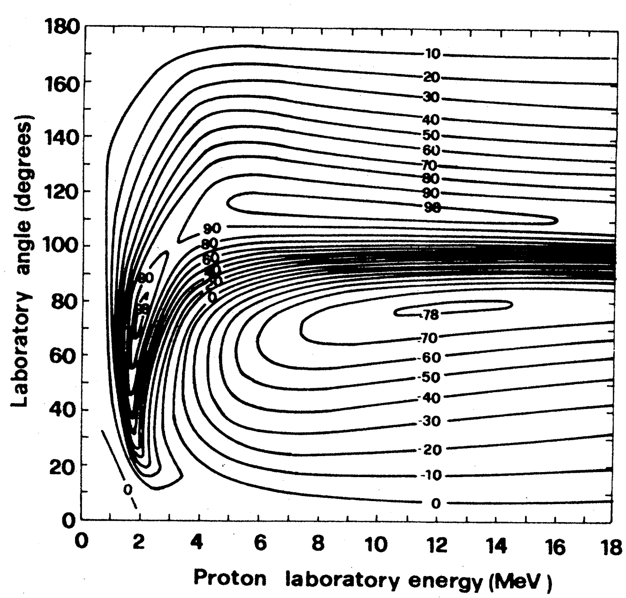

FIG. 4. Curves of constant polarization (in percent) as a function of proton laboratory energy and scattering angle, calculated from the effective range phase shifts (Schwandt *et al.*, 1971). Polarization contours below 3 MeV are based on the phase shifts of Brown *et al.* (1967).

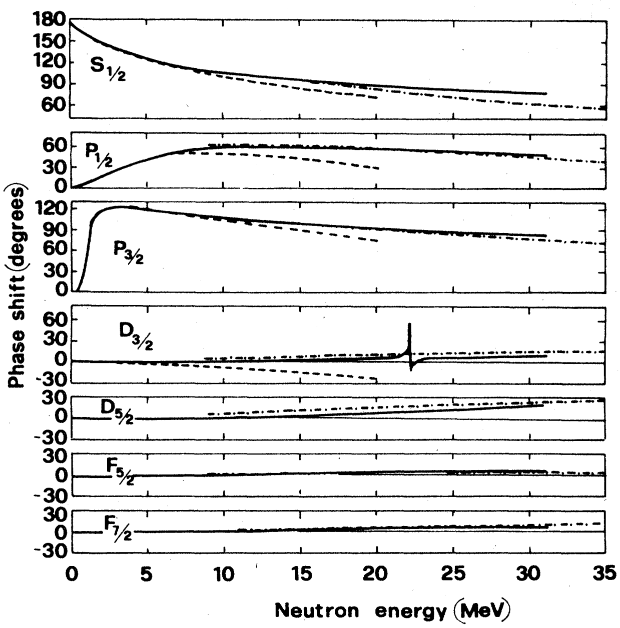

FIG. 5. s- and p-wave n-α phase shifts as functions of neutron laboratory energy (Hoop and Barschall, 1966). The solid curves represent the phase shifts of Hoop and Barschall. The dashed curves are the ones of Dodder and Gammer (1952) and Seagrave (1953); the dot-dashed curves are taken from Gammel and Thaler (1958) and Perkins (1960).

phase shifts modified slightly to give better agreement with the total cross-section data. Above 14 MeV, their observation was that the p-α phase shifts, derived by Weitkamp and Haeberli (1966) from their own proton polarization and cross-section data, were in agreement with their n-α data. Hoop and Barschall's analysis showed that for neutron energies below 6 MeV, the d waves could be neglected. It was shown that the s-wave phase shifts could be represented by a hard-sphere phase shift with a hard-sphere radius of 2.4 fm, a value very close to the one (2.48 fm) used by Brown and Trächslin (1967) in the analysis of the low-energy p-α data.

2. 10–20 MeV

The p-α phase shifts included in Table III for this region are the continuing ones of Schwandt *et al.* Although phase shifts have been quoted for a selected number of energies at which polarization meaurements and cross-section data were analyzed, those between 10 and 18 MeV have been calculated in intervals of 0.5 or 1 MeV. These are the phase shifts obtained by them with the use of the effective range expansion after the coefficients of the expansion were determined from a fit to the data at the energies of measurements. The phase shifts thus obtained join fairly smoothly with the ones quoted in the table, whose adequacy has already been discussed. The n-α phase shifts in this region are the ones of Hoop and Barschall. The derivation of these phases has just been mentioned.

In the energy ranges of 0–10 and 10–20 MeV, a number of R-matrix analyses have been performed, e.g., that of Morgan and Walter (1968) for n-α scattering from 0.2–7.0 MeV, of Stammbach and Walter (1972) for n-α and p-α scattering for energies up to 20 MeV, of Bond and Firk (1977) for n-α scattering below 21 MeV, and of Dodder *et al.* (1977) for p-α scattering in the energy region 0–17 MeV. The analysis of Dodder *et al.* is not only the most recent but also one of the richest in terms of inputs. The authors made accurate measurements of the p-α elastic scattering cross sections at energies of 11.157, 12.040, 13.600, and 14.230 MeV. They subjected their data and all available cross-section and spin-dependent measurements of p-α scattering between 0 and 18 MeV to a general purpose R-matrix analysis. Strict statistical criteria were followed for the elimination of data and the final search on 1131 data produced a unique R-matrix fit with a χ^2 per degree of freedom (weighted variance) of 1.001, which was within one standard deviation in χ^2 space.

Since, following the work of Lane and Thomas (1958), the R-matrix formalism has been frequently used in the literature, we shall not go into it but shall merely outline it in the way it has been used in the nucleon-alpha scattering. For the one-channel cases, the R-matrix reduces to an R function

$$R=\sum_{\lambda}\frac{\gamma_\lambda^2}{E_\lambda-E}\ ,$$

where the γ_λ are the reduced widths and E_λ are the eigenenergies. This function is used to describe the scattering phase shifts in terms of the model states of the nucleus. The boundary values B, at the channel radii a, are defined to be the ones which the logarithmic derivatives of the radial parts of the total wave function take at the eigenenergies. If one uses the equations given by Lane and Thomas, the phase shifts for a given l are related to the R function through the equation

$$\delta_l=\tan^{-1}[R_lP_l/(1-R_lS_l)]-\varphi_l+\omega_l\ ,$$

which Dodder *et al.* used. Here P_l, S_l, and φ_l are the penetration factor, shift function, and hard-sphere phase shifts, respectively. They are all energy dependent and can be computed from standard Coulomb functions. The ω_l are the Coulomb phase shifts. The nonresonant "background" contributions are not bracketed with the hard-sphere phase shifts but are included with the resonant contributions directly in the R function. The parameter space used by Dodder *et al.* was made up of s, p, d, and f states with an additional level each in the $P_{1/2}$ and $P_{3/2}$ states. For the $P_{3/2}$ and $P_{1/2}$ states, the R-matrix expansion was truncated to include two levels. One of these was a low-lying level to produce the observed resonance and the other a high-lying level to act as a distant background. Other states were described as single-level backgrounds. The values of a and B were taken to be $a=3.0$

TABLE V. p-α phase shifts (in degrees) of Dodder *et al.* (1977), obtained from R-matrix analysis.

Proton energy (MeV)	$s_{1/2}$	$p_{1/2}$	$p_{3/2}$	$d_{3/2}$	$d_{5/2}$	$f_{5/2}$	$f_{7/2}$
0.94	−11.034	1.539	6.050	−0.001	0.000	0.000	0.000
2.02	−22.342	7.343	49.982	−0.004	0.004	0.001	0.001
2.51	−26.480	11.331	79.135	−0.007	0.008	0.002	0.003
3.006	−30.270	15.596	97.046	−0.009	0.015	0.004	0.005
4.006	−36.952	25.425	110.387	−0.021	0.040	0.011	0.015
5.011	−42.733	34.944	113.491	−0.007	0.085	0.025	0.033
6.016	−47.819	42.782	113.557	0.012	0.158	0.048	0.064
7.50	−54.358	50.680	111.830	0.080	0.329	0.103	0.137
8.50	−58.235	53.962	110.245	0.162	0.498	0.158	0.211
10.0	−63.389	56.811	107.738	0.359	0.851	0.273	0.365
12.04	−69.302	58.323	104.478	0.807	1.555	0.503	0.675
13.65	−73.170	58.541	102.244	1.321	2.298	0.746	1.002
15.05	−76.032	58.424	100.408	1.957	3.167	1.027	1.383
17.84	−80.328	58.082	97.551	3.667	5.360	1.733	2.342

fm and $B=0$. The phase shifts obtained by the R-matrix fit to the scattering data are shown in Table V, where central values of the phase shifts have been quoted, and the corresponding R-matrix parameters are given in Table VI. It is seen that the background E_λ's for the P waves were fixed by Dodder *et al.* at 1000 MeV. These seemed to be unusually high. It was, however, pointed out that the search routine was unable to determine these parameters when they were treated as free and that no significant improvements could be achieved by placing these levels at low energies. The effect of having a high background E_λ was to make the background contribution essentially constant. An interesting new feature of the analysis of Dodder *et al.* was that the reduced width γ_l's for the same l but different J values were very similar. Comparing their phase-shift solutions with those of previous work in different parts of the energy region considered, Dodder *et al.* seemed to favor the phase-shift analysis of Arndt *et al.* (1971) and Stammbach and Walter (1972), although they emphasized that it is difficult to make such a comparison satisfactorily in view of the differences in the data sets. Their highest energy phases were compatible with the lowest energy phases of the (20—40)-MeV analysis of Plattner *et al.* (1972).

3. 20—50 MeV

The previous phase-shift analyses in this region were superseded for quite some time by that of Plattner *et al.* (1972), who made a phase-shift analysis of the cross-section and polarization data of Bacher *et al.* (1972) between 20- and 40-MeV proton laboratory energy. Because of the observation (Darriulat *et al.*, 1968; Bunker *et al.*, 1969) of the well-known resonance in ^{5}Li at an excitation energy of 16.7 MeV (corresponding to an incident proton energy of 23.39 MeV), measurements were made in small intervals of energy beteen 22 and 24 MeV in the overall energy range of 20—40 MeV. In this range, one encounters inelastic processes, the first inelastic threshold ($\alpha+p\rightarrow d+{}^3$He) being at the c.m. energy of 18.35 MeV, and the phase shifts have to be regarded as complex. Plattner *et al.* made a three-channel R-matrix parametrization of the $D_{3/2}$ phase shifts over the p-^{4}He resonance corresponding to the second excited state of ^{5}Li. The three channels considered were (1) $p+{}^4$He ($l=2$, $s=\frac{1}{2}$), (2) $d+{}^3$He ($l=0$, $s=\frac{1}{2}$), and (3) $d+{}^3$He ($l=2$, $s=\frac{1}{2}$ and $\frac{3}{2}$). The real parts of the phase shifts as well as the absorption or inelastic parameters extracted for all the states from $s_{1/2}$ to $g_{9/2}$ are shown in Table III and are plotted in Figs. 6 and 7. As can be seen from these figures, the phase shifts of Plattner *et al.* match very well with the previous values below 20 MeV and above 40 MeV. A look at the $d_{3/2}$ phase shift in the vicinity of 23.39 MeV shows its rapid variation pointing to the $\frac{3}{2}^+$ second state of ^{5}Li. The improved level parameters obtained for this state were $E_R=23.39$ MeV, corresponding to the second excited state, $\gamma_1^2=122$ keV,

TABLE VI. R-matrix parameters of Dodder *et al.* (1977).

	E_1 (MeV)	γ_1 (MeV)	E_2 (MeV)	γ_2 (MeV)
$s_{1/2}$	27.56	2.083		
$p_{1/2}$	3.296	4.655	1000.0 (fixed)	28.99
$p_{3/2}$	−8.73	4.70	1000.0 (fixed)	25.55
$d_{3/2}$	30.2	3.01		
$d_{5/2}$	29.6	3.15		
$f_{5/2}$	100.0 (fixed)	7.47		
$f_{7/2}$	100.0 (fixed)	8.66		

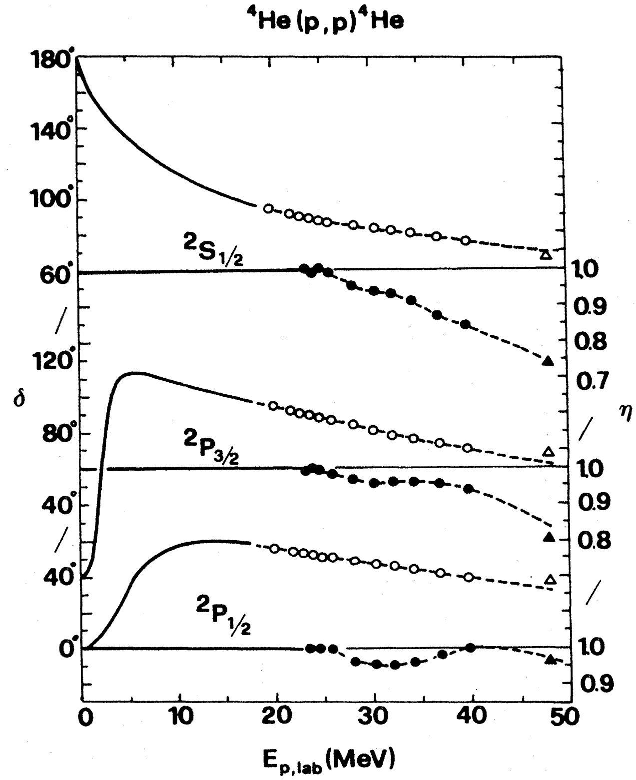

FIG. 6. s- and p-wave phase shifts for p-^{4}He elastic scattering (Plattner *et al.*, 1972). The open and the solid circles are the results of Plattner *et al.* for the real parts δ and the absorption parameter η, respectively. The solid lines below 18 MeV represent the energy-dependent set of phase shifts of Schwandt *et al.* (1971). The triangles at 48 MeV are the results of Davies *et al.* (1967).

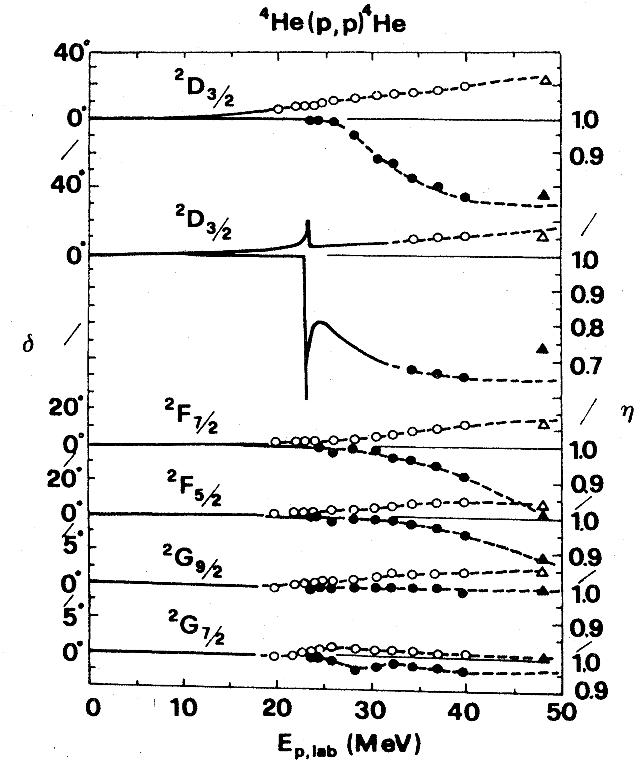

FIG. 7. d-, f-, and g-wave phase shifts for p-^{4}He elastic scattering (Plattner *et al.*, 1972); symbols as in Fig. 6.

$\gamma_2^2=-1580$ keV, $\gamma_3^2=1580$ keV, $\theta_1^2=0.014$, $\theta_2^2=0.765$, $\theta_3^2=0.765$, where 1, 2, and 3 refer to the channels considered earlier in the R-matrix analysis, and θ^2 is the ratio of the reduced width γ^2 to the Wigner limit $(3\hbar^2/2Ma^2)$; the channel radii used were $a_1=3$ fm, $a_2=5$ fm, and $a_3=5$ fm.

The most striking feature of the phase shifts of Plattner *et al.* was that they saw a dominant absorption in even l waves above the inelatic threshold of about 23 MeV. This is in sharp contrast with the analysis of Ramavataram *et al.* (1971), wherein rapid variation of both the $s_{1/2}$ and $d_{5/2}$ phase shifts had been found and were interpreted as evidence for the existence of two excited states around 20 MeV in ^{5}Li with $J^\pi=\frac{1}{2}^+$ and $\frac{5}{2}^+$. An unsatisfactory feature of the phase shifts of Plattner *et al.* was that below 26 MeV their predicted values of the absolute cross section were, on the average, 7—8 % higher than the experimental values. This discrepancy might be due to the inconsistencies of their data used for normalization. Also, there was no information on reaction cross section and hence no direct constraints could be placed on the inelastic parameters.

Thus, with a view to improving the available p-α data, Houdayer *et al.* (1978) measured p-α elastic scattering angular distributions at 13 energies between 20 and 55 MeV. The absolute scale of these measurements had an uncertainty of less than 2.5%. Their measurements were made, wherever possible, at the same energies as the polarization angular distributions of Bacher *et al.* (1972). These data, along with the angular distributions of differential cross section and analyzing power from selected references, were examined, and single-energy continuous phase shifts through G waves were obtained up to 45 MeV. These phase shifts, shown in Fig. 8, are not in striking disagreement with the ones of Plattner *et al.*, and we have included in Table III those phase shifts of Houdayer *et al.* which were obtained at energies higher than the ones considered by Plattner *et al.* The definition of χ^2 used by Houdayer *et al.* had been different from that [Eq. (2.1)] used in other analyses and has been explained at the bottom of Table III. The difference arises from the inclusion, in χ^2, of the total reaction data which were employed as a constraint on the imaginary parts of the phase shifts (Fig. 9).

The contour diagram of polarization of Houdayer *et al.* (Fig. 10) was based on the phase-shift solution of Plattner *et al.* up to and including the resonance region, on their own phase-shift solutions at higher energies and on an additional analyzing power angular distribution from Boschitz *et al.* (1965). This diagram shows the striking feature around the resonance region at 23.4 MeV

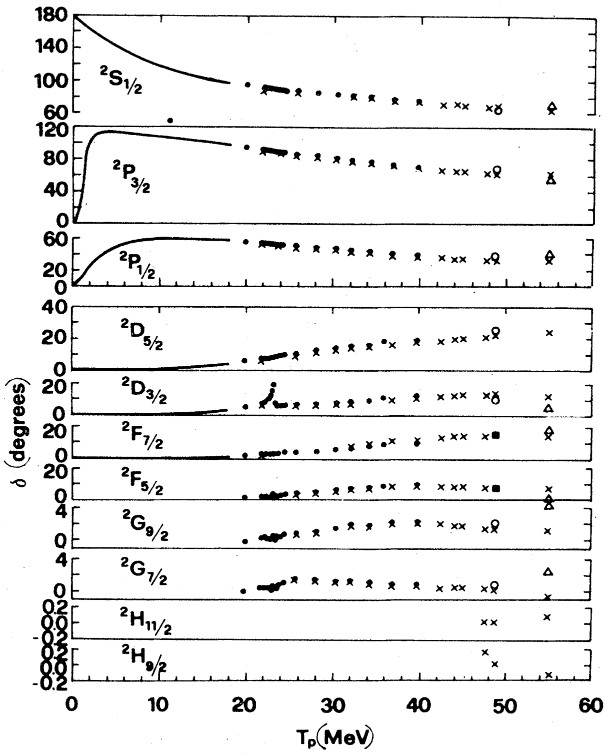

FIG. 8. Real parts of the *s*-, *p*-, *d*-, *f*-, *g*-, and *h*-wave phase shifts for p-^{4}He elastic scattering (Houdayer *et al.*, 1978). The crosses are the results of Houdayer *et al.* The solid lines below 18 MeV represent the energy-dependent phase-shift solution of Schwandt *et al.* (1971). The solid dots are the phase shifts of Plattner *et al.* (1972). The symbol ○ at 48.8 MeV is the result of Davies *et al.* (1967), and the triangle at 55 MeV is taken from the phase-shift analysis of Horikawa and Kanada (1965).

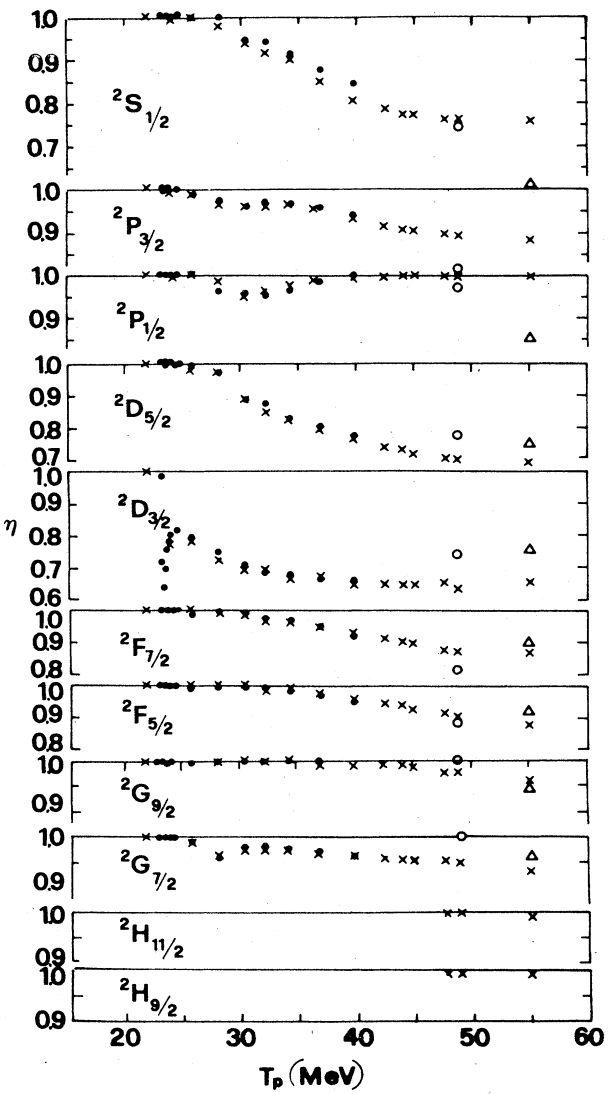

FIG. 9. Absorption parameters of the *s*-, *p*-, *d*-, *f*-, *g*-, and *h*-wave phase shifts for p-^{4}He elastic scattering (Houdayer *et al.*, 1978); symbols as in Fig. 8.

for the $d_{3/2}$ state, observed earlier by Plattner *et al.* The analysis of Houdayer *et al.* also supports the earlier finding that absorption is strong in even partial waves. They also obtained some improvement above 45 MeV with the inclusion of an h wave contribution. Thus with this analysis the p-α work in the energy region 20—55 MeV has been further strengthened.

The n-α work in the same region is, however, not very rich because of obvious experimental difficulties, namely, because of the lack of a calibrated source of polarized neutrons and by uncertainties in the properties of neutron polarization analyzers. In fact, the cross-section and polarization analysis of Hoop and Barschall (1966), which gives n-α phase shifts from 6 to 30 MeV was till recently the oft-quoted work. The field received further important inputs from the analyses, among others, of Broste *et al.* (1972), who made polarization measurements from 11.0 to 30 MeV, of Lisowski *et al.* (1976), who measured analyzing power from 20 to 30 MeV, and more recently of York *et al.* (1983), whose analyzing power measurement at 50.4 MeV confronted with that of Imai *et al.* (1979) at about the same energy, providing the first opportunity of comparing p-^{4}He and n-^{4}He analyzing power above 30 MeV. Hoop and Barschall's phase shifts below 22 MeV have already been shown in Table IV. We did not include their higher energy phase shifts in the present energy region, because Broste *et al.* in the analysis of their polarization measurements at 11.0, 17.1, 23.8, 25.7, 27.3, and 30.3 MeV observed that there are significant differences at the higher energies between actual experimental values for $P(\theta)$ and the predictions for $P(\theta)$ of the previously existing n-^{4}He scattering phase shifts. Broste *et al.* subjected these new polarization data along with other published cross-section and polarization measurements to a phase-shift analysis and claimed to have obtained an improved set of phase shifts above 20 MeV (shown in Table IV and Fig. 11). That such an improvement was necessary is evident from a plot of their polarizations at various energies (Fig. 12) where a comparison of their data with those obtained from the phase shifts of Hoop and Barschall indi-

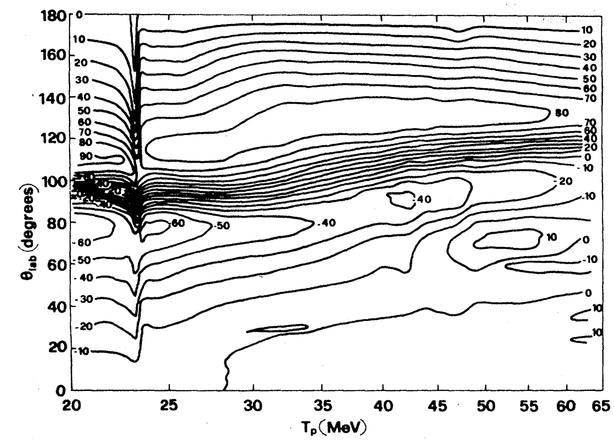

FIG. 10. Analyzing power contour diagram for p-^{4}He elastic scattering as function of energy, between 20 and 65 MeV, based on the phase-shift analyses of Plattner *et al.* (1972) and Houdayer *et al.* (1978) and on the data of Boschitz *et al.* (1965). [Figure from Houdayer *et al.* (1978).]

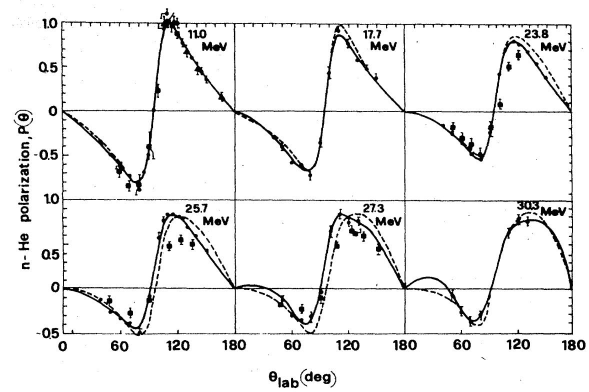

FIG. 12. Comparison of n-^{4}He polarization data (Broste *et al.*, 1972) with phase-shift solutions. The solid circles are the polarization data of Broste *et al.* The solid curves represent the predictions from their single-energy phase-shift solutions. The dashed curves are the predictions of polarization from the data of Hoop and Barschall (1966). The solid squares represent the data of May *et al.* (1963) at 10 and 23.7 MeV and of Arifkhanov *et al.* (1965) at 25 and 27.8 MeV; the solid triangles are the data of Büsser *et al.* (1966) at 12 MeV.

cate that the polarization predictions of previous phase-shift sets are found to be inadequate above 23 MeV. On the other hand, the single-energy phase-shift solutions of Broste *et al.* provided a better description of the polarization data and showed a smooth energy dependence up to 25.7 MeV. However, the phase-shift solutions at 27.3 and 30.3 MeV were rather poorly defined and the χ^2 values in the fits were rather on the higher side; the solution at 30.3 MeV was extrapolated from lower energy and could not claim uniqueness.

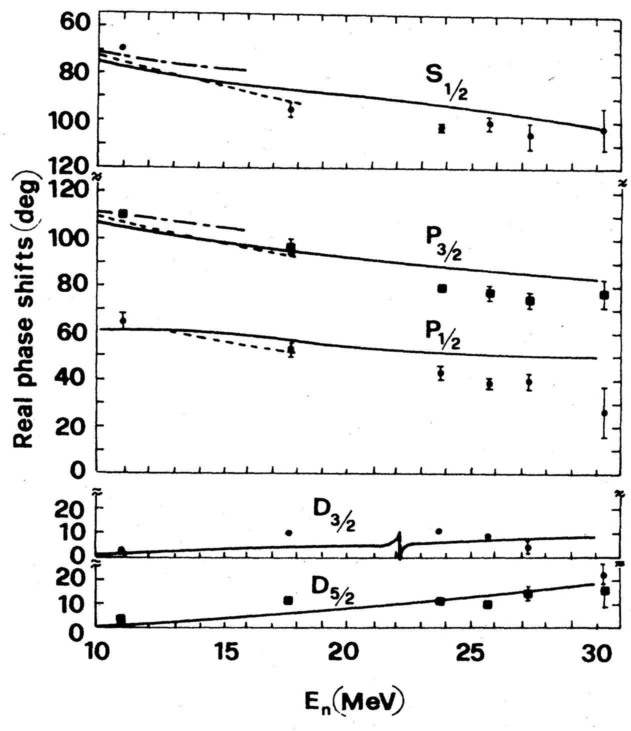

FIG. 11. Comparison of selected single-energy n-^{4}He phase-shift solutions (Broste *et al*, 1972). The data points represent the results of Broste *et al.* The solid curve is from Hoop and Barschall (1966). The dotted-dashed curve is from Arndt and Roper (1970), and the dashed curve is from Satchler *et al.* (1968).

Later, Lisowski *et al.* (1976), using the ^{3}H$(d,n)^4$He reaction as a calibrated polarized neutron source, measured the neutron analyzing power of ^{4}He$(n,n)^4$He from 20 to 30 MeV. They, for the first time, compared n-^{4}He data with the p-^{4}He data of Bacher *et al.* in this energy region and provided the first illustration of the equality of the analyzing powers of n-^{4}He and p-^{4}He scattering.

Above 30 meV, the n-α polarization measurements have been practically nonexistent. A limited set of asymmetry measurements was provided at 30.4 MeV by Arifkhanov *et al.* (1965), and very recently York *et al.* (1983) measured the n-^{4}He analyzing power at 50.4 MeV. This measurement again provided a further opportunity to make comparisons with p-^{4}He data and obtain a test of charge symmetry. The problem here was that the experiments were not done at the same energy; also, the Coulomb effects and neutron-proton mass differences between the p-^{4}He and n-^{4}He systems have to be accounted for. York *et al.* handled this problem through the mechanism of a phase-shift analysis. Their problem was that in order to obtain a set of n-^{4}He phase shifts at their energy of measurement, they needed a larger number of data sets. Assuming charge symmetry, these they obtained from the p-α data of Imai *et al.* (1979), who made p-α polarization and cross-section measurements at about the same energy (52 MeV) and a few other energies (45, 60, and 65 MeV). Saito (1979) made a phase-shift analysis of the data of Imai *et al.*, which we shall discuss below when we consider p-α data for proton energies over 50 MeV. By comparing their results for analyzing power and differential cross section (shown in Fig. 13) with the nearest 52.3-MeV data of Imai *et al.*, York *et al.* obtained good agreement when Coulomb correction to the phase shift was considered. According to the suggestion of Hoop and Barschall, the neutron and proton data should be compared at the c.m. energies equally displaced from the energies of the respective mass-5 excited states. Taking this into account, we note that the n-^{4}He polarization data of York *et al.* should have been strictly compared with p-^{4}He data at a laboratory energy of 51.7 MeV. Since the energy of 52.3 MeV is not too far from this, the similarity of n-^{4}He and p-^{4}He data, as is revealed by a comparison at this energy, is indeed quite impressive.

More recently, there has been a phase-shift analysis by Fröhlich *et al.* (1982) in an attempt to predict n-^{4}He phase shifts from p-^{4}He data between 20 and 55 MeV. The authors applied effective two-body Coulomb corrections to R-matrix n-^{4}He phase shifts below 20 MeV, obtaining charge symmetric phase shifts that were qualitatively consistent with the R-matrix p-^{4}He phase shifts. Above 20 MeV, the inverse procedure was followed—i.e., by applying Coulomb correction, n-^{4}He phase shifts were obtained from p-^{4}He phase-shift solutions. For energies between 20 and 30 MeV, the predicted n-^{4}He phase shifts seemed to be compatible with the available n-^{4}He data. In view of the fact that the n-^{4}He scattering data above 30 MeV are very sparse, it would indeed by very interesting to analyze the future n-^{4}He scattering data on the basis of firmly established p-^{4}He data.

Summarizing the experimental results for p-α and n-α scattering in the three regions (0—10, 10—20, and 20—50 MeV), we see that the measurements of nucleon-alpha differential scattering cross sections and polarization have been continually improved and we now have access to a significant amount of accurate p-α data, although the need for more n-α data in the higher energy side (> 30 MeV) is greatly felt. On the whole, the data for the ^{4}He$(p,p)^4$He and the ^{4}He$(n,n)^4$He reactions have not only

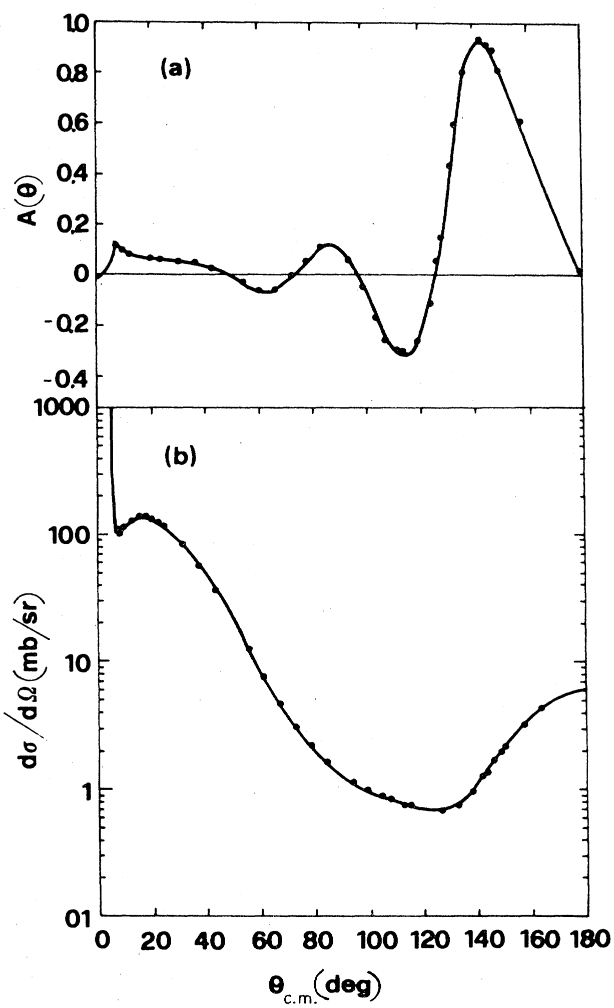

FIG. 13. (a) Analyzing power and (b) differential cross-section data of Imai *et al.* (1979) for the elastic scattering of 52.3-MeV protons from ^{4}He (York *et al.*, 1983). The solid curves represent the results of the phase-shift analysis of York *et al.*

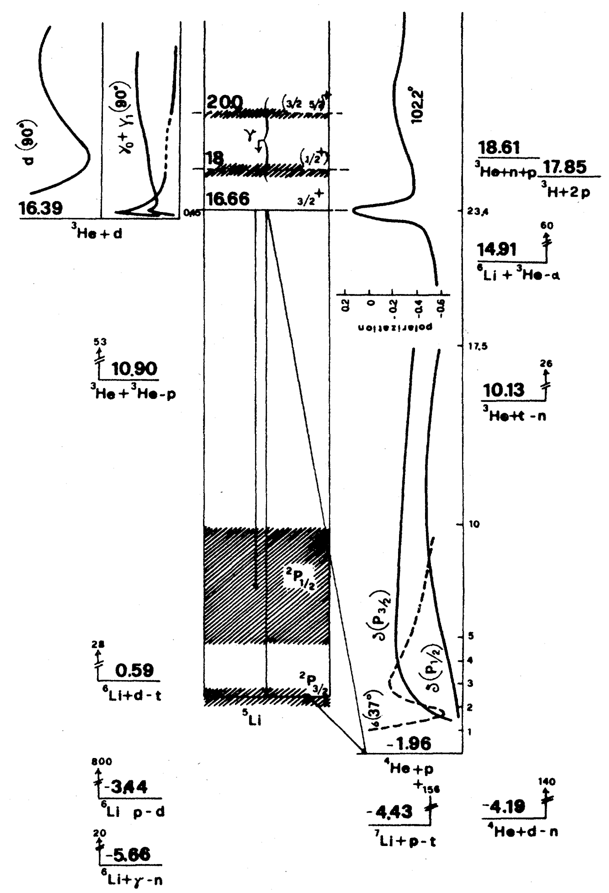

FIG. 14. Energy levels of ^{5}Li (Ajzenberg-Selove, 1984).

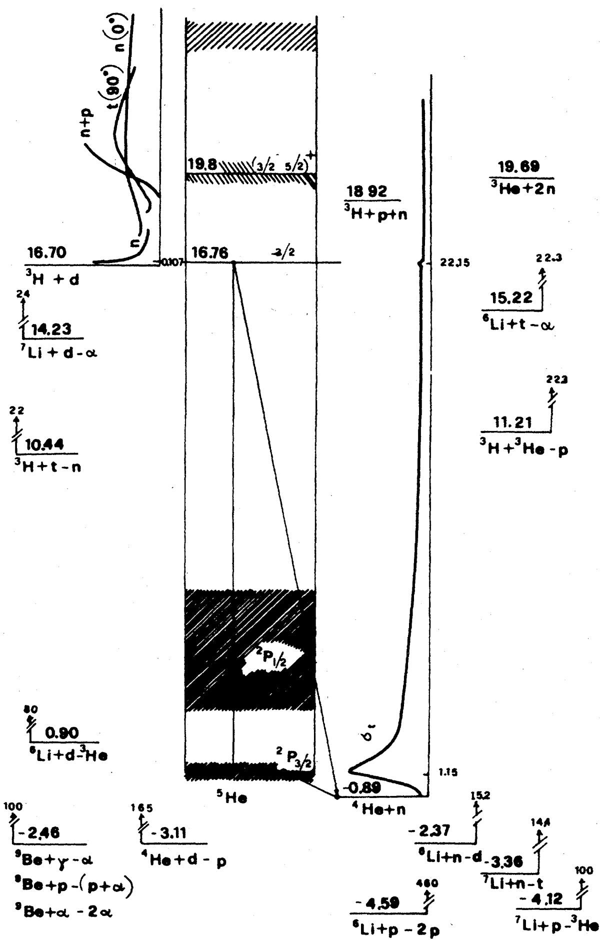

FIG. 15. Energy levels of ^{5}He (Ajzenberg-Selove, 1984).

created a suitable experimental basis for the understanding of the nucleon-α interaction but have also provided valuable inputs in the construction of the energy-level diagrams of ^{5}Li and ^{5}He (Figs. 14 and 15; see Tables VII and VIII for the energy-level parameters of ^{5}Li and ^{5}He, respectively). Other reactions which have been used for observing the levels in these nuclei have been discussed in detail by Ajzenberg-Selove (1984). As far as the informational content of nucleon-alpha scattering for level studies is concerned, it is found that the ground state of ^{5}He ($J^\pi=\frac{3}{2}^-$) can be reached at a neutron energy of about 1 MeV and manifests itself as a resonance in the $P_{3/2}$ phase shifts. A few MeV upwards, there is a broad state in ^{5}He, as is indicated by the $P_{1/2}$ phase shifts. A second resonance is observed at $E_n=22.15$ MeV corresponding to the excitation energy of 16.7 MeV of the $J^\pi=\frac{3}{2}^+$ state. In n-α scattering, one notices this state as resulting in a rapid variation with energy of the $D_{3/2}$ phase shifts. Beyond these three states, the n-α phase shifts vary smoothly with energy.

Concerning the relevance of the ^{4}He$(p,p)^4$He data to the level studies in ^{5}Li, we can see that the p-α $P_{3/2}$ phase shifts show a pronounced resonance corresponding to the 2.3-MeV ($J^\pi=\frac{3}{2}^-$) ground state of ^{5}Li. The slow variation of the $P_{1/2}$ phase shifts over a range of several MeV suggests that the first excted state ($\frac{1}{2}^-$) is very broad and is seated 5—10 MeV above the ground state. The reduced widths of the p-wave resonances are nearly the same. Thus the ground and first excited states of ^{5}Li are pure single-particle states consisting of a P-wave proton in the potential well of a closed s-shell α particle. This is borne out by the fact that the p-^{4}He s-wave phase shifts are accounted for by repulsive hard-sphere interaction scattering. The evidence for the second excited level in ^{5}Li ($J^\pi=\frac{3}{2}^+$) at 16.7 MeV excitation energy is obtained from the p-α phase-shift analysis below 50 MeV. A striking anomaly is observed in the analyzing power contour diagram for p-^{4}He elastic scattering at $E_p=23$ MeV and the $d_{3/2}$ phase shifts clearly show the $\frac{3}{2}^+$ state. The other phase shifts—$s_{1/2}$, $p_{1/2}$, $p_{3/2}$, $d_{5/2}$, $f_{5/2}$, $f_{7/2}$, $g_{7/2}$, and $g_{9/2}$—vary smoothly with energy. Absorption takes place mainly in the even partial waves, particularly in the $d_{3/2}$ and $d_{5/2}$ partial waves. The $p_{3/2}$ and $p_{1/2}$ inelastic parameters in the phase-shift analysis of p-α scattering show a somewhat anomalous behavior around an incident proton energy of 30 MeV; the absorption first increases and then decreases to stay rather constant at $E_p>40$ MeV. These results seem to be consistent with broad and overlapping states with $J^\pi=\frac{1}{2}^-$ and $\frac{3}{2}^-$ at excitation of $E_x\sim22$ MeV in ^{5}Li, which were predicted by Heiss and

TABLE VII. Energy levels of ^{5}Li.

E_x (MeV)	$J^\pi;T$	$\Gamma_{\text{c.m.}}$ (MeV)	Decay	Reactions	References
g.s.	$\frac{3}{2}^-;\frac{1}{2}$	$\simeq1.5$	p,α	^{4}He$(p,p)^4$He plus other reactions	Ajzenberg-Selove (1984)
5—10	$\frac{1}{2}^-;\frac{1}{2}$	5 ± 2	p,α	^{4}He$(p,p)^4$He plus other reactions	
16.66 ± 0.07	$\frac{3}{2}^+;\frac{1}{2}$	$\simeq0.3$	$\gamma,p,d,{}^3$He$,\alpha$	^{4}He$(p,p)^4$He plus other reactions	
18 ± 1	$(\frac{1}{2})^+;\frac{1}{2}$	broad	$\gamma,p,d,{}^3$He$,\alpha$	other reactions	
20.0 ± 0.5	$(\frac{3}{5},\frac{5}{2})^+;\frac{1}{2}$	$\simeq5$	$\gamma,p,d,{}^3$He$,\alpha$	other reactions	

TABLE VIII. Energy levels of ^{5}He.

E_x (MeV)	$J^\pi;T$	$\Gamma_{\mathrm{c.m.}}$ (MeV)	Decay	Reactions	References
g.s.	$\frac{3}{2}^-;\frac{1}{2}$	0.60±0.02	n,α	^{4}He$(n,n)^4$He plus other reactions	Ajzenberg-Selove (1984)
4±1	$\frac{1}{2}^-;\frac{1}{2}$	4±1	n,α	^{4}He$(n,n)^4$He plus other reactions	
16.76±0.13	$\frac{3}{2}^+;\frac{1}{2}$	0.10±0.05	γ,n,d,t,α	^{4}He$(n,n)^4$He plus other reactions	
19.8 ±0.4	$(\frac{3}{2},\frac{5}{2})^+;\frac{1}{2}$	2.5 ±0.5	n,d,t,α	other reactions	
24—25		broad		other reactions	

Hackenbroich (1971) and were explained as nucleon-^{4}He* (0^+ first excited state of ^{4}He) cluster structures. f-wave phase shifts show little splitting of real phase shifts up to 40 MeV, and there is only an indication from the $g_{7/2}$ phase shifts of a $\frac{7}{2}^+$ level around $E_p \approx 29$ MeV (corresponding to an excitation of 21 MeV). Above 40 MeV the phase shifts show smooth behavior as a function of energy. This behavior persists as will be clear in our discussion of the N-α data over 50 MeV.

The measurement of the analyzing power of n-^{4}He scattering in the (20—30)-MeV region by Broste *et al.* and Lisowski *et al.* and its comparison with the analyzing power of p-^{4}He scattering by Lisowski *et al.* would seem to provide, together with the same comparison by York *et al.* at 50.4 MeV, further experimental support for the charge symmetry hypothesis of nuclear forces.

4. 50 MeV and above

The n-α scattering experiments above 50 MeV are extremely limited in number, as can be seen from Table II. Of these, the one that has measured polarization and has been phase-shift-analyzed for both analyzing power and differential scattering cross section is that of York *et al.* (1983), which we have earlier discussed. The situation is a little better for p-α scattering; there, also, the number of experiments in the (50—100)-MeV range is limited, although a large number of experiments at high energies including the GeV region have been performed.

The recent p-α data crossing 50 MeV have been the ones of Imai *et al.* (1979) whose angular distributions of cross section and polarization at 45, 52, 60, and 65 MeV were measured in order to investigate the behavior of the phase shifts in an extended energy range. In particular, the measurements were made over a wide range of angles (between 15° and 160° lab), including the Coulomb interference region. The relative uncertainties of the analyzing power measurements were typically ±0.01. These measurements provided an accurate proton polarization analyzer up to 65 MeV. Interestingly, the analyzing power near $\theta_{\mathrm{c.m.}} = 140°$ exceeded 90% at all energies and showed very little energy dependence not only in shape but also in absolute value. Saito (1979) made a combined analysis of these analyzing power and cross-section measurements, in which $l = 0$—5 partial waves were considered. The analysis also made use of the experimental and theoretical information on total reaction cross section from the work of Sourkes *et al.* (1976) and Cairns *et al.* (1964). The results of this analysis did not agree with the contemporary results of Houdayer *et al.* and the ones of Plattner *et al.*, whose phase shifts, Saito noted, could not reproduce the analyzing power data of Imai *et al.* These phase shifts agreed roughly with those of Saito below 40 MeV but differed at higher energies. However, it should be pointed out that the phase-shift analysis of Saito produced at least two sets of phase shifts between 39.80 and 59.6 MeV and four sets at 64.9 MeV (values given in their paper). Although all of these sets reproduced equally well the experimental data of Imai *et al.*, the various phase-shift solutions were considerably different from each other and none could be uniquely established on its own merit. The difference was prominent in the absorption parameters also. Thus it is not at all obvious how far the comparison of the phase-shift sets of Saito with those of previous analyses would be of significance. It is to be further noted that the values of the spin rotation parameter calculated by Saito at given energies varied drastically at larger angles and at higher energies for the different phase-shift sets. This may provide a clue. An accurate experimental determination of the spin-rotation parameter together with precise measurements of more analyzing powers between 60 and 65 MeV, and studies of inelastic processes could presumably resolve the problem.

The next higher-energy p-α data below 100 MeV considered by us are the ones of Perez-Mendez *et al.* (1969). They measured the analyzing power of p-α elastic scattering at 70 and 80 MeV and made a phase-shift analysis based on their data, the polarization measurements at 63 and 96 MeV (Gotow, 1959; Conzett, 1968), and the differential cross-section measurements at 66 and 94 MeV (Cormack *et al.*, 1959). In order to obtain solutions at their energies of measurement, they interpolated between the differential cross-section data at 66 and 94 MeV. The justification given was that the differential cross sections at 55, 66, 93, and 147 MeV, when plotted as functions of momentum transfer $q=2k\sin\theta/2$, are nearly congruent over q in the range of 0.4—3.0 fm^{-1}, i.e., from 10° to 100° in the center of mass. The α-p phase shift of Conzett at 55 MeV was used as the starting point. Although it was recognized that phase-shift solutions at isolated energies are not unique, Perez-Mendez *et al.* found only one set of solutions that was consistent with the results at lower energies and had a plausible energy dependence up to 94 MeV. These phase shifts and the associated absorption parameters (quoted in their text in radians) are shown in Table III (in degrees). At each energy, partial waves up to $l=5$ were considered. The phase shifts obtained at the four energies are consistent with each other apart from being compatible with the results at lower energies. The s-wave phase shifts remain practically constant at $-135°$; the $p_{1/2}$ phase shift continues its gradual downward trend from resonance; the d phases stay within 10°—20°; the higher l phase shifts are small. Thus a slow variation of the phase shifts with energy is observed.

Above 100 MeV, a large number of p-α elastic scattering experiments have been performed at proton energies ranging from a few tenths of a GeV to a few GeV's. These experiments form a useful part of the overall program for hadron-nucleus scattering at intermediate and high energies. For the case of proton-nucleus scattering, the definition of intermediate energies can follow from the physical features of the N-N interaction, the lower limit of the energies being the onset of pion production and the upper being the disappearance of isobar resonances. The objective of performing the intermediate- and high-energy proton-nucleus scattering is to shed light on the mechanisms of interaction and, more specifically, to probe matter over very small intervals of space and time. Highly energetic particles traverse matter for extremely short periods of time. The questions that arise are the following: What structure of the target matter do these energetic probes see? Do they interact with the nucleus as a whole or individually with each one of its constituents? Also, at these energies, nucleons can actually "do" things which they can do only virtually inside the nucleus. Again, the question is, which of the suppressed degrees of freedom appear to make themselves felt in the interaction mechanisms? The helium nucleus, being a spin-isospin saturated, tightly bound spherically symmetric structure, serves as an applicational ground for testing some of the ideas in high-energy proton-nucleus scattering and for judging the adequacy of the theoretical tools in dealing with them.

The first high-energy proton-α scattering experiment was done at BNL at 1 GeV by Palevsky *et al.* (1967), who observed a deep diffraction minimum in their angular distribution data. A second measurement made at Saclay at 1.05 GeV by Baker *et al.* (1974) did not show the deep minimum in the BNL data; their dip was a shallow one (see Fig. 27 below). These two expeirments stimulated a lot of interest in both experimental and theoretical work on high-energy proton-α scattering. The BNL and the Saclay groups tried to understand each others' data better. The original Saclay data (referred to in the literature as *Saclay A*) was normalized to the Brookhaven data at small angles. Later, a normalized version of those data (Saclay B) has appeared in the literature (Aslanides *et al.*, 1977) with its own absolute normalization. These new data are in reasonable agreement with the Brookhaven experiment except for the deep dip reported earlier. The results of the BNL and the Saclay experiments initiated a large number of other high-energy p-α scattering experiments, covering a wide spectrum of s (total c.m. energy) and a wide range of t (square of the four-momentum transfer). These experiments exhibited a diffraction minimum or dip in the diffential scattering cross section. The structure is more pronounced at higher energies. A number of theoretical investigations have been made in order to understand the shape of the differential cross sections. A very good account of the experimental and theoretical work until 1978 has been given by Igo (1978) in a review of some intermediate and high-energy proton-nucleus research. Since then, a number of experiments at even higher energies have been performed and more theoretical investigations made. All these experiments have been listed in Table I and some of the latest analyses briefly reviewed in the section on the basic studies of the alpha-nucleon interaction.

III. PHENOMENOLOGICAL STUDIES OF ALPHA-NUCLEON INTERACTION

After having discussed the nucleon-alpha scattering data we now propose to deal with the phenomenological potentials that have been constructed so far from these data. A number of analyses have, in fact, been made of the low-energy scattering of nucleons from ^{4}He in terms of both local and nonlocal two-body interactions having central and spin-orbit terms.

A. Local phenomenological alpha-nucleon potential

We start with the post-1950 period, when more and more α-N data were becoming available. Blanchard *et al.* (1950), Blanchard and Avery (1951), and Adair (1951,1952) suggested that the alpha-nucleon interaction could be looked upon as a one-body interaction, i.e., with the nucleon moving in the average potential of the closed-shell core of the α-particle. They postulated a central and spin-orbit force between the nucleon and the α-particle. This idea gained support from the work of Mayer (1949,1950) and of Haxel *et al.* (1949) and from that of Koester *et al.* (1951). Hochberg (1953) used a square-well potential of the form

$$V=(1+\beta\boldsymbol{l}\cdot\boldsymbol{\sigma})V(r)\ ,$$

with

$$V(r)=\begin{cases} V_0 & \text{for } r<a \\ 0 & \text{for } r>a \end{cases},$$

and found a good fit to the experimental s- and p-wave phase shifts with

$$V_0=-70.9 \text{ MeV}, \quad a=2.5 \text{ fm}, \quad \text{and} \quad \beta=0.15 .$$

Earlier Bürgel (1952) found the best-fit values of $V_0=-33.0$ MeV, $a=2.55$ fm, and $\beta=0.103$, using similar calculation to that of Hochberg. Sack *et al.* (1954) fitted the $P_{1/2}$ and $P_{3/2}$ p-α phase shifts up to 10 MeV by using a central potential along with a Thomas-type spin-orbit interaction which is a derivative of the central part. Their potential had the form

$$V(r)=\left[1-\beta \mathbf{l}\cdot\boldsymbol{\sigma}\frac{1}{r}\frac{d}{dr}\right]f(r),$$

where $\beta=(\alpha/4)(\hbar/mc)^2$ and α is a parameter.

For $f(r)$, exponential Gaussian, and square-well shapes were used. The Gaussian well was found to give an overall good fit to the experimental phase shifts. It was also observed that the exponential well gave a splitting increasing too rapidly with energy while the square well gave splitting increasing rather slowly with energy. The parameters for the central part of the Gaussian potential

$$V_c(r)=-V_0\exp(-K^2r^2)$$

were $V_0=47.32$ MeV, $K^2=0.17$ fm^{-2}, and $\beta=7.4(\hbar/mc)^2$. Feingold (1956) used the variational method to calculate the splitting of the p-α doublet for Gaussian and Yukawa potentials. He found that for a reasonable choice of the nuclear radius the splitting was within an order of magnitude of the experimental value.

Herzenberg and Squires (1960) also used the Gaussian interaction to describe the p-α scattering at 40 and 90 MeV, taking into consideration the effects due to the antisymmetry of the incident and bound nucleons, incoherent multiple scattering, and the distortion of the incident plane wave and of the nuclear wave function. For the nuclear potential, they took

$$V_{ij}=-f(r_{ij})(V_0+V_\sigma\boldsymbol{\sigma}_i\cdot\boldsymbol{\sigma}_j+V_\tau\boldsymbol{\tau}_i\cdot\boldsymbol{\tau}_j + V_{\sigma\tau}\boldsymbol{\sigma}_i\cdot\boldsymbol{\sigma}_j\boldsymbol{\tau}_i\cdot\boldsymbol{\tau}_j),$$

with $f(r_{ij})=\exp(-\beta r_{ij}^2)$; $\beta=0.37$ fm^{-2}.

The other parameters were adjusted to give a singlet-even strength $V_0-3V_\sigma+V_\tau-3V_{\sigma\tau}=37$ MeV and a triplet-even strength $V_0+V_\sigma-3V_\tau-3V_{\sigma\tau}=62$ MeV. Experimental values of the singlet scattering length and effective range and the triplet scattering length were reproduced well with these parameters. Though the fitting was not very good, the calculated differential cross section showed the qualitative features of p-α scattering at 40 and 90 MeV. Herzenberg and Squires were aware of the fact that the nuclear potential they used was rather too simple and should have contained a repulsive core. However, they gave arguments suggesting that the tail of the nuclear potential gave the principal effects in this problem at least for forward angles while the effect of the repulsive core was probably important at larger angles when the exchange effects predominated. It was concluded that to give a qualitatively correct account of p-α scattering around 100 MeV it was necessary to include the effects due to both nucleon exchange and target distortion.

Assuming a two-body effective potential, Gammel and Thaler (1958) obtained a precision fit to both s- and p-wave phase shifts below 9 MeV. The angular distributions of 40 and 17.5 MeV protons scattered off helium were calculated with the following potential:

$$V(r)=\begin{cases} +\infty, & r\le r_c \\ -[V_c(r)+V_{LS}(r)\mathbf{L}\cdot\mathbf{S}], & r>r_c \end{cases},$$

where

$$V_c(r)=\frac{V_c}{1+(r/D-1)\exp[(r-R)/D]},$$

$$V_{LS}(r)=-\frac{D^2}{r}V_c(r)\left[\frac{V_{LS}}{V_c}\right].$$

At 40 MeV this potential with

$$R=2.0 \text{ fm}, \quad D=1.0 \text{ fm}, \quad V_{LS}=22.5 \text{ MeV}$$

gave

$$\delta(s_{1/2})=-110^\circ, \quad \delta(P_{3/2})=82^\circ, \quad \delta(P_{1/2}=58.9^\circ)$$

with

$$r_c=0.183 \text{ fm} \quad \text{and} \quad V_c=46.6 \text{ MeV}$$

and

$$\delta(s_{1/2})=-105^\circ$$

with

$$r_c=0.5 \text{ fm} \quad \text{and} \quad V_c=-55.4 \text{ MeV}.$$

The analysis was also done at 17.5 MeV, and it was found that the potential strength $V_c(r)$ was energy dependent and different in odd and even angular momentum states. An interesting feature of $\delta(s_{1/2})$ phase shifts was observed, namely, that almost the same values of $\delta(s_{1/2})$ were produced by central potentials with very different strengths and signs. This was also obvious later from the analysis of Pearce and Swan (1966), who obtained phase-equivalent potentials from s- and p-wave scattering for n-α scattering up to 12 MeV using a potential shape of the type

$$V(r)=\sum_\rho U_\rho\exp(-r/\rho b).$$

They observed that there was practically no difference between the phase shifts calculated by the barrier solution or by a well solution for the s wave. For example, a 2.5-GeV repulsive barrier with a radius of 1.2 fm gave the same phase shifts as that given by a 2.1-GeV well with a radius of 1.2 fm. Thus the inner part of the potential cannot really be determined from the low-energy phase shifts over a rather limited interval. A similar situation has also been observed for nonlocal separable N-α potentials (see Sec. III.B). This observation is also consistent with a later calculation of Swan (1967), who observed that the phase/binding energy equivalent of an n-α potential in the s state should have a Pauli barrier $3\hbar^2/\mu r^2$ MeV arising from the exclusion principle. Swan used a distorted inverse square barrier wave approximation and deduced from experimental phase shifts an entirely repulsive potential for $l=0$ phase shifts.

So far we have discussed only real phenomenological potentials for nucleon-alpha scattering. Complex potentials have also been used in describing the α-N system. Bunch *et al.* (1964) applied an optical model analysis for p-α scattering with 31-MeV protons to test the validity of the optical model for a tightly bound light nucleus like ^{4}He and to get information on ^{4}He$(p,d)\,^3$He reaction cross sections. The analysis was carried out with a potential

$$V_{\text{opt}}=V_{\text{CN}}+V_{\text{SO}}+V_{\text{Coul}} ,$$

where V_{CN} and V_{SO} were, respectively, the complex central and spin-orbit potentials, and the Coulomb potential V_{Coul} was that corresponding to a uniformly charged sphere of radius R. The real part of V_{CN} was defined according to Nodvic *et al.* (1962):

$$\text{Re}(V_{\text{CN}})=-Vf(r)$$

with

$$f(r)=\left[1+\exp\left[\frac{r-R}{a}\right]\right]^{-1} , \quad R=R_0A^{1/3} ,$$

and its imaginary part was taken to be

$$\text{Im}(V_{\text{CN}})=-W_1\exp[-(r-R)^2/b^2] - W[1+\exp(r-R)/0.69b] ,$$

which accounted for both volume and surface absorption. The spin-orbit potential was taken to be

$$V_{\text{SO}}=-\left[\frac{\hbar}{m_\pi c}\right]^2(V_s+iW_s)\left[\frac{1}{r}\right]\frac{df}{dr}\sigma\cdot l .$$

Fits to the elastic scattering cross-section data were made by minimizing the values of χ^2. The minimum values of χ^2 were obtained for values of R_0 betwen 1.1 and 1.3 fm, and accordingly several sets of optical model parameters were obtained. A typical set is, for example,

$$R_0=1.2 \text{ fm}, \quad a=0.284 \text{ fm} , \quad b=0.9 \text{ fm} ,$$

$$V=48.8 \text{ MeV} , \quad W=4.0 \text{ MeV} , \quad W_1=-1.0 \text{ MeV} ,$$

$$V_s=-5.2 \text{ MeV} , \quad \sigma_R \ (\text{fm}^2)=6.91 , \quad \chi^2=166.9 .$$

An attempt on the line of the above analysis was made for just one energy and it seemed to indicate that the optical model might reasonably describe the scattering of nucleons from as light a nucleus as ^{4}He. Later an extensive analysis of nucleon-alpha scattering below the inelastic threshold was carried out by Satchler *et al.* (1968) using real optical potentials of Saxon-Woods shape. This potential is often quoted in the literature. The potential has the form

$$U(r)=U_N(r)+U_C(r) ,$$

where

$$U_N(r)=-V(e^x+1)^{-1} + \left[\frac{\hbar}{m_\pi c}\right]^2 V_s\mathbf{L}\cdot\boldsymbol{\sigma}\frac{1}{r}\frac{d}{dr}(e^{x_s}+1)^{-1} ,$$

and U_c is the Coulomb potential from a uniformly charged sphere of radius R_C, so $U_C=0$ for neutron scattering:

$$x=\frac{r-R}{a} , \quad x_s=\frac{r-R_s}{a_s}$$

$$R=r_0\left[\frac{M_\alpha}{M_p}\right]^{1/3} , \quad R_s=\left[\frac{M_\alpha}{M_p}\right]^{1/3} r_s .$$

Several sets of parameters were given. The parameters which gave the best compromise fits to the experimental data (differential scattering cross sections and polarizations) were the following:

$$V_n=41.8 \text{ MeV (for neutrons)} ,$$

$$V_{sn}=(3.0+0.1E_n) \text{ MeV} ,$$

$$V_p=43.0 \text{ MeV (for protons)} ,$$

$$V_{sp}=(2.7+0.1E_p) \text{ MeV} ,$$

$$r_0=(1.50-0.01E) \text{ fm} ,$$

$$r_s=1.0 \text{ fm} ,$$

$$a=a_s=0.25 \text{ fm} .$$

Figures 16 and 17 give the p-α and n-α phase shifts, respectively, calculated with the above parameters. These parameters were found to be energy dependent and were chosen to give good fit near the resonance region, i.e., around 1.2 MeV for E_p and E_n. It was found that the s-wave phase shifts were affected more by changes in the strength of the central potential V than by changes in r_0 and that they were affected hardly at all by changes in a. Though the p-wave phases were affected by the changes in spin-orbit parameter, they were less affected by changes in a. It was found that these parameters were no different from the optical model parameters of other nuclei. Although the analysis of Satchler *et al.* up to 20 MeV with a real Saxon-Woods form gave an adequate representation of the experimental data, it would seem interesting to perform the analysis for higher energies, as well, which could give information about the imaginary part of the potential. In fact, such an extension was made by Thompson *et al.* (1970) for p-α scattering at 31, 40, 46, and 55 MeV with a potential of the form

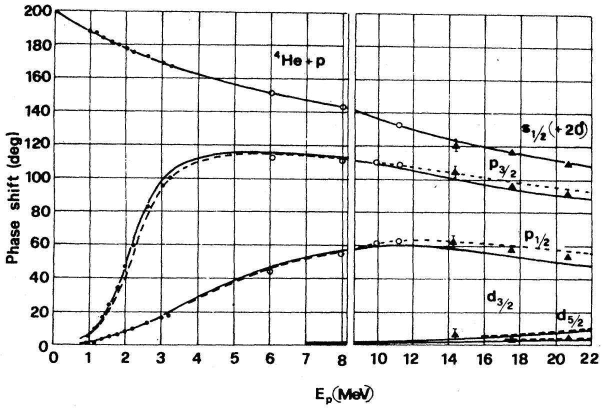

FIG. 16. The optical-model p-α phase shifts as a function of proton energy (Satchler *et al.*, 1968). The solid curve is the calculation of Satchler *et al.* for the optical parameter set described in the text. The dashed curve is for the reduced value of $V_p = 42.8$ MeV. The dotted curve corresponds to the radius $r_0 = 1.475 - 0.007E_p$. The experimental phase shifts (circles and triangles) are taken from Brown *et al.* (1967) and from Weitkamp and Haeberli (1966), respectively.

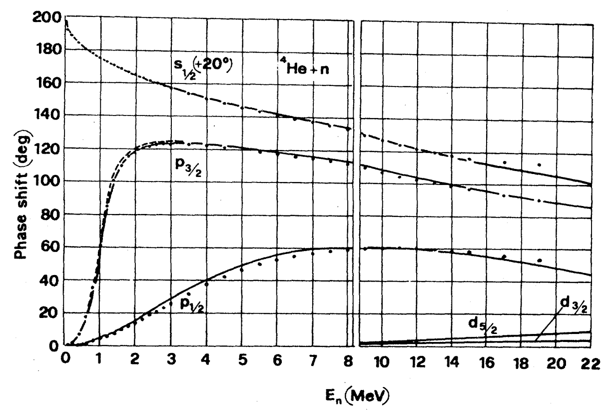

FIG. 17. The n-α optical-model phase shifts as a function of neutron energy (Satchler *et al.*, 1968). The solid curve is the calculation of Satchler *et al.* with the optical parameter set described in the text. The dashed curve is for the increased value of $V_n = 41.9$ MeV. The dots are the phase-shift values of Morgan and Walter (1968).

$$U(r) = V_c(r) - V(e^x+1)^{-1} - i\left[W - 4W_1\frac{d}{dx_1}\right](e^{x_1}+1)^{-1} + \left[\frac{\hbar}{m_\pi c}\right]^2 \sigma\cdot l(V_s + iW_s)\frac{1}{r}\left[\frac{d}{dr}\right](e^{x_{\rm SO}}+1)^{-1},$$

where

$$x = \frac{r - r_0 A^{1/3}}{a},$$

$$x_1 = \frac{r - r_1 A^{1/3}}{a_1},$$

and

$$x_{\rm SO} = \frac{r - r_{\rm SO} A^{1/3}}{a_{\rm SO}}.$$

A search was made for an optimum set of optical model parameters which would give best values for the differential cross-section and polarization data. The energy dependence of the central part was found from the relation $V = 74 - 0.57E$ MeV. While the imaginary part, the spin-orbit part, and the radius also showed some energy dependence, the calculated real phase shifts seemed to follow the trend of the low-energy data, and the inelastic parameter $[= e^{2i\delta} = |\eta| \exp(2iR_e\delta)]$ was found to be evenly distributed among various partial waves. An optical potential with an exchange term given by

$$U(r) = V(k,r) + iW(k,r) + (-1)^l W_{\rm ex}(k,r) + V_{\rm SO}(k,r)$$

was used by Goldstein *et al.* (1970) to analyze the scattering of 100-MeV protons off ^{4}He and specifically to investigate the backward peak in the angular distribution. The other parts of the potential consisted of a real part of the familiar Woods-Saxon type, possessing a variable radius, diffuseness, and strength. A spin-orbit interaction of the standard form was included and possessed the same radius and diffuseness as the real part. Parameters which gave the best fit were

E (MeV)	V (MeV)	W (MeV)	a (fm)	b (fm)	R (fm)	$V_{\rm SO}$ (MeV)	$W_{\rm ex}$ (MeV)	$a_{\rm ex}$ (fm)	χ^2
31.0	61.6	5.5	0.05	0.42	1.55	7.8	4.9	0.32	1.1
40.0	65.8	13.5	0.54	0.24	1.55	4.3	5.8	0.22	2.7
55.0	46.2	19.5	0.56	0.13	1.74	6.9	−3.2	0.44	14.0
100.0	1.9	14.8	0.24	0.42	1.67	8.4	0.65	0.66	3.8

The agreement with the experimental data was very good, indicating that the backward peak might be due to exchange phenomena. Although one may wonder whether it is permissible to use the optical model shape for the exchange term, it is found that in the Born-approximation calculation their structures are the same and differ only by $(-1)^l$ factor.

Though the magnitudes of the exchange potentials for diferent energies were reasonable, the negative value at 55 MeV was difficult to explain. The analyses at 31, 40, and 55 MeV were done for comparison of results for optical potential with or without an exchange term by Bunch *et al.* and Thompson *et al.*, and it was found that the agreement was quite good. Although there have not been many significant optical-model analyses of low-energy nucleon-alpha scattering since that of Satchler *et al.*, such analysis has recently been extended to intermediate-energy p-^{4}He scattering. This will be discussed in Sec. IV together with Glauber theory, another tool employed in high-energy p-α scattering.

B. Nonlocal potentials for alpha-nucleon interaction

So far we have dealt with local phenomenological nucleon-alpha potentials. As we will shortly see in Sec. IV the basic studies of N-α interactions starting from first principles show that these interactions, when constructed from two-body N-N forces, are nonlocal as well as l and energy dependent. Phenomenologically, however, it has been possible to admit of energy-dependent local N-α interactions. Nevertheless, it would seem interesting to introduce phenomenological nonlocal separable (NLS) potentials to describe the N-α interaction. Considerable interest has recently been aroused in the studies of N-α systems using NLS potentials. Although the nonlocality of N-α potentials is an accepted feature, its separability remains an ansatz. For certain special shapes of the two-body N-N forces (e.g., Gaussian), the nonlocal N-α interaction can presumably be recast in the same manner as the α-α interaction, using Hille's formula (Leung and Park, 1969), as the sum of a very large number of separable terms. However, in practice, one usually employs a finite rank separable potential. Thus the separability of the nonlocal N-α interaction still remains a convenient assumption. The interest in separable interaction has further been enhanced because of the ease with which three-body problems involving N-α interactions can be tackled. Till recently, all the analyses of N-α data with nonlocal separable interaction were made in momentum representation. The first such analysis was performed for neutron-alpha scattering by Mitra *et al.* (1962). They considered the s- and p-wave interactions and found that the spin-orbit potential was much smaller than the central potential. Their attractive s-wave interaction admitted a bound state. The next attempt was by Barguil *et al.* (1971), who studied the elastic scattering of nucleons off ^{4}He below 22 MeV using a one-term separable potential based on their method (Pigeon *et al.*, 1970). Using a form factor of the Yukawa type, they reproduced the neutron-alpha and proton-alpha s- and p-wave phase shifts up to 20 MeV rather accurately. Later, they extended their analyses up to 50 MeV, by making the interaction complex (Pigeon *et al.*, 1971). It is known that an adequate description of p-α phase shifts needs to take into account the Coulomb interactions in an exact way. This can be done both in the coordinate and in the momentum representations. Although Pigeon *et al.* calculated the Coulomb effect exactly in the momentum representation, their analyses were rather involved. This effect can be accounted for in a much simpler way in the coordinate representation (Ali *et al.*, 1972,1974; Rahman *et al.*, 1974). A typical outline of their method (Ali *et al.*, 1972) is given below. One added advantage of using the coordinate representation is that for a given nonlocal separable potential one may have some insight into the corresponding local potential obtained by a suitable prescription.

C. Method

The nonlocal Schrödinger equation with Coulomb forces may be written as

$$\left[\frac{d^2}{dr^2}+k^2-\frac{l(l+1)}{r^2}-\frac{2nk}{r}\right]\psi_l(r)=\int_0^\infty K_l(r,r')\psi_l(r')dr' \tag{3.1}$$

following the usual notation.

If $K_l(r,r')$ is separable and is of the type

$$K_l(r,r')=\sum_{l=1}^{N}\lambda_l^i g_l^i(r)g_l^i(r') , \tag{3.2}$$

the solution of Eq. (3.1) is

$$\psi_l(r)=F_l(r)+\sum_{i=1}^{N}a_l^i Z_l^i(r) , \tag{3.3}$$

where $F_l(r)$ and $Z_l(r)$ satisfy the equations

$$\left[\frac{d^2}{dr^2}+k^2-\frac{l(l+1)}{r^2}-\frac{2nk}{r}\right]F_l(r)=0 , \tag{3.4}$$

$$\left[\frac{d^2}{dr^2}+k^2-\frac{l(l+1)}{r^2}-\frac{2nk}{r}\right]Z_l^i(r)=\lambda_l^i g_l^i(r) \tag{3.5}$$

with boundary conditions

$$\begin{aligned} &F_l(0)=0 ,\\ &Z_l^i(0)=0 ,\\ &Z_l^i(r)\underset{r\to\infty}{\to}\frac{\lambda_l^i}{k}G_l(r)\int_0^\infty F_l(r)g_l^i(r)dr . \end{aligned} \tag{3.6}$$

The functions $F_l(r)$ and $G_l(r)$ are the regular and irregular Coulomb wave functions, respectively.

From the asymptotic form of $\psi_l(r)$ one obtains

$$\tan\delta_l=-\frac{1}{k}\sum a_l^i C_l^i \lambda_l^i \tag{3.7}$$

and

$$\sum_{j=1}^{N}(\delta_{ij}-\tau_l^{ij})a_l^j=C_l^i , \tag{3.8}$$

where

$$\tau_l^{ij}=\int_0^\infty g_l^i(r)Z_l^j(r)dr \tag{3.9}$$

and

$$C_l^i=\int_0^\infty g_l^i(r)F_l(r)dr . \tag{3.10}$$

The formal solution of Eq. (3.5) is

$$Z_l^i(r)=\lambda_l^i\int_0^\infty G_l(r,r')g_l^i(r')dr' ,$$

with

$$G_l(r,r')=\begin{cases}\frac{1}{k}F_l(r)G_l(r') & r'>r\\ \frac{1}{k}F_l(r')G_l(r) & r'<r .\end{cases}$$

With this formulation, analyses have been done for proton-alpha and neutron-alpha scattering by Ahmad *et al.* (1975) and Rafiqullah *et al.* (1975), respectively. Figures 18 and 19 give the calculated phases of Ahmad *et al.* together with the experimental phase shifts. For the above analyses a one-term potential was chosen with a form factor of simple exponential type

$$K_l(r,r')=\lambda_l g_l(r)g_l(r')$$

with

$$g_l(r)=r^l e^{-\alpha r} .$$

The above one-term separable potential was found to be quite adequate in describing the elastic scattering of nucleons off helium, especially for p-α scattering, where higher partial waves up to $l=3$ were fitted accurately; and for n-α scattering the equivalent local potentials were

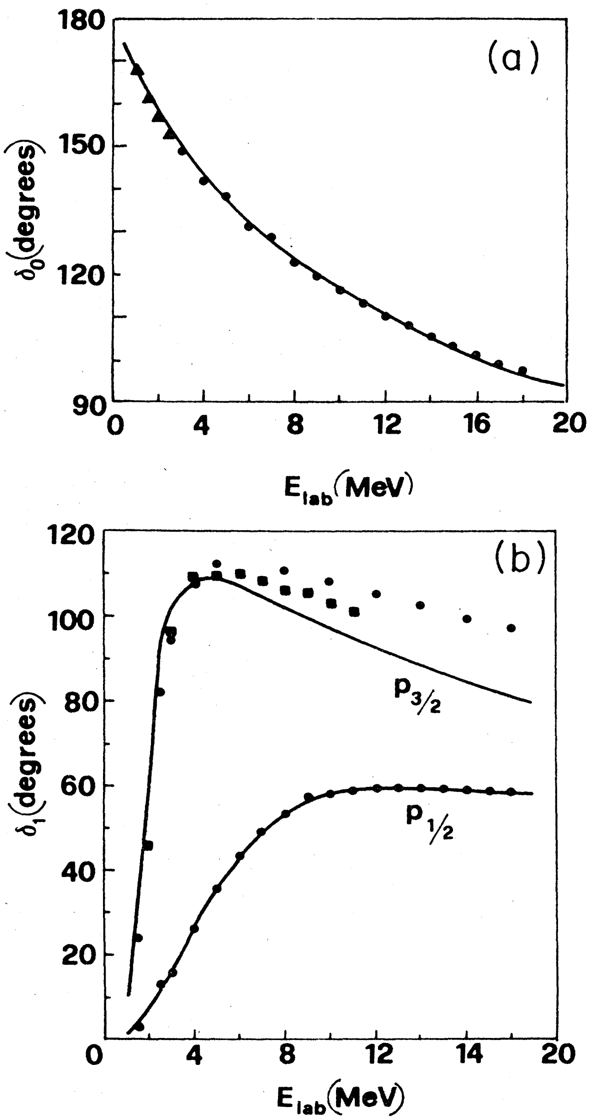

FIG. 18. (a) s-wave and (b) p-wave p-α phase shifts obtained by Ahmad *et al.* (1975) with the use of the nonlocal separable potential described in the text. The experimental points are denoted by triangles (▲) taken from Brown *et al.* (1967), dots (●) taken from Schwandt *et al.* (1971), and squares (■) taken from Barnard *et al.* (1964). The best-fit parameters were $\lambda_0=-6.5$ fm^{-3}, $\beta_0=0.8$ fm^{-1} (for $s_{1/2}$), $\lambda_1=-0.8$ fm^{-5}, $\beta_1=1.25$ fm^{-1} (for $p_{1/2}$), and $\lambda_1=-11.25$ fm^{-5}, $\beta_1=1.25$ fm^{-1} (for $p_{3/2}$ phase shifts).

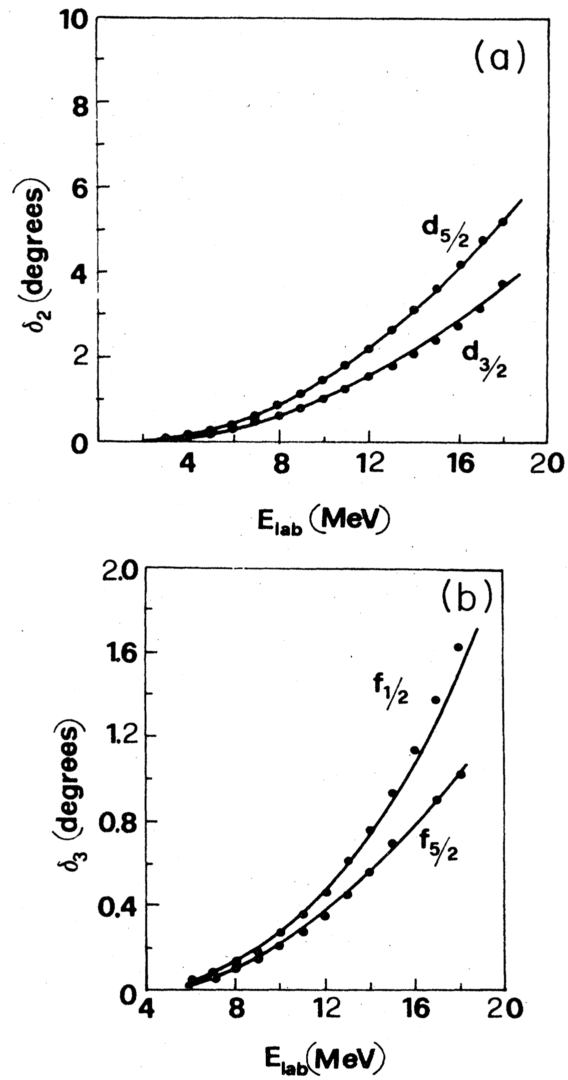

FIG. 19. (a) d-wave and (b) f-wave p-α phase shifts obtained by Ahmad *et al.* (1975) with the use of a nonlocal separable potential. The best-fit parameters were $\lambda_2=-33.0$ fm^{-7}, $\beta_2=2.0$ fm^{-1} (for $d_{3/2}$), $\lambda_2=-43.0$ fm^{-7}, $\beta_2=2.0$ fm^{-1} (for $d_{5/2}$), $\lambda_3=-12.0$ fm^{-9}, $\beta_3=2.0$ fm^{-1} (for $f_{5/2}$), and $\lambda_3=-15.0$ fm^{-9}, $\beta_3=2.0$ fm^{-1} (for $f_{7/2}$ phase shifts). The experimental phase shifts were taken from Schwandt *et al.* (1971).

also calculated using the prescription of Husain and Ali (1970). One of the most interesing features which was observed in the behavior of s-wave phase shifts with different strengths of potential was that equally good fitting for an s-wave could be obtained with an attractive potential of strength $\lambda_0=-6.5$ fm^{-3} and $\beta_0=0.8$ fm^{-1} and with repulsive potential of strength $\lambda_0=17.0$ fm^{-3} and $\beta_0=0.39$ fm^{-1} (Fig. 20), which implies that it is virtually impossible to distinguish between attraction and repulsion at lower energies, a point which we noted earlier in the discussion of the s-wave experimental phase shifts.

A separable potential approach to nucleon-nucleus scattering with the exact treatment of Coulomb effects was also made by Cattapan *et al.* (1975) in the Coulomb state representation using form factors of the modified Yukawa type $g_l(r)=\exp(-\alpha r)r^l/r$. In this work, Cattapan *et al.* considered the p-α as well as the n-α phase shifts for the energy region 0–5 MeV, where the details of the $\frac{3}{2}^-$ single-particle resonances are well evidenced. In spite of calculational differences, the results of Ahmad *et al.* and those of Cattapan *et al.* were consistent with each other.

More recently, in a folding model approach (in which projectile-nucleon interactions are folded into the nucleonic density distribution of the target to generate projectile-target potentials), Lee and Robson (1982) generated a nonlocal nucleon-nucleus optical potential by using a separable N-N potential in the folding procedure. In the case of n-^{4}He scattering, they used the Tabakin, the Doleschall, and the Strobel N-N potentials of Yukawa and Gaussian forms with variable parameters for each partial wave. Spin-orbit and tensor forces were included. Their resultant nonlocal potential, with the N-N potential fitted to the N-N data, reproduced the $s_{1/2}$ scattering well

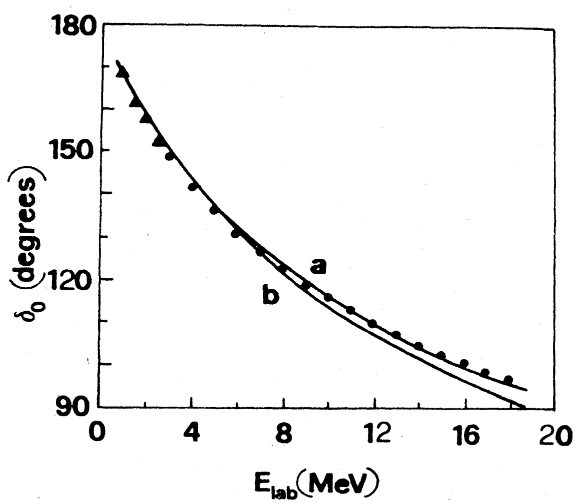

FIG. 20. s-wave phase shifts of p-α scattering calculated by Ahmad *et al.* (1975) by using (a) a purely attractive and (b) a purely repulsive nonlocal separable potential. The parameters of the purely repulsive potential were $\lambda_0=17.0$ fm^{-3}, $\beta_0=0.39$ fm^{-1}. The experimental phases are the ones of Brown *et al.* (1967) and Schwandt *et al.* (1971).

but failed to describe the $p_{1/2}$ and $p_{3/2}$ resonances. However, they had to consider the higher-order corrections (in the first order, the N-N interaction is actually the phenomenological N-N interaction) and introduce an effective N-N potential in the G-matrix concept in order to reproduce the $p_{1/2}$ and $p_{3/2}$ resonances.

IV. BASIC STUDIES OF THE ALPHA-NUCLEON INTERACTION

By *basic studies of the α-N interaction* we mean those studies which attempt to build an interaction between an α particle and a nucleon from rather first principles, using the two-nucleon interaction as the building block. Such microscopic studies have, in fact, been made more or less within the framework of the resonating group method (RGM) of Wheeler (Bransden and McKee, 1954; Hochberg *et al.*, 1954,1955; Van der Spuy, 1956; Sugie *et al.*, 1957; Nagata *et al.*, 1959; Lasker *et al.*, 1961; Kanada *et al.*, 1963a,1963b; Franco, 1968; Thompson *et al.*, 1969; Heiss and Hackenbroich, 1970,1971; Omojola, 1970; Reichstein and Tang, 1970; Thompson and Tang, 1971; Thompson *et al.*, 1972; Chwieroth *et al.*, 1974; Hackenbroich *et al.*, 1974; Thompson *et al.*, 1977).

A typical outline of the RGM as applicable to the α-N system is given below.

The wave function describing the scattering of a nucleon from an α particle is assumed, in the one-channel approximation (namely, pure elastic scattering), to be

$$\psi_{\alpha N}=\mathcal{A}[\varphi F(\mathbf{R}-\mathbf{r}_5)\xi(\sigma,\tau)] \ . \tag{4.1}$$

Here $\mathcal{A}$ is the antisymmetrization operator, ξ denotes the appropriate charge-spin function, φ describes the spatial behavior of the α cluster, and $F(r)$ describes the motion of the nucleon relative to the α cluster. If, for example, the two neutrons and the two protons in the α particle are labeled "particles 1 and 2" and "particles 3 and 4," respectively, and if the outside nucleon is denoted as "particle 5," then

$$\mathcal{A}=[1-H(15)-H(25)]$$

when the outside nucleon is a neutron, and

$$\mathcal{A}=[1-H(35)-H(45)]$$

when the outside nucleon is a proton. $H(15)$ is the Heisenberg exchange operator exchanging the space and spin coordinates of particles 1 and 5, and so on.

The basic idea, then, is to start from the antisymmetric wave function (4.1) and the total Hamiltonian of the system

$$H=-\frac{\hbar^2}{2m}\sum_{i=1}^{5}\nabla_i^2+\sum_{i<j=1}^{5}V_{ij} \ , \tag{4.2}$$

where V_{ij} is the two-nucleon force, and derive an equation of motion for $F(r)$, thereby reducing the five-body problem into a two-body one. This is usually accomplished by determining $F(r)$ from the variational principle:

$$\delta\int\psi^*(H-E')\psi d_\tau=0\ , \tag{4.3}$$

where E' is the total energy. The calculational scheme is as follows.

The function φ is usually assumed to be of the form

$$\varphi=\exp\left[-\frac{\alpha}{2}\sum_{i=1}^{4}(\mathbf{r}_i-\mathbf{R})^2\right], \tag{4.4}$$

where $\mathbf{R}$ is the position vector of the c.m. of the α cluster. The width parameter α is usually fixed by a fit to the rms radius of matter distribution of the alpha particle as observed from electron scattering data and is thus determined to be $\alpha=0.514$ for $\langle r^3\rangle^{1/2}=1.44$ fm.

For the nucleon-nucleon potential V_{ij}, generally a central Gaussian form with exchange terms is chosen:

$$V_{ij}=-V_0\exp(-\beta r_{ij}^2)(\omega+mP_{ij}^r+bp_{ij}^\sigma-hP_{ij}^\tau)+\frac{e^2}{4r_{ij}}(1+\tau_{iz})(1+\tau_{jz})\ , \tag{4.5}$$

with

$$w+m+b+h=1\ , \tag{4.5a}$$

$$w+m-b-h=x \text{ (ratio of singlet to triplet interaction)}\ . \tag{4.5b}$$

For values of $V_0=72.98$ MeV, $\beta=0.46$ fm^{-2}, and $x=0.656$, the potential (4.5) yields the correct values of the two-nucleon effective range parameters (Afzal and Ali, 1970).

With the above expressions for φ and V_{ij}, one now uses Eqs. (4.1) and (4.3) along with the partial-wave expansion

$$F(\mathbf{r})=\sum_l\frac{f_l(r)}{r}P_l(\cos\theta) \tag{4.6}$$

and obtains an integro-differential equation for $F_l(r)$

$$\left[\frac{\hbar^2}{2\mu}\left[\frac{d^2}{dr^2}-\frac{l(l+1)}{r^2}\right]+E-V_D(r)-V_c(r)\right]f_l(r)=\int_0^\infty K_l(r,r')f_l(r')dr'\ , \tag{4.7}$$

where $E=E'-E_\alpha$ (binding energy of the α particle) is the relative energy in the c.m. system. μ is the reduced mass of the α-N system. $V_c(r)$ is the Coulomb potential applicable to the α-proton system. $V_D(r)$ is the direct part of the α-N interaction (corresponding to no interchange between constituents of the α particle and the N). The term $k_l(r,r')$ is the nonlocal kernel interaction whose origin lies in the antisymmetrization of the wave function. Since the latter ensures that particles having the same spin and charge should not overlap appreciably, $k_l(r,r')$ does incorporate the general character of a repulsion. Equation (4.7) is solved numerically with proper boundary conditions for α-N scattering phase shifts using standard procedures (e.g., the method of finite differences). It should be noted that Gaussian shapes are assumed for φ and V_{ij} in order that the calculation of $k_l(r,r')$ be done analytically. The expression for $k_l(r,r')$ is a rather complicated one and is a function of w, m, b, h, V_0, β, α, and $E'(=E+E_\alpha)$. The ways of determining V_0, β, and α have already been mentioned. To determine w, m, b, and h one needs further relations between them besides Eq. (4.5a). Such relations are provided if one writes V_{ij} as a linear combination of the Serber potential V_{Serb} and the Rosenfeld potential V_{Rosen}

$$V=yV_{\text{Serb}}+(1-y)V_{\text{Rosen}}\ . \tag{4.8}$$

V_{Serb} and V_{Rosen} are given by Eq. (4.5) with $(w=m, b=h)$ and $(m=2b, h=2w)$, respectively. In calculations where specific distortion effects (i.e., distortion effects over and above what is implied by the antisymmetrization procedure) are not taken into account as a result of not using many channels or not using improved wave functions in the region of strong interactions, y is usually treated as an adjustable parameter in order to compensate for such omissions. With the admission of proper distortion effects, the value of y has been expected to be around unity. More discussion about it is given later.

Early one-channel RGM calculations of α-N scattering did not take into account the spin-orbit component of the α-N force needed to account for the splitting of the $p_{1/2}$ and $p_{3/2}$ phase shifts. These calculations [e.g., the ones of Thompson *et al.* (1969)] considered as baseline data the s- and p-wave phase shifts produced by the real part of the optical potential of Satchler *et al.* (1968), obtained from a phenomenological analysis of α-N scattering. A fair fit to these phase-shift data was obtained for $y=0.95$. A good fit required either a low value of y (around $y\approx0.65$) or an adjustment in the α value, from $\alpha=0.514$ fm^{-2} to $\alpha=0.43$ fm^{-2} for $y=0.95$. However, no physical meaning could be attributed to such *ad hoc* adjustments.

Later, one-channel RGM calculatons of Reichstein and Tang (1970) used a slightly improved N-N potential which had different depths and ranges in the singlet and triplet N-N interactions and had also a spin-orbit part:

$$V_{ij}=[\tfrac{1}{2}(1+P_{ij}^\sigma)V_t+\tfrac{1}{2}(1-P_{ij}^\sigma)V_s]\left[\frac{u}{2}+\tfrac{1}{2}(2-u)P_{ij}^\sigma\right]-V_\lambda\exp(-\lambda r_{ij}^2)(\mathbf{r}_i-\mathbf{r}_j)\times(\mathbf{p}_i-\mathbf{p}_j)\cdot(\boldsymbol{\sigma}_i+\boldsymbol{\sigma}_j)\frac{1}{2\hbar}+\frac{e^2}{4r_{ij}}(1+\tau_{iz})(1+\tau_{jz})\ , \tag{4.9}$$

where V_t and V_s are the s-wave triplet and singlet potentials assumed to be

$$V_t = -V_{0t}\exp(-K_t r^2) ,$$
$$V_s = -V_{0s}\exp(-K_s r^2) .$$

A fit to the N-N effective range parameters is obtained for $V_{0t}=66.92$ MeV, $K_t=0.415\ \mathrm{fm}^{-2}$, $V_{0s}=29.05$ MeV, and $K_s=0.292\ \mathrm{fm}^{-2}$. The parameter u is the exchange mixture parameter [i.e., the same as y in Eq. (4.8)]. u, V_λ, and λ were determined from a fit to α-N data. While the reason for treating u as a parameter has been given earlier, the use of V_λ and λ as free parameter would appear to be somewhat unsatisfactory. Nevertheless, Reichstein and Tang argue that since in the energy range considered only the s-wave N-N interaction is pertinent, the spin-orbit parameters cannot be determined from the s-wave data and hence are left free to be determined from α-N. Of course, a more desirable feature would be the introduction of a tensor interaction for the description of the $\frac{3}{2}^+$ resonance, especially for its decay into N-α, although the calculations would be somewhat complicated. However, Reichstein and Tang observed that without the spin-orbit term, their second potential (4.9) came closer, in a phase-shift fit, to the central part of the potential of Satchler *et al.* than the earlier potential (4.8). With this improved potential, Reichstein and Tang calculated the differential scattering cross section $d\sigma/d\Omega$, polarization P, and spin-rotation parameter β, the definitions of which are rewritten here for the sake of convenience:

$$\frac{d\sigma}{d\Omega}=|g|^2+|h|^2 ,$$
$$P=\frac{2\,\mathrm{Re}(g^*h)}{|g|^2+|h|^2} , \tag{4.10}$$
$$\beta=\arctan\left[\frac{2\,\mathrm{Im}(gh^*)}{|g|^2-|h|^2}\right] ,$$

where $g(\theta)$ and $h(\theta)$ are the spin-independent and spin-dependent scattering amplitudes

$$g(\theta)=f_c(\theta)+\frac{1}{k}\sum_l[(l+1)e^{i\delta_l^+}\sin\delta_l^+ + le^{i\delta_l^-}\sin\delta_l^-]e^{2i\delta_l}P_l(\cos\theta) ,$$
$$h(\theta)=\frac{i}{k}\sum_l(e^{i\delta_l^+}\sin\delta_l^+ - e^{i\delta_l^-}\sin\delta_l^-)\times e^{2i\delta_l}\sin\theta\frac{dP_l(\cos\theta)}{d\cos\theta} . \tag{4.11}$$

In (4.11) f_c is the pure Coulomb scattering amplitude and σ_l the Coulomb phase shift. δ_l^+ and δ_l^- are the nuclear phase shifts for $J=l+\frac{1}{2}$ and $J=l-\frac{1}{2}$, corresponding to whether l and s are parallel or antiparallel, respectively. Thus $|d\sigma/d\Omega|$, P, and β are computed from the numerical solution of the integro-differential equation obtained for the α-N system

$$\left[\frac{\hbar^2}{2\mu}\left[\frac{d^2}{dr^2}-\frac{l(l+1)}{r^2}\right]+E-V_D(r)-V_c(r)-\eta_{jl}V_{\mathrm{SO}}(r)\right]f_{jl}(r)=\int_0^\infty[k_l^N(r,r')+k_l^c(r,r')+\eta_{jl}k_l^{\mathrm{SO}}(r,r')]f_{jl}(r')dr' . \tag{4.12}$$

In (4.12), η_{jl} is defined by

$$\eta_{l+1/2,l}=l\ ,\quad \eta_{l-1/2,l}=-(l+1)\ ,\quad \eta_{1/2,0}=0\ .$$

$V_D(r)$, $V_C(r)$, and $V_{\mathrm{SO}}(r)$ are the direct parts of the nuclear central potential, the Coulomb potential, and the spin-orbit potential, respectively, and k_l^N, k_l^C, and k_l^{SO} denote the corresponding exchange contributions. Other symbols have the same meaning as in (4.7). In earlier calculations, only the direct Coulomb potential was considered. Anyway, the results of Reichstein and Tang indicated that the exchange Coulomb interaction plays a minor role—especially for the s-wave phase shifts—and thus its omission is not very serious. With the full nonlocal potential of Eq. (4.12), they performed calculations for a very wide range of values of u, V_λ, and λ. Finally, two sets (their sets I and III) emerged to be satisfactory:

	λ (fm^{-2})	V_λ (MeV)	u
set I	0.46	11.0	0.97
set III	2.0	224.8	0.95

Some typical plots of n-α and p-α phase shifts and also those of $d\sigma/d\Omega$ and P for p-α scattering for the above two sets are shown in Figs. 21—24.

These results suggest that a single-channel RGM calculation of the α-N interaction gives a moderate fit to the experimental results. More detailed fits, of course, would need taking into account the reaction channels in the calculations. One thus needs to do complete coupled-channel calculations, which are, however, rather involved. Thus as a first step towards taking care of the reaction channels, Thompson *et al.* (1972) incorporated into the RGM Eq. (4.12) a phenomenological imaginary potential W which included both a nonexchange component and a Majorana exchange (i.e., space exchange) component and had the form

$$W=(1+C_IP^r)U(r)\equiv[1+C_I(-1)^l]U(r) ,$$

where for the radial form $U(r)$, a Woods-Saxon volume plus surface term was used. The observation of Thompson *et al.* had been that above the α-p reaction threshold

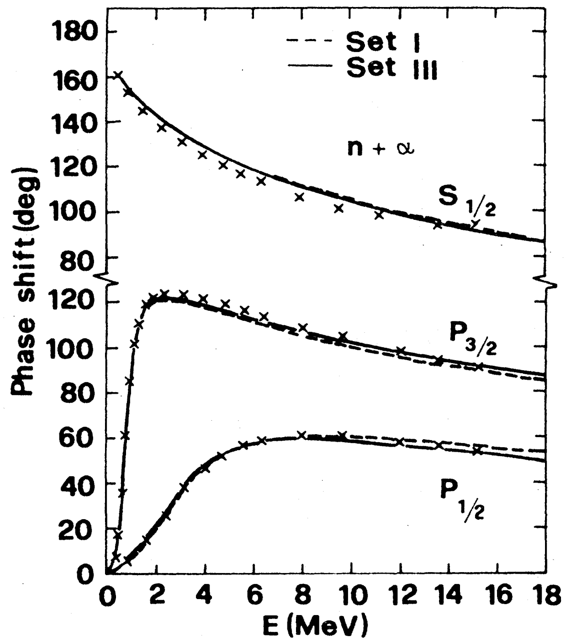

FIG. 21. Resonating group model (RGM) phase shifts for n-α scattering (Reichstein and Tang, 1970). The dashed line and the solid line correspond to their sets I and III described in the text. The data points represent the empirical phase shifts of Morgan and Walter (1968).

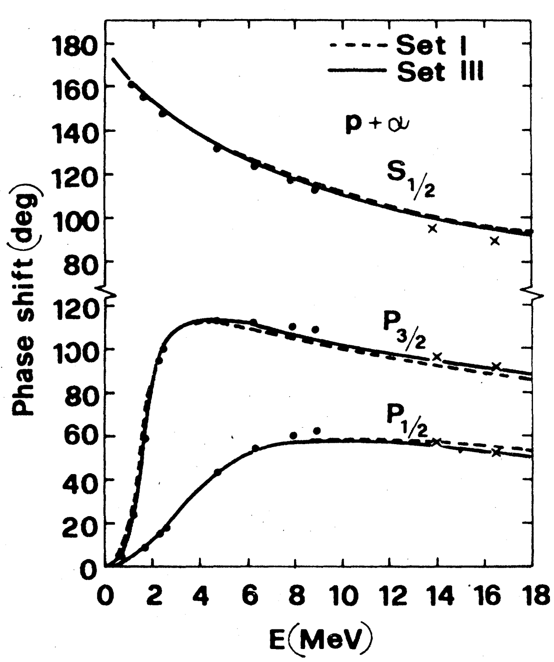

FIG. 22. RGM phase shifts for p-α scattering (Reichstein and Tang, 1970). The dashed line and the solid line correspond to their sets I and III, respectively. The data points represent the empirical phase shifts of Satchler *et al.* (1968), Brown *et al.* (1967), and Weitkamp and Haeberli (1966).

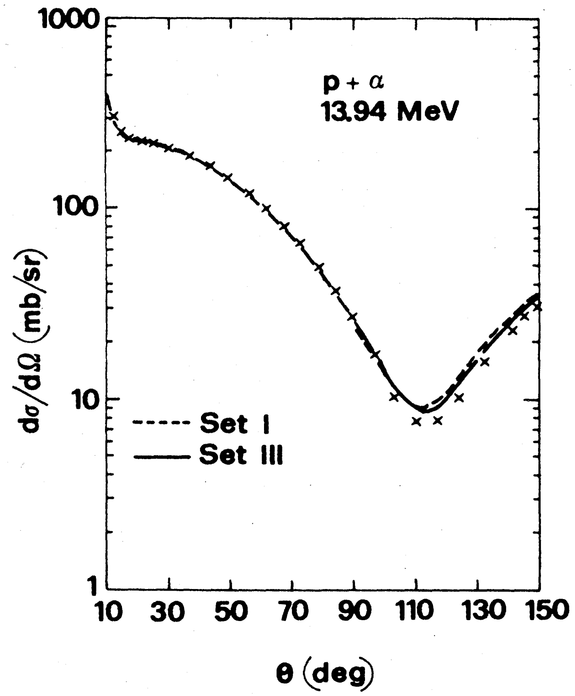

FIG. 23. Comparison of the RGM p-α differential scattering cross section calculation by Reichstein and Tang (1970) for their sets I and III with the experimental data at 13.94 MeV of Brockman (1956). [Figure from Reichstein and Tang (1970).]

of 18.35 MeV (c.m.) the experimental data on differential cross section, polarization, and the spin-rotation parameter in the energy range 23—75 MeV (c.m.) could be fitted rather satisfactorily except for some discrepancies in the

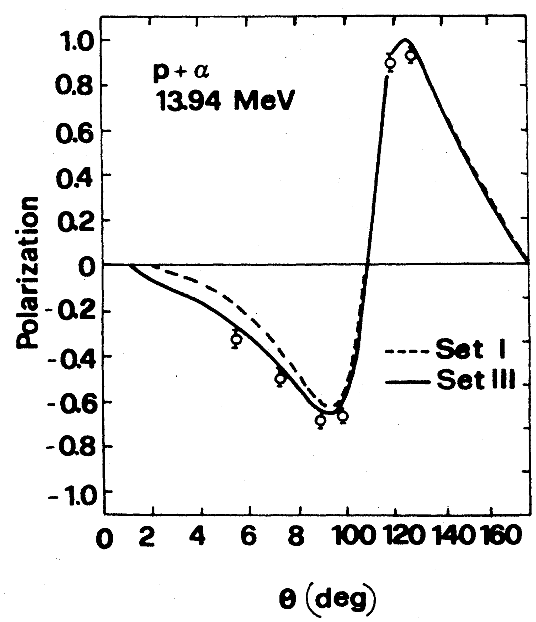

FIG. 24. Comparison of RGM calculation of p-α polarization with the experimental data of Weitkamp and Haeberli (1966) at 13.94 MeV (Reichstein and Tang, 1970).

forward angle polarization. It was also observed that at most energies the values of C_I were negative, indicating that the absorption is stronger in odd angular momentum states than in even. However, no physical interpretation could be given for the rather wide variation of the strength parameter C_I with energy. This, taken together with the fact that the above calculations were a combination of phenomenology of the optical-model type and basic studies of the RGM type, would seem to indicate that these first calculations of Thompson *et al.* could be regarded as a convenient parametrization of the effect of coupled reaction channels. However, encouraged by the success of these calculations, Chwieroth *et al.* (1974) made elaborate microscopic coupled-channel study of the five-nucleon system with the RGM, using the purely central two-nucleon potential, i.e., potential (4.9) without the spin-orbit term. Apart from knowing the influence of a second channel, the purpose of their calculations was also to explore the adequacy of the RGM in studying nuclear reactions in light systems. To this end, they included the channels $d+{}^3\text{He}$ (or $d+{}^3\text{H}$) and the $p+\alpha$ (or $n+\alpha$) channels in the five-nucleon system. Incidentally, it is worth mentioning that coupled-channel calculations for N-α scattering were, in fact, initiated by Lasker *et al.* (1961) and by Heiss and Hackenbroich (1971). However, the investigations of Chwieroth *et al.*, although having the essential content of earlier studies, were more comprehensive, in that they admitted a large number of partial waves which are experimentally warranted because of the diffuse structures, e.g., $d+{}^3\text{He}$ in the five-nucleon system. Also, the effects of three- and more-body breakup were not included in earlier calculations. Chwieroth *et al.* took account of these latter effects by incorporating into the formulation an imaginary potential. Thus the mathematical recipe involved in the RGM formulation of the coupled-channel study of the α-N system is practically the same as that described earlier for the one-channel case except that now one antisymmetrizes a two-component wave function describing the two channels and eventually obtains a pair of coupled integro-differential equations to solve for the wave function of relative motion of the p-α (or n-α) and d-${}^3\text{He}$ (or d-${}^3\text{H}$) systems. From a solution of the coupled equations the p-α and d-${}^3\text{He}$ scattering phase shifts are computed and so are $(d\sigma/d\Omega)(p+\alpha\rightarrow p+\alpha)$, $(d\sigma/d\Omega)(d+{}^3\text{He}\rightarrow d+{}^3\text{He})$, and also $(d\sigma/d\Omega)(p+\alpha\rightarrow d+{}^3\text{He})$ and $(d\sigma/d\Omega)(d+{}^3\text{He}\rightarrow p+\alpha)$. Now, the results Chwieroth *et al.* obtained by varying the parameters of the imaginary potential and again by treating the exchange parameter u as an adjustable one show that the p-α phase shifts are essentially unaffected by the addition of the $d+{}^3\text{He}$ channel. Also, they found that for the $p+\alpha$ and $d+{}^3\text{He}$ differential scattering cross sections the calculated values are in close agreement with experiment. However, for the $p+\alpha\leftrightarrows d+{}^3\text{He}$ differential reaction cross sections, the agreement is not very satisfactory. Also, since in this calculation only central forces are used, polarization data cannot be reproduced. Thus the RGM description of the α-N interaction in the coupled-channel version with central forces seems to be only generally satisfactory. Further refinements could include, among other things, the coupling between the spin-$\frac{1}{2}$ and spin-$\frac{3}{2}$ channels through the introduction of noncentral components in the nucleon-nucleon potential. Such refinements have subsequently been made, although within the framework of a somewhat different cluster model reaction theory, by Hackenbroich *et al.* (1974), who calculated elastic α-p scattering below 30 MeV using a nucleon-nucleon potential which contained spin-orbit and tensor forces and had been successfully employed in reaction calculations for other light systems. They obtained quantitative agreement for their α-p cross-section and polarization values with experimental data.

More recently the result of a RGM p-α phase shift calculation using both $p+\alpha$ and $d+{}^3\text{He}$ channels but with the inclusion of spin-orbit and tensor forces was reported by Wildermuth and Tang (1977). They pointed out that the single-channel $d+{}^3\text{He}$ calculation of Chwieroth *et al.* (1973) showed $4s_{3/2}$ resonance level occurring very near the $d+{}^3\text{He}$ threshold and a refinement in the $p+\alpha$ single-channel calculation should take into account the $d+{}^3\text{He}$ channel with the relative orbital angular momentum between the clusters equal to 0 and total spin equal to $\frac{3}{2}$. It is no wonder that central and spin-orbit potentials cannot effect any coupling between the $p+\alpha$ channel, having $l=2$ and $s=\frac{1}{2}$, and the $d+{}^3\text{He}$ channel, having $l=0$ and $s=\frac{3}{2}$; tensor force is needed. The results of the calculation with both central and spin-orbit and tensor forces, as reported by Wildermuth and Tang, are shown in Fig. 25, where a comparison of the calculated phase shifts with the experimental point of Plattner *et al.* (1972) is made. Since the calculated d-${}^3\text{He}$ threshold energy was found to be 21.8 MeV, which is about 2.83 MeV higher than the value of 18.35 MeV (c.m.) determined experimentally, the data points of Plattner *et al.* have been plotted with an energy shift of 2.83 MeV toward the right, thus taking into account the mismatch between the calculated and experimental values of the d-${}^3\text{He}$ threshold energy. It can be seen from Fig. 25 that the single-channel calculation (with the tensor force set equal to zero) does not give the resonance behavior of the phase shifts, while fair agreement with empirical values is obtained in the coupled-channel calculation. At larger energies, the calculated values are smaller, perhaps reflecting the fact that $l=2$, $s=\frac{1}{2}$, and the $l=2$, $s=\frac{1}{2}$ and $\frac{3}{2}$, values were not considered for the $d+{}^3\text{He}$ channel.

All in all, the RGM calculations demonstrate that the $d+{}^3\text{He}$ channel is seen to influence the $p+\alpha$ elastic scattering in the energy region around the $\frac{3}{2}^+$ resonance. Thus, although the anomaly in the p-α analyzing power measurement at $E_p=23$ MeV and the resonance of the $d_{3/2}$ phase shifts near this energy clearly show the 16.7-MeV $\frac{3}{2}^+$ second excited state in ${}^5\text{Li}$, an accurate description of this state should take into account both the α-p and the d-${}^3\text{He}$ structures.

The use of the RGM calculations of p-α scattering has also been extended to comparatively higher c.m. energies

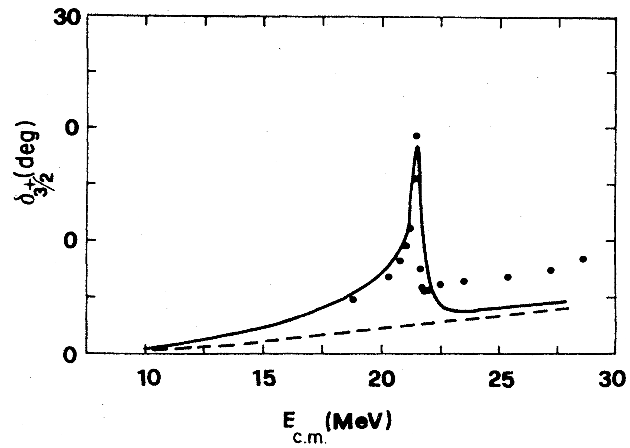

FIG. 25. Calculated and empirical values of the p-α phase shifts $\delta_{(3/2)^+}$ as a function of c.m. energy (Wildermuth and Tang, 1977). The solid and dashed curves represent the results of the coupled-channel and the single-channel calculations, respectively. The empirical data points are those of Plattner *et al.* (1972) and are plotted with an energy shift of 2.83 MeV in order to compensate for the mismatch between calculated and experimental $d+{}^3\text{He}$ threshold energies. [Adapted from Heiss and Hackenbroich (1969).]

of 60, 80, and 124.8 MeV by Thompson *et al.* (1977), who, using a nucleon-nucleon potential with a weakly repulsive core, reproduced reasonably well the two-nucleon scattering data and the essential properties of the α particle. These authors find that because of the use of a totally antisymmetric wave function in the RGM which automatically includes the exchange effects the scattering behavior at large angles was adequately described.

Since the RGM interaction is nonlocal, it does not obviously lend itself to a graphic representation. On the other hand, for purposes of comparison with the phenomenological local potentials and also for purposes of practical applications, it would be desirable to seek an effective local representation of the microscopic RGM interaction so that the general features of the interaction could be visualized. This basically means that one now must replace the nonlocal potential in the integro-differential equation

$$\left[\frac{h^2}{2\mu}\left[\frac{d^2}{dr^2}-\frac{l(l+1)}{r^2}\right]+E-V_D(r)\right]f_l(r)=\int_0^\infty k_l(r,r')f_l(r')dr' \quad (4.13)$$

by an effective local potential $V^{\text{eff}}(r)$ entering in a differential equation

$$\left[\frac{h^2}{2\mu}\left[\frac{d^2}{dr^2}-\frac{l(l+1)}{r^2}\right]+E\right]f_l(r)=V_l^{\text{eff}}(r)f_l(r)\ . \quad (4.14)$$

Obviously such a replacement is possible if V_l^{eff} is defined as

$$V_l^{\text{eff}}(r)=V_D(r)+\frac{1}{f_l(r)}\int_0^\infty k_l(r,r')f_l(r')dr'\ . \quad (4.15)$$

Note that (4.13) is the same as (4.7) except that the Coulomb potential $V_c(r)$ has now been included in the direct potential $V_D(r)$. Now, generally speaking, in the replacement of the nonlocal potential by an equivalent local one, the simple choice (4.15) leads to difficulties with singularities whenever $f_l(r)$ is zero. One thus seeks prescriptions (Fiedeldey, 1967) which avoid this difficulty. Such prescriptions introduce r-dependent proportionality factors $g_l(r)$ between the wave function of the nonlocal potential and that of the equivalent local one, and the equivalent local potential is then constructed as a function of the proportionality factor and its derivatives. However, Thompson *et al.* (1969) reasoned that the potential $V_l^{\text{eff}}(r)$ contains singularities in the region where the clusters overlap considerably and hence has more academic inerest than practical. Thus they used another effective potential $\widetilde{V}_l^{\text{eff}}(r)$, defined by

$$\widetilde{V}_l^{\text{eff}}=\begin{cases}\infty\ , & r<r_0\\ V_l^{\text{eff}}(r)\ , & r>r_0\ ,\end{cases} \quad (4.16)$$

where r_{l0} is the distance at which $f_l(r)$ has its outermost node in the region of strong overlap. The core radius r_0 is chosen as a first approximation to be energy independent in view of the observation that the positions of the nodes of the radial scattering functions are only weakly energy dependent. Since $f_l(r)$ in (4.15) is energy dependent, the potential $\widetilde{V}^{\text{eff}}(r)$ is local and energy dependent. The manner of construction of $\widetilde{V}^{\text{eff}}(r)$ makes it evident that both the RGM nonlocal potential and its local representation $\widetilde{V}^{\text{eff}}(r)$ [or $V_l^{\text{eff}}(r)$] would yield exactly the same phase shifts. The effective potentials thus constructed for the α-N system show some interesting features as are evident from Fig. 26.

It is seen that the potentials for different partial waves contain varying degrees of repulsion, the potential $\widetilde{V}_0$ having a hard core radius of 2.21 fm followed by a very weak attractive part, the potential V_1 being purely attractive, and the potential V_2 having no hard core but displaying moderate repulsion for small values of r. However, not too much physical significance should be attributed to the hard core in view of the fact that the hard core in the present case is not a result of dynamical calculations but is only an artifice of avoiding the region below the position of the outermost node where clusters are expected to overlap. Calculations done also at other energies showed energy dependence of the potentials, although rather slight. Incidentally, the odd-even feature (in which the potentials in the odd states are different from those in the even-l states), which was first observed by Gammel and Thaler (1958) in the phenomenological analysis of α-p scattering data using a local potential, is also seen to be present to some extent in the long-range part of the calculated effective potentials. Thus both the nonlocal α-N interactions obtained from microscopic studies and the effective local ones derived from them

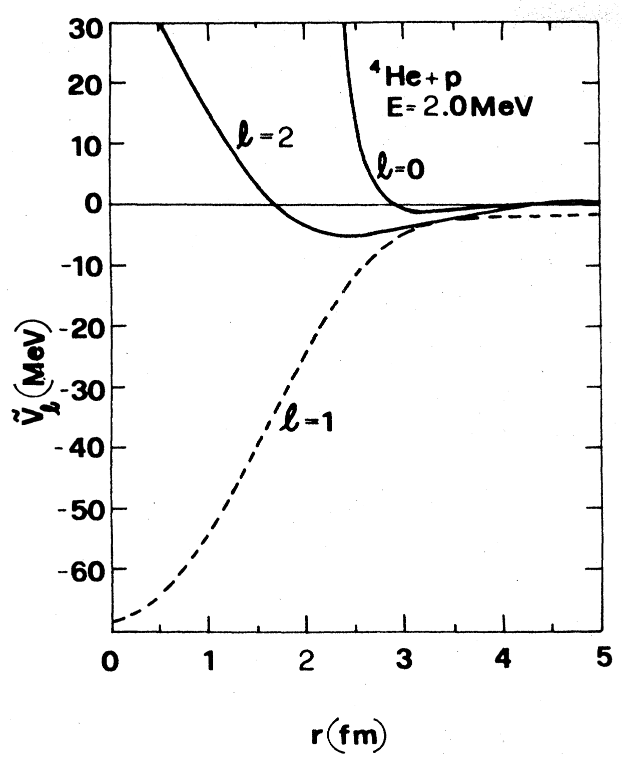

FIG. 26. Effective α-p potentials $\widetilde{V}_l$ for $l=0$, 1, and 2 at 2.0 MeV (Reichstein and Tang, 1970).

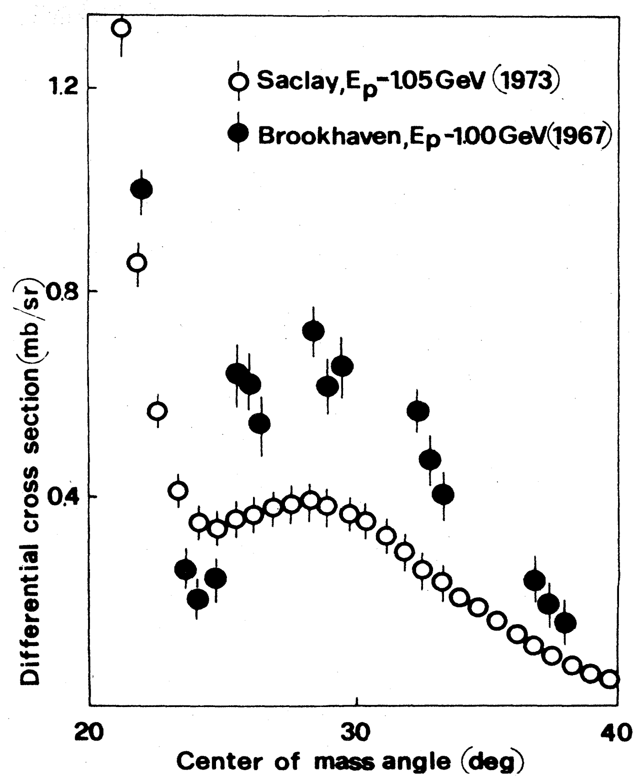

FIG. 27. Angular distribution of 1-GeV protons elastically scattered from ^{4}He. The solid circles and the open circles represent the data of Palevsky *et al.* (1967) and Baker *et al.* (1974), respectively.

have features similar to those of the phenomenological potentials and provide, within limitations, a fairly adequate description of the α-N scattering data.

So far, we have discussed several aspects of the low-energy α-N interaction. Since, with the availability of high-energy proton beams at the particle accelerators, a large number of p-α experiments in the GeV range have been performed, it is worthwhile to take at least a summary look at the situation prevailing in the experimental and theoretical areas. Experimentally, structures have been observed in the differential scattering cross sections. The first GeV experiment at the BNL showed a deep minimum near $t=-0.25$ (GeV/c)^2, where t is the four-momentum transfer squared; the dip is followed by a secondary maximum (see Fig. 27). Such a structure has been more pronounced at higher energies. Here the hope has been that such structures can tell us something about the nucleon correlations in the nucleus. Since at these energies the high-momentum components of the nuclear wave functions could be involved, the short-distance behavior of the N-N correlations are likely to be revealed. Theoretically, attempts have been made to explain the shape and structure of the differential cross sections, keeping in mind the fact that it is one thing to talk of the interaction of the proton with the nucleus as a whole, while it is quite another to talk of the multiple interactions of the proton with the nucleons of the nucleus. In the latter case, nucleon-nucleon amplitudes are involved and a correct parametrization of these nucleon amplitudes is expected to form an essential part of the description of the interaction process. Relativistic energies are involved, so one may have to use the Dirac equation instead of the Schrödinger equation. At the high energies involved, the excitation of the nucleon and thus the appearance of the Δ isobar may assume importance. Also, if multiparticle scatterings are induced, for which the essential property of the nucleus is its high density, which is to a certain extent realized in the tightly bound helium nucleus, then there must be a theory to test these multiple scatterings. In fact, that theory is the Glauber multiple scattering theory. One of the objectives of high-energy p-α scattering is to treat the helium nucleus as a microlaboratory for testing the theories of high-energy proton-nucleus scattering. Two types of tools have so far been used in analyzing such scattering. One of these is the familiar optical potential model with its different versions and the other is the Glauber theory of multiple scattering just mentioned.

In the Glauber model, the full scattering amplitude is a coherent sum of single, double, triple, and quadrupole scatterings from the four nucleons in ^{4}He. In between two scatterings, the proton may get excited as long as it comes back to the ground state before leaving the nucleus. Thus intermediate inelastic collisions of nucleons, where at the end both projectile and target emerge in their ground states, have also been included in the Glauber model calculations. The assumptions and approximations involved in the Glauber model (Glauber, 1959) are the restriction to small scattering angle θ ($\theta^2 kd \leq 1$, when d is the nuclear force range and k the wave number), the high-energy conditon ($V/T \leq 1$, and $ka \gg 1$, where a is the range and T the projectile kinetic energy), dynamical approximation (phase shifts due to scatterings from nucleons may be added together), and the frozen nucleus approximation (meaning that for the very short period for which the projectile traverses the nucleus the nucleons in the nucleus do not rearrange themselves, i.e., they freeze themselves). With these assumptions one may obtain the physical amplitude for elastic scattering $F_{f0}(q)$ in the Glauber model by averaging the transition amplitude $F(\mathbf{q},\mathbf{r}_1,\mathbf{r}_2,\ldots,\mathbf{r}_A)$ over the nucleon distribution. Thus

$$F_{f0}(\mathbf{q}) = \langle f \,|\, F(\mathbf{q},\mathbf{r}_1,\mathbf{r}_2,\ldots,\mathbf{r}_A) \,|\, 0 \rangle = \frac{k}{2\pi i}\left\langle f \left| \int e^{i\mathbf{q}\cdot\mathbf{r}}\Gamma(\mathbf{b},\mathbf{s}_1,\ldots,\mathbf{s}_A)\,d^2b \right| 0 \right\rangle .$$

Here $|0\rangle$ and $|f\rangle$ are the intrinsic initial and final nuclear wave functions depending on $A-1$ coordinates, $\mathbf{s}_n$ is the transverse component of the vector position of a nucleon $\mathbf{r}_n$, and b is the impact parameter. The nucleon-nucleon profile function Γ is related to the phase function χ through

$$\Gamma(b) = 1 - \exp[i\chi(b)] .$$

There are many finer points of the model, and corrections to multiple scattering have also been proposed. We shall not go into all this but refer the reader to a recent review by Igo (1978) on intermediate- and high-energy proton-nucleus research, in which the results of high-energy p-α scattering experiments up to 1978 and their theoretical analyses have been discussed. We shall therefore comment on a few selected experiments and their theoretical interpretation since this last review. One such experiment is the cross-section and polarization measurements of Courant *et al.* (1979) for 0.5—1.73 GeV showing structure at $t=-0.25$ (GeV/c)^2 which decreases in magnitude with energy. Earlier the differential cross-section and analyzing power data at 1.03 GeV were fitted by Wallace and Alexander (1977), who suggested that the inclusion of noneikonal terms in a multiple-scattering model could give a fit to the cross-section data to within 5% but that both cross-section and analyzing power data could not be fitted without the inclusion of the inelastic intermediate state (IIS) in the multiple-scatttering formalism. The necessity of including such inelastic processes has been earlier emphasized by many authors (see, e.g., Alberi and Bertocchi, 1969) and was also pointed out in two later experiments by Bujak *et al.* (1981) and Burq *et al.* (1981), who measured p-^{4}He differential scattering cross sections at energies ranging from 40 to 400 GeV. The region $0.2 < -t < 0.4$ (GeV/c)^2 was found to be most sensitive to the $N^*(1232)$ production. With the inclusion of the intermediate state the cross-section dip is filled in and the maximum analyzing power is reduced from 0.8 to 0.4. The experimental data of Courant *et al.* were in agreement with these calculations. In the model of Wallace and Alexander a fit to the analyzing power required $\alpha_{pn} = -0.35$, where α is the ratio of the real to the imaginary part of the scattering amplitude, the value of α_{pp} at this energy being -0.06. Thus it seems that high-energy p-α data can yield information about the previously unknown N-N scattering amplitudes.

At the same energy of 1.03 GeV, Mercer *et al.* (1978) fitted the cross-section and analyzing power data using an optical potential model. They used a relativistically correct model having a scalar and a fourth-component vector potential. A fit to the analyzing power gave a vector-scalar ratio of -0.72, which was consistent with previous meson exchange theory calculations. Having obtained a fit to 1.03-GeV data, Mercer *et al.* reproduced the cross-section and polarization data at the energies of measurement in the experiment of Courant *et al.*

At the lower energy of 500 MeV, optical-model fits of Leung and Sherif (1978) and van Oers *et al.* (1982) seemed to be unsuccessful. The situation did not improve, as was noted by Cooper (1981), even if the Dirac equation was used instead of the Schrödinger equation. However, in a more recent investigation, Greben and Gaurishanker (1983) have argued that the inclusion of the Wolfenstein R-parameter data as measured recently by Moss *et al.* (1983) is of great value in providing a lot of information on the geometries of the various components of the potential. Using a local optical-model potential with the same terms as contained in the analysis of Satchler *et al.* (1968) discussed earlier, but with the inclusion of imaginary parts in both central and spin-orbit terms, Greben and Gaurishankar reproduced the p-^{4}He elastic scattering data at 500 MeV, using the Born approximation.

Last, we present in Fig. 28 the results of two of the most recent experiments (Ambrosio *et al.*, 1982; Bell *et al.*, 1982) and the results of their analysis (Proriol *et al.*, 1982), as reported by Faessler (1983). The points below and up to the diffraction minimum are those of Ambrosio *et al.*, while the points above the first dip are the ones of Bell *et al.* The curves are the calculations of Proriol *et al.* The dashed line shows the results of pure Glauber-model calculations with an effective radius of 1.66 fm. The continuous line includes a correction for intermediate inelastic states in the double scattering term. This inclusion increases the double scattering amplitude, which has a negative sign, and thus the cross section in the t region $[0.2 < -t < 0.8$ (GeV/c)$^2]$, where double elastic scattering dominates, is likely to decrease. However, the accuracy of the data and the agreement between the data and the calculations are such as not to warrant a choice between the two calculations, which differ by only about 20%.

Sumarizing the data and analyses of intermediate- and high-energy p-α scattering, one finds that in the multiple scattering model, the data in the region $-t < 0.25$

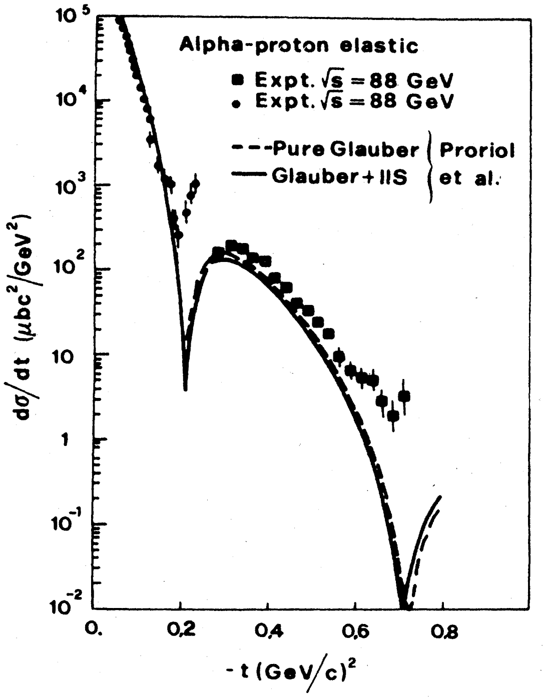

FIG. 28. Differential elastic α-p cross section as a function of t, the invariant four-momentum transfer squared (Faessler, 1983). The experimental points below the diffraction minimum are the data of Ambrosio *et al.* (1982) while the points beyond the dip are taken from Bell *et al.* (1982).

$(\mathrm{GeV}/c)^2$ are represented primarily by single scattering, while near the region at 0.25 $(\mathrm{GeV}/c)^2$ the first minimum arises due to the single and double scattering amplitudes' interfering destructively; then there is a secondary maximum followed by another region of interference between double and triple scattering; triple scattering dominates near the region at $t=1.45$ $(\mathrm{GeV}/c)^2$. The data do not show a sign of quadrupole dominance. There is certainly a need for more energy-dependent data in general and for more polarization measurements in particular. The nucleon-nucleon amplitudes in the GeV region need also be known, particularly that for p-n. At the moment it is difficult to decide whether the multiple scattering models or the optical potential models give a better representation of the experimental data. As far as obtaining information about correlations within the ^{4}He nucleus is concerned, the earlier calculations do not suggest (Igo, 1978) that finer details of the ^{4}He wave function are necessary beyond what is obtained from electron scattering studies. However, the most recent CERN experiments indicate (Faessler, 1983) that the differential scattering cross sections at $\sqrt{2}=88$ GeV (total c.m. energy) show sensitivity to details of the ^{4}He wave function. Obviously, more data with greater accuracy could settle the issue.

V. CONCLUDING REMARKS

The alpha-nucleon problem has been one of the few simple and meaningful two-body problems in nuclear physics. Since the manner of construction, especially of the basic interaction for this two-body system is practically the same as that for most two-cluster systems, the α-N interaction could be treated as a good ground for testing various assumptions and approximations involved in the microscopic studies of interactions between more complicated systems.

From the experimental point of view, there have been continual improvements in the measurements of N-α scattering data (differential scattering cross section and polarization). Abundant p-^{4}He elastic scattering data of high precision exist below 20 MeV, in which region a number of phase-shift analyses have been made. Above the inelastic threshold near 23 MeV, more data with better accuracy have recently been available (Plattner *et al.*, 1972; Houdayer *et al.*, 1978). However, there is still a lack of sufficient data, especially of analyzing powers, above 40 MeV. In the energy region 40—65 MeV, a number of phase-shift solutions exist (Houdayer *et al.*, 1978; Saito, 1979) which are fairly consistent with the phase-shift sets at lower energies. In order to distinguish among these solutions, more measurements of analyzing powers, preferably at the same energies, together with accurate measurements of the spin-rotation parameters at backward angles are necessary. With the analyses of p-α scattering made so far only the 16.7 MeV $\frac{3}{2}^+$ second excited state in ^{5}Li has been studied with some precision. The study of analyzing powers and the phase-shift behavior of the d-phase shifts around 23 MeV clearly show this state. Beyond this state, the phase shifts behave as smooth function of energy, and no other level of ^{5}Li has been unambiguously identified through p-α scattering. The theoretical calculations show that the second excited state does not have a predominantly $p+\alpha$ cluster structure; the $d+{}^3$He channel has also to be brought in. At higher excitation energy, a study of d-^{3}He scattering together with multiparticle breakup reactions would be essential for the level studies of ^{5}Li. The polarization measurements in p-α scattering show that ^{4}He is an excellent polarization analyzer. Except for a strong anomaly around 23.4 MeV corresponding to the $D_{3/2}$ resonance in ^{5}Li, the analyzing power contour diagram does not show a striking energy dependence, especially in the backward hemisphere, for proton energies ranging from 20 to 60 MeV; a weak anomaly is observed around 30 MeV; analyzing power as high as 90% or more has been observed at $\theta_{\mathrm{c.m.}}=140°$. Thus the analyzing power measurements provide an accurate polarization analyzer up to 65 MeV.

For the case of n-^{4}He scattering, intensive work has been done over the last two decades, and below 20 MeV, the most widely used phase shifts have been those of Hoop and Barschall (1966). Again near 20 MeV, there are still some discrepancies between the various phase shifts of different authors. Since in the 20-MeV region, the n-^{4}He system is widely used as a neutron polarization analyzer, it is desirable that such discrepancies be removed through better analyses. Above 20 MeV, improved phase-shift solutions have been proposed (Broste *et al.*, 1972) from a combined analysis of polarization and cross-section data. But the uniqueness of the phase-shift solutions has not been established and there is clearly need for more data on both cross sections and polarization in the range of 20—30 MeV. Above 30 MeV, the neutron analyzing power measurements have been practically nonexistent apart from some measurements around 34 and 50 MeV. The lack of neutron analyzing power data above 30 MeV has been a serious handicap in determining final-state polarizations. Charge symmetric n-^{4}He phases have, however, been predicted (Fröhlich *et al.*, 1982) by applying Coulomb corrections to the best available p-^{4}He phase shifts between 20 and 55 MeV. A comparison of these predictions with the future neutron data at higher energies could be very useful. For the moment, the comparison of n-^{4}He and p-^{4}He analyzing powers between 20 and 30 MeV by Broste *et al.* (1972) and Lisowski *et al.* (1976) and at 50.4 MeV by York *et al.* (1983) as well as considerations of the known energy levels of ^{5}He and ^{5}Li would seem to provide support to the charge symmetry hypothesis of nuclear forces. The availability, in the future, of accurate high-energy n-^{4}He analyzing power measurements in the same energy ranges in which p-^{4}He data have been considered would permit a more elaborate treatment of the charge-symmetry issue from the alpha-nucleon point of view.

There has been a mounting interest in intermediate- and high-energy p-α scattering in recent years. The experimental data in the GeV region, characterized by a deep diffraction minimum followed by a secondary maximum, have generated a number of theoretical investigations based on the multiple scattering models and the optical potential models. The structures in the p-^{4}He experimental data admit of interpretations in terms of the coherent sum of single, double, triple, and quadruple scatterings of the incident proton, from the four nucleons in ^{4}He. The optical-model analyses in the intermediate-energy region also provide a fair representation of the data, and the Wolfenstein R-parameter data have been found to be of great use in such analyses (Greben and Gaurishankar, 1983). While some recent experiments (Bujak *et al.*, 1981) support the early finding that the inclusion of intermediate inelastic scattering is important in the region of the diffractive cone as well as in the secondary maximum observed in the differential scattering cross sections, the results of analyses of more recent α-p experiments at CERN (Faessler, 1983) indicate that the experimental data are not of sufficient precision to decide between calculations with and without intermediate inelastic scattering. Also, while some experiments do not insist on more detailed information of the ^{4}He wave function than is known at present, others (Bujak *et al.*, 1981; Faessler, 1983) indicate a great sensitivity of the results to the details of the ^{4}He wave function and demand a better understanding of this wave function. Thus the situation in intermediate- and high-energy p-α scattering is far from being conclusive. More cross-section and polarization data supporting each other are needed. The polarization data would be of great use in providing useful information about the nucleon-nucleon scattering amplitudes (particularly for p-n), which have not yet been firmly determined experimentally.

On the phenomenological plane, although a number of careful α-N potential constructions (both local and nonlocal) have been made, it would be worthwhile to obtain over a very large energy interval separable potential model analyses of α-N scattering in coordinate space, preferably with Gaussian form factors. The latter could be useful for possible applications to α-nucleus scattering in the spirit of the folding model.

Although the α-N interaction is a sufficiently interesting topic by itself, it is nevertheless connected with the general fabric of nuclear physics. The connection arises from the fact that while on the one hand α-N interaction can be built from the N-N forces, on the other, the former can be used as an input in generating the α-nucleus interaction. Thus it is of interest to inquire as to how the phenomenology of α-N interaction is related to that of N-N and α-nucleus interaction.

As far as the first part of the above inquiry is concerned, the nucleon-alpha potential is but only one of the nucleon-nucleus optical model potentials which are seen to be energy dependent. The energy dependence can be interpreted in terms of the density dependence or the nonlocality of the N-N forces. Density-dependent N-N forces have already been used by Majka (1978), for example, in generating a nucleon-alpha potential by averaging an adequate nucleon-nucleon interaction over the nucleon density distribution of the target nucleus. It was found that the "Woods-Saxon" potentials extracted from the phenomenological studies of Satchler *et al.* (1968) and Thompson *et al.* (1970) fitted the tail of N-α potential thus generated in a larger part at higher energy. This observation could be taken to mean that the energy dependence of the phenomenological potentials simulated effects which could be included through the energy dependence of the N-N forces. It should be noted, however, that since the N-N potential considered here is that between a free nucleon and a nucleon which is bound inside the alpha particle, the N-N force has to be regarded as an effective one.

More recently, Lee and Robson (1982) employed separable N-N potentials in the "averaging" procedure. Using phenomenological N-N interactions of the Tabakin, the Doleschall, and the Strobel N-N types, for which Yukawa and Gaussian forms with variable parameters for each partial wave were considered along with the inclusion of spin-orbit and tensor forces, they found that the resultant n-α potentials reproduced approximately the same $S_{1/2}$ phase shifts for elastic n-α scattering. However, in order to reproduce the resonances in the $p_{1/2}$ and $p_{3/2}$ phase shifts, an effective N-N force of the form of the G matrix had to be derived from the V matrix. The analysis of Lee and Robson showed that for the $S_{1/2}$ scattering most of the contributions come from the S waves of the N-N potential, while for the $p_{1/2}$ and $p_{3/2}$ n-α scattering the p-waves of the N-N potential play a significant role; the contribution of the d waves was found to be negligible. Single nucleon knockout exchange was considered throughout the analysis.

The more microscopic theory which uses antisymmetric wave function and generates nonlocal α-N interaction from local N-N forces is, of course, the resonating group method, discussed earlier. The RGM calculations have shown reasonably good agreement with the experimental results (cross section and polarization) for α-N scattering and have at the same time pointed out the need for including the $d+{}^3\mathrm{He}$ channel in an accurate description of the $\frac{3}{2}^+$ second excited state in ${}^5\mathrm{Li}$. However, almost all RGM calculations have been made with rather simple N-N potentials. The difficulties of using more realistic N-N interactions are mostly numerical. As a step towards understanding better the sensitivity of certain aspects of interactions between heavy clusters to refinements in the N-N interaction, it would nevertheless seem profitable to make further basic studies of the α-N system with a variety of N-N potentials. This, of course, would mean employing considerable computational skill.

A feature of the RGM calculations of the α-N interaction which appears somewhat less satisfactory is the fact that in most of these calculations employing a single-term α-particle wave function, the parameter α of the wave function [see Eq. (4.4)] has been fixed, on most occasions, not *variationally* from a calculation of the α-particle binding energy with chosen N-N forces, as should have been the case, but rather from the rms radius of the α particle. Some variational calculations for the α particle have, of course, been done by Le-Chi-Niem *et al.* (1971), who, employing a soft-core N-N interaction, obtained an α-particle wave function by a variational procedure but obtained an α-particle binding energy of 21.5 MeV, 6.5 MeV smaller that the experimental value. However, since the kernel depends strongly on the total energy $E=E_{\mathrm{rel}}+E_\alpha$, differences in the values of E_α used can have a sizable effect on the phase shifts. An argument which is often given in favor of fixing α from the rms radius of the α particle is that N-N forces used are nonsaturating and hence would not prevent collapse. In fact, the rms radius of the α-particle determined by the variational parameters is found to be only 10—15 % smaller than the experimentally observed value. An interesting point to note in this connection is that the RGM calculations of the α-N interaction together with a variational determination of E_α could reduce the Serber component considerably [as shown in the α-α case by Afzal and Ali (1976)], and thus the conclusions about the force mixture may also be altered.

The effective α-N potentials derived from the RGM α-N interaction provide a reasonable link between the microscopic calculations and the phenomenological potentials. However, as has been discussed earlier, in the construction of such effective potentials, a hard core has often been placed at the outermost node in the region of strong overlap, thus deemphasizing the inside region and avoiding singularities which appear in single-channel RGM calculations whenever the radial function $f_1(r)$ goes to zero. In multichannel calculations, where possible, reaction channels open at higher energies, $f_1(r)$ is complex and the real and imaginary parts of $f_1(r)$ are not expected to go to zero simultaneously. However, it should be noted that in single-channel RGM calculations, singularities occur in the surface region where the potential depth is rather low. It has been claimed that since these singularities are extremely narrow and since at relatively lower energies the wavelength λ is large, the narrow singularities have very little effect on scattering and thus the effective potentials may be smoothed out. While this claim is not unjustified, it would nevertheless be instructive to construct equivalent local α-N potentials from the nonlocal ones using adequate prescriptions (Fiedelday, 1967; Husain and Ali, 1970; Ali *et al.*, 1985).

Concerning the second part of the inquiry posed earlier regarding the relation between the α-N and the α-nucleus interactions, one notices that such a relation is, in fact, provided by the folding model. Through use of this model, α-nucleus potentials have been derived by folding an effective α-N interaction into the density distribution of the target nucleus. The fits to α-particle scattering from a number of nuclei using the folding model are improved appreciably over those produced by the standard optical model and are sensitive to the choice of the matter distribution parameters (Rebel, 1974). The rms matter radii deduced have also been in good agreement with other estimates.

In all these calculations it has been assumed that the interaction between the α-particle projectile and the nucleus is actually replaced by a sum of interactions of the α with each individual nucleon, thus avoiding many-body features. For a struck nucleon which is bound one needs to consider the off-energy shell matrix elements of the α-nucleon interaction. However, the α particle has been found to be a strongly absorbed particle with the effect that the interaction takes place in the surface region where the matter density is low. Thus, in the absence of substantial clustering, the effects of multiple scattering and the Pauli principle constraints should be reduced compared to nucleon scattering. In that case, the effective interaction between an α particle and a bound nucleon would tend to approach the free alpha-nucleon interaction. This has been borne out by the results of Batty *et al.* (1971), who fitted the data for α scattering by calcium and nickel isotopes using nuclear matter distributions derived from single-particle wave functions generated by reliable bound-state potentials. The observation of Batty *et al.* has been that the best choice for a local effective interaction is a simple Gaussian form and that the effective α-N interaction is only slightly different from the free α-N interaction that reproduces the nonresonant features of the α-N scattering data. Thus the effective α-N interaction seems to be quite well determined and the microscopic model for α scattering from complex nuclei appears to be rather consistent.

It would be interesting to see detailed folding model calculations of α-N interactions using either a nonlocal separable N-N interaction or a local interaction but taking due account of the antisymmetrization effect and the density dependence of the nuclear forces. In fact, such calculations have only just been introduced (Lassaut and Vinh Mau, 1980; Lee and Robson, 1982). Also, it would be worthwhile to use nonlocal separable α-N interactions of different shapes in the folding models for α-nucleus scattering. The use of nonlocal α-N interaction could take account of the observed energy dependence of the α-nucleus potential [Singh *et al.* (1975) and references cited therein].

Finally, there are still a number of important gaps in the understanding of the N-α problem. To mention a few, on the experimental side there is a dearth of n-α cross-section and polarization measurements above 30 MeV. Such measurements could, besides determining final-state polarizations, shed further light on the charge symmetry hypothesis of nuclear forces. The p-α data are comparatively richer, although resolving of the ambiguities in some of the phase-shift solutions above 50 MeV will require an experimental determination of precise analyzing powers of p-α scattering between 60 and 65 MeV together with measurements of the spin-rotation parameter and a study of the inelastic processes. At intermediate and high energies, the p-α scattering situation is far from being conclusive. Although many of the features of the multiple scattering theory have been understood, the data still do not permit one to decide between the multiple scattering models or the optical potential models. Also, in order to make more definite conclusions about the importance of the intermediate inelastic states, the sensitivity of the high-energy p-α scattering results to the finer details of the ^{4}He wave function, and the relative phases of the spin-dependent and spin-independent parts of the averaged nucleon-nucleon amplitude, more accurate data on the high-energy p-α cross section and polarization are wanted. On the low-energy theoretical side, although there has been reasonable agreement between the microscopic theory and the N-α scattering data, more calculations with realistic N-N forces are still needed. Also, considering the importance of the α-N interaction in generating α-nucleus potentials for describing the α-nucleus scattering data, the use of different types of density-dependent and nonlocal α-N forces in the generating procedure would be desirable.

To sum up, alpha-nucleon scattering, apart from being sufficiently interesting by itself in the way of being an excellent polarizer as well as an analyzer of polarization, will continue to act as a laboratory for testing various assumptions involved in proton-nucleus scattering. Thus a deeper study of the alpha-nucleon interaction is expected to provide valuable information towards understanding the detailed features of nucleon-nucleus as well as alpha-nucleus interactions.

ACKNOWLEDGMENTS

The authors are grateful to Professor H. A. Weidenmüller and Professor D. Fick of the Max Planck Institute, Heidelberg, for reading parts of the manuscript and making useful comments. One of us (S.A.) would like to thank Professor Abdus Salam, the International Atomic Energy Agency, and UNESCO for hospitality at the International Center for Theoretical Physics, Trieste, where part of this work was completed.

REFERENCES

Adair, R. K., 1951, Phys. Rev. **82**, 750.

Adair, R. K., 1952, Phys. Rev. **86**, 155.

Ad'yasevich, B. P., V. G. Antonenko, Yu. P. Polunin, and D. E. Famenko, 1966, Yad. Fiz. **5**, 933 [Sov. J. Nucl. Phys. **5**, 665 (1967)].

Afzal, S. A., and S. Ali, 1970, Nucl Phys. A **157**, 353.

Afzal, S. A., and S. Ali, 1976, in *Few-Body Dynamics*, edited by Asoke N. Mitra, Ivo Slaus, V. S. Bhasin, and V. K. Gupta (North-Holland, Amsterdam), p. 70.

Ahmad, A. A. Z., S. Ali, N. Ferdous, and M. Ahmed, 1975, Nuovo Cimento A **30**, 385.

Ajzenberg-Selove, F., 1984, Nucl. Phys. A **413**, 1.

Alberi, G., and L. Bertocchi, 1969, Nuovo Cimento A **61**, 201.

Alekseev, N. V., U. R. Arifkhanov, N. A. Vlasov, V. V. Davydov, and L. N. Samoilov, 1963, Zh. Eksp. Teor. Fiz. **45**, 1416 [Sov. Phys.—JETP **18**, 979 (1964)].

Alekseev, N. V., U. R. Arifkhanov, N. A. Vlasov, V. V. Davydov, and L. N. Samoilov, 1964, Zh. Eksp. Teor. Fiz. **47**, 433 [Sov. Phys.—JETP **20**, 287 (1965)].

Ali, S., A. M. Khan, and G. Schiffrer, 1985, Phys. Rev. C **32**, 318.

Ali, S., M. Rahman, and D. Husain, 1972, Phys. Rev. D **6**, 1178.

Ali, S., M. Rahman, and D. Husain, 1974, Phys. Rev. C **9**, 1657.

Allison, P. W., and R. Smythe, 1968, Nucl. Phys. A **121**, 97.

Ambrosio, M., G. Anzivino, G. Barbarino, U. Becker, G. Carboni, V. Cavisinni, T. Del Prete, G. Kantardjian, D. Lloyd Owen, M. Morganti, J. Paradiso, G. Peternoster, S. Patricelli, M. Steuer, and M. Valdata-Nappi, 1982, Phys. Lett. **113**, 347.

Arifkhanov, U. R., N. A. Vlasov, V. V. Davydov, and L. N. Samoilov, 1965, Yad. Fiz. **2**, 239 [Sov. J. Nucl. Phys. **2**, 170 (1966)].

Arndt, R. A., and L. D. Roper, 1970, Phys. Rev. C **1**, 903.

Arndt, R. A., L. D. Roper, and R. L. Shotwell, 1971, Phys. Rev. C **3**, 2100.

Aslanides, E., T. Bauer, R. Bertini, R. Beurtey, A. Boudard, F. Brochard, G. Bruge, A. Chaumeaux, H. Catz, J. M. Fontaine, R. Frascaria, D. Garreta, P. Gorodetzky, J. Guyot, F. Hibou, D. Legrand, M. Matoba, Y. Terrien, J. Thirion, and E. Lambert, 1977, Phys. Lett. **68B**, 221.

Austin, S. M., H. H. Barschall, and R. E. Shamu, 1962, Phys. Rev. **126**, 1532.

Bacher, A. D., G. R. Plattner, H. E. Conzett, D. J. Clark, H. Grunder, and W. F. Tivol, 1972, Phys. Rev. C **5**, 1145.

Baicker, J. A., and K. W. Jones, 1960, Nucl. Phys. **17**, 424.

Baker, S. D., R. Beurtey, G. Bruge, A. Chaumeaux, J. M. Durand, J. C. Faivre, J. M. Fontaine, D. Garreta, D. Legrand, J. Saudinos, J. Thirion, R. Bertini, F. Brochard, and F. Hibou, 1974, Phys. Rev. Lett. **32**, 839.

Barguil, J., J. Pigeon, C. Fayard, G. H. Lamot, and E. El Baz, 1971, Nuovo Cimento A **1**, 285.

Barnard, A. C. L., C. M. Jones, and J. L. Well, 1964, Nucl. Phys. **50**, 604.

Barschall, H. H., and M. H. Kanner, 1940, Phys. Rev. **58**, 590.
Bashkin, S., F. P. Mooring, and B. Petree, 1951, Phys. Rev. **82**, 378.
Battat, M. E., R. O. Bondelid, J. H. Coon, L. Cranberg, R. B. Day, F. Edeskuty, A. H. Frentrop, R. L. Henkel, R. L. Mills, R. A. Nobles, J. E. Perry, D. D. Phillips, T. R. Roberts, and S. G. Sydoriak, 1959, Nucl. Phys. **12**, 291.
Batty, C. J., E. Friedman, and D. F. Jackson, 1971, Nucl. Phys. A **175**, 1.
Bell, W., K. Braune, G. Claesson, D. Drijard, M. A. Faessler, H. G. Fischer, H. Frehse, R. W. Frey, S. Garpman, W. Geist, P. C. Gugelot, P. Hanke, M. Heiden, P. G. Innocenti, T. G. Ketel, E. E. Kluge, G. Mornacchi, T. Nakada, I. Otterlund, B. Povh, A. Putzer, E. Stenlund, T. J. M. Symons, R. Szwed, O. Ullaland, and Th. Walcher, 1982, Phys. Lett. **117B**, 131.
Berthot, J. G., J. Douhet, L. Gardès, L. Meritet, M. Querrou, A. Tetefort, F. Vazeille, J. P. Burg, M. Chemarin, M. Chevallier, B. Ille, M. Lambert, J. P. Marin, J. P. Gerber, and C. Voltolini, 1975, in *High-Energy Physics and Nuclear Structure,* proceedings of the Sixth International Conference, Sante Fe and Los Alamos, edited by D. E. Nagle *et al.* (AIP, New York), paper VI.A.8.
Beznokikh, G. G., V. A. Budilov, P. Devenski, V. I. Inozemtsev, L. F. Kirillova, N. K. Zhidkov, V. A. Nikitin, P. V. Nomokonov, V. Skveres, V. I. Khachko, M. G. Shafranova, A. Bujak, P. Zelinsky, M. Szawlowski, T. Szczepankowski, and V. V. Avdeichikov, 1978, Yad. Fiz. **27**, 710 [Sov. J. Nucl. Phys. **27**, 380 (1978)].
Blanchard, C. H., and R. Avery, 1951, Phys. Rev. **81**, 35.
Blanchard, C. H., R. Avery, and R. G. Sachs, 1950, Phys. Rev. **78**, 292.
Bond, J. E., and F. W. K. Firk, 1976, Nucl. Phys. A **258**, 189.
Bond, J. E., and F. W. K. Firk, 1977, Nucl. Phys. A **287**, 317.
Bonner, T. W., F. W. Prosser, Jr., and J. Slattery, 1959, Phys. Rev. **115**, 398.
Boreli, F., V. Lazarevic, and N. Radisic, 1965a, in *Proceedings of the Second International Symposium on Polarization Phenomena of Nucleons,* edited by P. Hubert and H. Schopper (Birkhäuser, Basel), p. 520.
Boreli, F., V. Lazarevic, and N. Radisic, 1965b, Nucl. Phys. **66**, 301.
Boschitz, E. T., M. Chabre, M. E. Conzett, E. Shield, and R. J. Slobodrian, 1965, in *Proceedings of the Second International Symposium on Polarization Phenomena of Nucleons,* edited by P. Hubert and H. Schopper (Birkhäuser, Basel), p. 328.
Boschitz, E. T., W. K. Roberts, J. S. Vincent, M. Blecher, K. Gotow, P. C. Gugelot, C. F. Perdrisat, L. W. Swenson, and J. R. Priest, 1972, Phys. Rev. C **6**, 457.
Braden, C. H. 1951, Phys. Rev. **84**, 762.
Brandan, M. E., G. R. Plattner, and W. Haeberli, 1976, Nucl. Phys. A **263**, 189.
Bransden, B. H., and J. S. McKee, 1954, Philos. Mag. **45**, 869.
Brockman, K. W., 1956, Phys. Rev. **102**, 391.
Brockman, K. W., 1957, Phys. Rev. **108**, 1000.
Brockman, K. W., 1958, Phys. Rev. **110**, 163.
Broste, W. B., G. S. Mutchler, J. E. Simmons, R. A. Arndt, and L. D. Roper, 1972, Phys. Rev. C **5**, 761.
Brown, L., W. Haeberli, and W. Trächslin, 1967, Nucl. Phys. A **90**, 339.
Brown, L., and W. Trächslin, 1967, Nucl. Phys. A **90**, 334.
Brown, R. I., W. Haeberli, and J. X. Saladin, 1963, Nucl. Phys. **47**, 212.
Brussel, M. K., and J. H. Williams, 1957, Phys. Rev. **106**, 286.
Bruton, P. C., C. S. Curran, J. K. Davies, T. Ekelöf, S. M. Fisher, E. Hagberg, A. J. Herz, F. F. Heymann, D. C. Imrie, S. Kullander, G. J. Lush, J. P. Nassalski, and A. L. Read, 1978, Nucl. Phys. B **142**, 365.
Bujak, A., P. Devensky, A. Kuznetsov, B. Morozov, V. Nikitin, P. Nomokonov, Yu. Pilipenko, V. Smirnov, E. Jenkins, E. Malamud, M. Miyajima, and R. Yamada, 1981, Phys. Rev. D **23**, 1895.
Bunch, S. M., H. H. Forster, and C. C. Kim, 1964, Nucl. Phys. **53**, 241.
Bunker, S. N., J. M. Cameron, M. B. Epstein, G. Paić, J. R. Richardson, J. G. Rogers, P. Tomaš, and J W. Verba, 1969, Nucl. Phys. A **133**, 537.
Bürgel, B., cited in Huber and Baldinger (1952), p. 439.
Burq, J. P., M. Chemarin, M. Chevallier, A. S. Denisov, T. Ekelof, J. Fay, P. Grafstrom, L. Gustafsson, E. Hagberg, B. Ille, A. P. Kashchuk, G. A. Korolev, A. V. Kulikov, M. Lambert, J. P. Martin, S. Maury, J. L. Paumier, M. Querroll, V. A. Schegelsky, I. I. Tkatch, M. Verbeken, and A. A. Vorobyov, 1981, Nucl. Phys. B **187**, 205.
Busse, W., J. Christiansen, D. Hilscher, U. Morfeld, J. A. Scheer, and W. U. Schröder, 1967, Nucl. Phys. A **100**, 490.
Büsser, F. W., F. Niebergall, G. Sohngen, and J. Christiansen, 1966, Nucl. Phys. **88**, 593.
Cairns, D. J., T. C. Griffith, G. J. Lush, A. J. Metheringham, and R. H. Thomas, 1964, Nucl. Phys. **60**, 369.
Carroll, H., 1941, Phys. Rev. **60**, 702.
Cattapan, G., G. Pisent, and V. Vanzani, 1975, Nucl. Phys. A **241**, 204.
Chadwick, J., and E. S. Bieler, 1921, Philos. Mag. **42**, 923.
Chamberlain, O., E. Segre, R. D. Tripp, C. Wiegand, and T. Ypsilantis, 1956, Phys. Rev. **102**, 1659.
Christiansen, J., F. W. Büsser, F. Niebergall, and G. Sohngen, 1965, Nucl. Phys. **67**, 133.
Chwieroth, F. S., R. E. Brown, Y. C. Tang, and D. R. Thompson, 1973, Phys. Rev. C **8**, 938.
Chwieroth, F. S., Y. C. Tang, and D. R. Thompson, 1974, Phys. Rev. C **9**, 56.
Comparat, V., R. Frascaria, N. Fujiwara, N. Marty, M. Morlet, P. G. Roos, and A. Willis, 1975, Phys. Rev. C **12**, 251.
Conzett, H. E., 1966, Lawrence Radiation Laboratory Report No. UCRL-16767 (unpublished).
Conzett, H. E., 1968, private communication with V. Perez-Mendez.
Conzett, H. E., G. Igo, and A. Nir, 1960, Helv. Phys. Acta, Suppl. **6**, 253.
Cooper, E. D., 1981, Ph.D. thesis, University of Alberta.
Cork, B., 1953, Phys. Rev. **89**, 78.
Cork, B., and W. Hartsough, 1954, Phys. Rev. **96**, 1267.
Cormack, A. M., J. N. Palmieri, N. F. Ramsey, and R. Wilson, 1959, Phys. Rev. **115**, 599.
Courant, H., K. Einsweiler, T. Joyce, H. Kagan, Y. I. Makdisi, M. L. Marshak, B. Mossberg, E. A. Peterson, K. Ruddick, T. Walsh, G. J. Igo, R. Talaga, A. Wriekat, and R. Klem, 1979, Phys. Rev. C **19**, 104.
Craddock, M. K., R. C. Hanna, L. P. Robertson, and B. W. Davies, 1963, Phys. Lett. **5**, 335.
Cramer, D. S., and L. Cranberg, 1972, Nucl. Phys. A **180**, 273.
Critchfield, C. L., and D. C. Dodder, 1949, Phys. Rev. **76**, 602.
Daehnick, W. W., 1959, Phys. Rev. **115**, 1008.
Darriulat, P., D. Garreta, A. Tarrats, and J. Testoni, 1968, Nucl. Phys. A **108**, 316.
Davies, B. W., M. K. Craddock, R. C. Hanna, Z. J. Moroz, and L. P. Robertson, 1967, Nucl. Phys. A **97**, 241.
Demanins, F., G. Pisent, G. Poiani, and C. Villi, 1962, Phys.

Rev. **125**, 318.
Dodder, D. C., and J. L. Gammel, 1952, Phys. Rev. **88**, 520.
Dodder, D. C., G. M. Hale, N. Jarmie, J. H. Jett, P. W. Keaton, Jr., R. A. Nisley, and K. Witte, 1977, Phys. Rev. C **15**, 518.
Drigo, L., C. Manduchi, G. C. Nardelli, M. T. Russo-Manduchi, and G. Zannoni, 1964, Nucl. Phys. **60**, 441.
Dubbeldam, P. S., and R. L. Walter, 1961, Nucl. Phys. **28**, 414.
Enge, H. A., 1966, *Introduction to Nuclear Physics* (Addison-Wesley, Reading, Mass.).
Faessler, Martin A., 1983, Nucl. Phys. A **400**, 525.
Fain, J., J. Gardes, A. Lefort, L. Meritet, J. F. Pauty, G. Peynet, M. Querrou, F. Vazeille, and B. Ille, 1976, Nucl. Phys. A **262**, 413.
Feingold, A. M., 1956, Phys. Rev. **101**, 258.
Fiedeldey, H., 1967, Nucl. Phys. A **96**, 463.
Franco, V., 1968, Phys. Rev. Lett. **21**, 1360.
Freemantle, R. G., T. Grotdal, W. M. Gibson, R. Mckeague, D. T. Prowse, and J. Rotblat, 1954, Philos. Mag. **45**, 1090.
Freier, G., E. Lampi, W. Sleator, and J. H. Williams, 1949, Phys. Rev. **75**, 1345.
Fröhlich, J., H. Kriesche, L. Streit, and H. Zankel, 1982, Nucl. Phys. A **384**, 97.
Gaerttner, E. R., L. A. Pardue, and J. F. Streib, 1939, Phys. Rev. **56**, 856.
Gammel, J. L., and R. M. Thaler, 1958, Phys. Rev. **109**, 2041.
Garreta, D., J. Sura, and A. Tarrats, 1969, Nucl. Phys. A 132, 204.
Geaga, J. V., M. M. Gazzaly, G. J. Igo, J. B. McClelland, M. A. Nasser, A. L. Sagle, H. Spinka, J. B. Carroll, V. Perez-Mendez, and E. T. B. Whipple, 1977, Phys. Rev. Lett. 38, 1265.
Glauber, R. J., 1959, in *Lectures in Theoretical Physics,* edited by W. E. Brittin (Interscience, New York), Vol. I, p. 315.
Goldstein, N. P., A. Held, and D. G. Stairs, 1970, Can. J. Phys. **48**, 2629.
Gotow, K., 1959, University of Rochester Report No. NYO-2532 (unpublished).
Goulding, C. A., P. Stoler, and J. D. Seagrave, 1973, Nucl. Phys. A **215**, 253.
Greben, J. M., and R. Gaurishankar, 1983, Nucl. Phys. A **405**, 445.
Greeniaus, L. G., D. A. Hutcheon, C. A. Miller, G. A. Moss, G. Roy, R. Dubois, C. Amsler, B. K. S. Koene, and B. T. Murdoch, 1979, Nucl. Phys. A **322**, 308.
Griffith, T. C., D. C. Imrie, G. J. Lush, and L. A. Robbins, 1965, in *Proceedings of the Second International Symposium on Polarization Phenomena of Nucleons,* edited by P. Hubert and H. Schopper (Birkhäuser, Basel), p. 325.
Griffith, T. C., D. C. Imrie, G. J. Lush, and L. A. Robbins, 1966, Phys. Rev. **146**, 626.
Hackenbroich, H. H., P. Heiss, and Le-Chi-Niem, 1974, Phys. Lett. **51B**, 334.
Hall, T. A., and P. G. Koontz, 1947, Phys. Rev. **72**, 196.
Hardekopf, R. A., and G. G. Ohlsen, 1977, Phys. Rev. C **15**, 514.
Harris, P., 1950, Phys. Rev. **80**, 20.
Haxel, O., J. H. D. Jensen, and H. E. Suess, 1949, Phys. Rev. **75**, 1766.
Hayakawa, S., N. Horikawa, R. Kajikawa, K. Kikuchi, H. Kobayakawa, K. Matsuda, S. Nagata, and Y. Sumi, 1964, Phys. Lett. **8**, 330.
Heiss, P., and H. H. Hackenbroich, 1969, Phys. Lett. **30B**, 373.
Heiss, P., and H. H. Hackenbroich, 1970, Z. Phys. **231**, 230.
Heiss, P., and H. H. Hackenbroich, 1971, Nucl. Phys. A **162**, 530.
Herzenberg, A., and E. J. Squires, 1960, Nucl. Phys. **19**, 280.
Heusinkveld, M., and G. Freier, 1952, Phys. Rev. **85**, 80.
Heydenberg, N. P., and N. F. Ramsey, 1941, Phys. Rev. **60**, 42.
Heydenberg, N. P., and R. B. Roberts, 1939, Phys. Rev. **56**, 1092.
Hillman, P., R. H. Stahl, and N. F. Ramsey, 1954, Phys. Rev. **96**, 115.
Hochberg, S., 1953, Ph.D. thesis, London.
Hochberg, S., H. S. W. Massey, H. Robertson, and L. H. Underhill, 1955, Proc. Phys. Soc. London, Sect. A **68**, 746.
Hochberg, S., H. S. W. Massey, and L. H. Underhill, 1954, Proc. Phys. Soc. London, Sect. A **67**, 957.
Hodgson, P. E., 1958, Adv. Phys. **7**, 1.
Hoop, B., Jr., and H. H. Barschall, 1966, Nucl. Phys. **83**, 65.
Hoop, B., Jr., and P. Huber, 1967, Helv. Phys. Acta **40**, 710.
Horikawa, N., and H. Kanada, 1965, J. Phys. Soc. Jpn. **20**, 1758.
Houdayer, A., N. E. Davison, S. A. Elbakr, A. M. Sourkes, W. T. H. van Oers, and A. D. Bancher, 1978, Phys. Rev. C **18**, 1985.
Huber, P., and E. Baldinger, 1952, Helv. Phys. Acta **25**, 435.
Husain, D., and S. Ali, 1970, Phys. Rev. C **2**, 1587.
Hwang, C. F., D. H. Nordby, S. Suwa, and J. H. Williams, 1962, Phys. Rev. Lett. **9**, 104.
Igo, G. J., 1978, Rev. Mod. Phys. **50**, 523.
Imai, K., K. Hatanaka, H. Smimizu, N. Tamura, K. Egawa, K. Nisimura, T. Saito, H. Sato, and Y. Wakuta, 1979, Nucl. Phys. A **325**, 397.
Jahns, M. F., and E. M. Bernstein, 1967, Phys. Rev. **162**, 871.
Jewell, R W., W. John, J. E. Sherwood, and D. H. White, 1966, Phys. Rev. **142**, 687.
Juveland, A. C., and W. Jentschke, 1956, Z. Phys. **144**, 521.
Kanada, H., S. Nagata, S. Otsuki, and Y. Sumi, 1963a, Prog. Theor. Phys. **29**, 610.
Kanada, H., S. Nagata, S. Otsuki, and Y. Sumi, 1963b, Prog. Theor. Phys. **30**, 475.
Keaton, P. W., Jr., D. D. Armstrong, R. A. Hardekopf, P. M. Kurjan, and Y. K. Lee, 1972, Phys. Rev. Lett. **29**, 880.
Koester, L. J., H. L. Jackson, and R. K. Adair, 1951, Phys. Rev. **83**, 1250.
Klem, R., G. Igo, R. Talaga, A. Wriekat, H. Courant, K. Einsweiler, T. Joyce, H. Kagan, Y. Makdisi, M. Marshak, B. Mossberg, E. Peterson, K. Ruddick, and T. Walsh, 1977, Phys. Lett. **70B**, 155.
Kraus, L., and I. Linck, 1974, Nucl. Phys. A **224**, 45.
Kreger, W. E., W. K. Jentschke, and P. G. Kruger, 1954, Phys. Rev. **93**, 837.
Kreger, W. E., R. O. Kerman, and W. K. Jentschke, 1952, Phys. Rev. **86**, 593.
Lane, A. M., and R. G. Thomas, 1958, Rev. Mod. Phys. **30**, 257.
Laskar, W., C. Tate, B. Pardoe, and P. G. Burke, 1961, Proc. Phys. Soc. London **77**, 1014.
Lassaut, M., and N. Vinh Mau, 1980, Nucl. Phys. A **349**, 372.
Le-Chi-Niem, P. Heiss, and H. H. Hackenbroich, 1971, Z. Phys. **244**, 346.
Lee, Chew-Lean, and D. Robson, 1982, Nucl. Phys. A **379**, 11.
Leung, C. C. H., and S. C. Park, 1969, Phys. Rev. **187**, 1239.
Leung, S. W. L., and H. S. Sherif, 1978, Can. J. Phys. **56**, 1116.
Levintov, I. I., A. V. Miller, and V. N. Shamshev, 1957, Nucl. Phys. **3**, 221.
Lisowski, P. W., T. C. Rhea, and R. L. Walter, 1975, in *Proceedings of the Fourth International Symposium on Polari-*

zation Phenomena in Nuclear Reactions, edited by W. Grübler and V. König (Birkhäuser, Basel), p. 534.

Lisowksi, P. W., R. L. Walter, G. G. Ohlsen, and R. A. Hardekopf, 1976, Phys. Rev. Lett. **37**, 809.

Majka, Z., 1978, Phys. Lett. **76B**, 161.

Malaroda, R., G. Poiani, and G. Pisent, 1963, Phys. Lett. **5**, 205.

Manduchi, C., G. C. Nardelli, M. T. Russo-Manduchi, and G. Zannoni, 1964, Nucl. Phys. **53**, 605.

May, T. H., W. Benenson, R. L. Walter, and P. Vander Maat, 1962, Bull. Am. Phys. Soc. **7**, 268.

May, T. H., R. L. Walter, and H. H. Barschall, 1963, Nucl. Phys. **45**, 17.

Mayer, M. G., 1949, Phys. Rev. **75**, 1969.

Mayer, M. G., 1950, Phys. Rev. **78**, 16.

Mayer, M. G., and J. H. Jensen, 1955, *Elementary Theory of Nuclear Shell Structure* (Wiley, New York).

McManigal, P. G., R. D. Eandi, S. N. Kaplan, and B. J. Moyer, 1965, Phys. Rev. B **137B**, 620.

Measday, D. F., and J. N. Palmieri, 1966, Nucl. Phys. **85**, 129.

Mercer, R. L., L. G. Arnold, and B. C. Clark, 1978, Phys. Lett. **73B**, 9.

Miller, P. D., and G. C. Phillips, 1958, Phys. Rev. **112**, 2043.

Mitra, A. N., V. S. Bhasin, and B. S. Bhakar, 1962, Nucl. Phys. **38**, 316.

Mohr, C. B. O., and G. E. Pringle, 1937, Proc. R. Soc. London, Ser. A **160**, 190.

Morgan, G. L., and R. L. Walter, 1968, Phys. Rev. **168**, 1114.

Moss, G. A., C. A. Davis, J. M. Greben, L. G. Greeniaus, G. Roy, J. Uegaki, R. Abegg, D. A. Hutcheon, C. A. Miller, and W. T. H. van Oers, 1983, Nucl. Phys. A **392**, 361.

Mutchler, G. S., W. B. Broste, and J. E. Simmons, 1971, Phys. Rev. C **3**, 1031.

Nagata, S., T. Sasakawa, T. Sawada, and R. Tamagaki, 1959, Prog. Theor. Phys. **22**, 274.

Nasser, M. A., M. M. Gazzaly, J. V. Geaga, B. Hoistad, G. J. Igo, J. B. McClelland, A. L. Sagle, H. Spinka, J. B. Carroll, V. Perez-Mendez, and E. T. B. Whipple, 1978, Nucl. Phys. A **312**, 209.

Niiler, A., M. Drosg, J. C. Hopkins, J. D. Seagrave, and E. C. Kerr, 1971, Phys. Rev. C **4**, 36.

Nodvik, J. S., C. B. Duke, and M. A. Malkanoff, 1962, Phys. Rev. **125**, 975.

Ohlsen, Gerald G., J. L. McKibben, G. P. Lawrence, P. W. Keaton, Jr., and D. D. Armstrong, 1971, Phys. Rev. Lett. **27**, 599.

Omojola, D. A. F., 1970, J. Phys. A **3**, 630.

Palevsky, H., J. L. Friedes, R. J. Sutter, G. W. Bennett, G. J. Igo, W. D. Simpson, G. C. Phillips, D. M. Corley, N. S. Wall, R. L. Stearns, and B. Gottschalk, 1967, Phys. Rev. Lett. **18**, 1200.

Palmieri, J. N., and R. Goloskie, 1964, Nucl. Phys. **59**, 253.

Pasma, P. J., 1958, Nucl. Phys. **6**, 141.

Pearce, W. A., and P. Swan, 1966, Nucl. Phys. **78**, 433.

Perez-Mendez, V., J. M. Sperinde, and A. W. Stetz, 1969, Phys. Lett. **288**, 648.

Perkins, R. B., 1960, as cited by Hoop and Barschall (1966), p. 65.

Perkins, R. B., and C. Glashausser, 1964, Nucl. Phys. **60**, 433.

Perkins, R. B., and J. E. Simmons, 1961, Phys. Rev. **124**, 1153.

Phillips, G. C., and P. D. Miller, 1959, Phys. Rev. **115**, 1268.

Pigeon, J., J. Barguil, C. Fayard, G. H. Lamot, and E. El Baz, 1970, Nucl. Phys. A **145**, 319.

Pigeon, J., J. Barguil, C. Fayard, G. H. Lamot, and E. El Baz, 1971, Phys. Rev. C **4**, 704.

Plattner, G. R., A. D. Bacher, and H. E. Conzett, 1972, Phys. Rev. C **5**, 1158.

Plummer, D. J., T. A. Hodges, K. Ramavataram, D. G. Montague, and N. S. Chant, 1968, Nucl. Phys. A **115**, 253.

Plummer, D. J., K. Ramavataram, T. A. Hodges, D. G. Montague, A. Zucker, and N. K. Ganguly, 1971, Nucl. Phys. A **174**, 193.

Proriol, J., S. Maury, and B. Jargeaix, 1982, Phys. Lett. **110B**, 95.

Putnam, T. M., 1952, Phys. Rev. **87**, 933.

Putnam, T. M., J. E. Brolley, and L. Rosen, 1956, Phys. Rev. **104**, 1303.

Rafiqullah, A. K., S. Hossain, N. Chowdhury, A. Begum, and N. Ferdous, 1975, Dacca Univ. Stud. B **23**(2), 5.

Rahman, M., D. Husain, and S. Ali, 1974, Phys. Rev. C **10**, 1.

Ramavataram, K., D. J. Plummer, T. A. Hodges, and D. G. Montague, 1971, Nucl. Phys. A **174**, 204.

Rebel, H., 1974, Lectures given at the International Summer School of Nuclear Physics, Predeal, Romania, KFK Report No. 2065 (unpublished).

Reichstein, I., and Y. C. Tang, 1970, Nucl. Phys. A **158**, 529.

Rosen, L., and J. E. Brolley, Jr., 1957, Phys. Rev. **107**, 1454.

Sack, S., L. C. Biedenharn, and G. Breit, 1954, Phys. Rev. **93**, 321.

Saito, T., 1979, Nucl. Phys. A **331**, 477.

Sanada, J., 1960, Helv. Phys. Acta, Suppl. **6**, 249.

Satchler, G. R., L. W. Owen, A. J. Elwyn, G. L. Morgan, and R. L. Walter, 1968, Phys. Rev. **112**, 1.

Sawers, J. R., Jr., G. L. Morgan, L. A. Schaller, and R. L. Walter, 1968, Phys. Rev. **168**, 1102.

Schwandt, P., T. B. Clegg, and W. Haeberli, 1971, Nucl. Phys. A **163**, 432.

Schwinger, J., 1946, Phys. Rev. **69**, 681.

Schwinger, J., 1948, Phys. Rev. **73**, 407.

Scott, M. J., 1958, Phys. Rev. **110**, 1398.

Scott, M. J., and R. E. Segel, 1955, Phys. Rev. **100**, 1244.

Seagrave, J. D., 1953, Phys. Rev. **92**, 1222.

Selove, W., and J. M. Teem, 1958, Phys. Rev. **112**, 1658.

Shamu, R. E., and J. G. Jenkin, 1964, Phys. Rev. **135**, 99B.

Shamu, R. E., G. G. Ohlsen, and P. G. Young, 1963, Phys. Lett. **4**, 286.

Singh, P. P., P. Schwandt, and G. C. Yang, 1975, Phys. Lett. **59B**, 113.

Smith, J. R., 1954, Phys. Rev. **95**, 730.

Sourkes, A. M., N. E. Davison, S. A. Elbakr, J. L. Horton, A. Houdayer, W. T. H. van Oers, and R. F. Carlson, 1974, Phys. Lett. **51B**, 232.

Sourkes, A. M., A. Houdayer, W. T. H. van Oers, R. F. Carlson, and Ronald E. Brown, 1976, Phys. Rev. C **13**, 451.

Stammbach, Th., J. Taylor, G. Spalek, and R. L. Walter, 1970, Phys. Rev. C **2**, 434.

Stammbach, Th., and R. L. Walter, 1972, Nucl. Phys. A **180**, 225.

Staub, H., and W. E. Stephens, 1939, Phys. Rev. **55**, 131.

Staub, H., and H. Tatel, 1940a, Phys. Rev. **57**, 936.

Staub, H., and H. Tatel, 1940b, Phys. Rev. **58**, 820.

Stetz, A. W., and A. Stetz, 1968, UCRL Report No. 18088 (unpublished).

Striebel, H. R., and P. Huber, 1957, Helv. Phys. Acta **30**, 67.

Sugie, A., P. E. Hodgson, and H. H. Robertson, 1957, Proc. Phys. Soc. London, Sect. A **70**, 1.

Swan, P., 1967, Phys. Rev. Lett. **19**, 245.

Swartz, C., 1952, Phys. Rev. **85**, 73.

Tannenwald, P. E., 1953, Phys. Rev. **89**, 508.
Thompson, D. R., R. E. Brown, M. LeMere, and Y. C. Tang, 1977, Phys. Rev. C **16**, 1.
Thompson, D. R., I. Reichstein, W. McClure, and Y. C. Tang, 1969, Phys. Rev. **185**, 1351.
Thompson, D. R., and Y. C. Tang, 1971, Phys. Rev. C **4**, 306.
Thompson, D. R., Y. C. Tang, and R. E. Brown, 1972, Phys. Rev. C **5**, 1939.
Thompson, G. E., M. B. Epstein, and T. Sawada, 1970, Nucl. Phys. A **142**, 571.
Trostin, I. S., and V. A. Smotryaev, 1963, Zh. Eksp. Teor. Fiz. **44**, 1160 [Sov. Phys.—JETP **17**, 784 (1963)].
Trostin, I. S., V. A. Smotryaev, and I. I. Levintov, 1961, Zh. Eksp. Teor. Fiz. **41**, 725 [Sov. Phys.—JETP **14**, 524 (1962)].
Van der Spuy, E., 1956, Nucl. Phys. **1**, 381.
van Oers, W. T. H., B. T. Murdoch, B. K. S. Koene, D. K. Hasell, R. Abegg, D. J. Margaziotis, M. B. Epstein, G. A. Moss, L. G. Greeniaus, J. M. Greben, J. M. Cameron, J. G. Rogers, and A. W. Stetz, 1982, Phys. Rev. C **25**, 390.
Vaughn, F. J., W. L. Imhof, R. G. Johnson, and M. Walt, 1959, Phys. Rev. **118**, 683.
Velicho, G. N., A. A. Vorob'ëv, Yu. K. Zalite, G. A. Korolëv, E. M. Maev, N. K. Terent'ev, Y. Terrien, and A. V. Khanzadeev, 1982, Yad. Fiz. **35**, 270 [Sov. J. Nucl. Phys. **35**, 154 (1982)].
Verbeck, S. L., J. C. Fong, G. J. Igo, C. A. Whitten, Jr., D. L. Hendrie, Y. Terrien, V. Perez-Mendez, and G. W. Hoffmann, 1975, Phys. Lett. **59B**, 339.
Votta, L. G., P. G. Roos, N. S. Chant, and R. Woody III, 1974, Phys. Rev. C **10**, 520.
Wallace, S. J., and Y. Alexander, 1977, Phys. Rev. Lett. **38**, 1269.
Walter, R. L., W. Benenson, P. S. Dubbeldam, and T. H. May, 1962, Nucl. Phys. **30**, 292.
Walter, R. L., W. Benenson, T. H. May, and A. S. Mahajan, 1962, Bull. Am. Phys. Soc. **7**, 268.
Weitkamp, W. G., and W. Haeberli, 1966, Nucl. Phys. **83**, 46.
White, R. E., and F. J. M. Farley, 1957, Nucl. Phys. **3**, 476.
Wildermuth, K., and Y. C. Tang, 1977, *A Unified Theory of the Nucleus,* Clustering Phenomena in Nuclei (Vieweg, Braunschweig), Vol. I.
Williams, J. H., and S. W. Rasmussen, 1955, Phys. Rev. **98**, 56.
Wolfenstein, L., 1949, Phys. Rev. **75**, 1664.
Wolfenstein, L., 1956, Ann. Rev. Nucl. Sci. **6**, 43.
York, R. L., J. C. Heibert, H. L. Woolverton, and N. C. Northcliffe, 1983, Phys. Rev. C **27**, 46.